VOL.107 NO.TE1. JAN. 1981

TRANSPORTATION ENGINEERING JOURNAL OF ASCE

PROCEEDINGS OF
THE AMERICAN SOCIETY
OF CIVIL ENGINEERS

AEROSPACE
AIR TRANSPORT
HIGHWAY
PIPELINE
URBAN TRANSPORTATION

VOL.107 NO.TE1. JAN. 1981

TRANSPORTATION ENGINEERING JOURNAL OF ASCE

PROCEEDINGS OF
THE AMERICAN SOCIETY
OF CIVIL ENGINEERS

AEROSPACE
AIR TRANSPORT
HIGHWAY
PIPELINE
URBAN TRANSPORTATION

Copyright© 1981 by
American Society
of Civil Engineers
All Rights Reserved
ISSN 0569-7891

AMERICAN SOCIETY OF CIVIL ENGINEERS

BOARD OF DIRECTION

President
Irvan F. Mendenhall

Past President
Joseph S. Ward

President Elect
James R. Sims

Vice Presidents
Robert D. Bay — Lyman R. Gillis
Francis J. Connell — Albert A. Grant

Directors
Martin G. Abegg — Paul R. Munger
Floyd A. Bishop — William R. Neuman
L. Gary Byrd — Leonard S. Oberman
Larry J. Feeser — John D. Parkhurst
John A. Focht, Jr. — Celestino R. Pennoni
Sergio Gonzalez-Karg — Robert B. Rhode
James E. Humphrey, Jr. — S. Russell Stearns
Richard W. Karn — William H. Taylor
Leon D. Luck — Stafford E. Thornton
Arthur R. McDaniel — Robert E. Whiteside
Richard S. Woodruff

EXECUTIVE OFFICERS

Eugene Zwoyer, *Executive Director*
Julie E. Gibouleau, *Assistant to the Executive Director*
Louis L. Meier, *Washington Counsel/Assistant Secretary*
William H. Wisely, *Executive Director Emeritus*
Michael N. Salgo, *Treasurer*
Elmer B. Isaak, *Assistant Treasurer*

STAFF DIRECTORS

Donald A. Buzzell, *Managing Director for Education and Professional Affairs*
Robert A. Crist, Jr., *Managing Director for Publications and Technical Affairs*
Alexander Korwek, *Managing Director for Finance and Administrative Services*
Alexandra Bellow, *Director, Human Resources*
David Dresia, *Director, Publications Production and Marketing*
Barker D. Herr, *Director, Membership*
Richard A. Jeffers, *Controller*
Carl E. Nelson, *Director, Field Services*
Don P. Reynolds, *Director, Policy, Planning and Public Affairs*
Bruce Rickerson, *Director, Legislative Services*
James M. Shea, *Director, Public Communications*
Albert W. Turchick, *Director, Technical Services*
George K. Wadlin, *Director, Education Services*
R. Lawrence Whipple, *Director, Engineering Management Services*

COMMITTEE ON PUBLICATIONS

Stafford E. Thornton, *Chairman*
Martin G. Abegg — Richard W. Karn
John A. Focht, Jr. — Paul R. Munger
William R. Neuman

PUBLICATION SERVICES DEPARTMENT

David Dresia, *Director, Publications Production and Marketing*

Technical and Professional Publications
Richard R. Torrens, *Manager*
Joseph P. Cerami, *Chief Copy Editor*
Linda Ellington, *Copy Editor*
Thea C. Feldman, *Copy Editor*
Meryl Mandle, *Copy Editor*
Joshua Spieler, *Copy Editor*
Shiela Menaker, *Production Co-ordinator*
Richard C. Scheblein, *Draftsman*

Information Services
Elan Garonzik, *Editor*

PARTICIPATING GROUPS

AEROSPACE DIVISION

Executive Committee
Nicholas C. Costes, *Chairman*
William F. Bates, Jr., *Vice Chairman*
Edward G. Anderson — Walter J. Horn
Harold D. Laverentz, *Secretary*
Stewart W. Johnson, *Management Group C Contact Member*

Publications Committee
W. David Carrier, III, ***Chairman***
Randall Brown — David N. Markey
Samuel P. Clemence — Balakrishna Rao
Wesley P. James — Kentaro Tsumi
Charles E. S. Ueng
Edward G. Anderson, *Exec. Comm. Contact Member*

AIR TRANSPORT DIVISION

Executive Committee
J. C. Orman, *Chairman*
Donald M. Arntzen, *Vice Chairman*
Frederic M. Isaac — Adib K. Kanafani
Edward C. Regan, *Secretary*
Andy M. Attar, *Management Group C Contact Member*

Publications Committee
Frederick J. Wegmann, ***Chairman***
Milton B. Meisner, ***Vice Chairman***
Edwin H. Clark — Bernard A. Vallerga
H. K. Friedland — Gordon Y. Watada
Everett S. Joline — Jason C. Yu
A. Kanafani, *Exec. Comm. Contact Member*

HIGHWAY DIVISION

Executive Committee
Robert H. Wortman, *Chairman*
Edward M. Whitman, *Vice Chairman*
Richard St. John — Phillip G. Manke
Sanford La Hue, *Secretary*
William B. Drake, *Management Group C Contact Member*

Publications Committee
John A. Dearinger, ***Chairman***
Bob M. Galloway — William F. Land
T. Allan Hailburton — Rex K. Rainer
Douglas I. Hanson — N. J. Rowan
Fred M. Hudson — Bob L. Smith
Robert L. Janes — Robert L. Vecellio
R. E. Johnson — Edward M. Whitlock

PIPELINE DIVISION

Executive Committee
Mercel J. Shelton, *Chairman*
Jerry Machemehl, *Vice Chairman*
Michael A. Collins — Charles H. Klohn
B. Jay Schrock, *Secretary*
William F. Quinn, *Management Group E Contact Member*

Publications Committee
Walter W. Hu, ***Chairman***
Michael A. Collins — Allan S. Humphreys
Robert Faddick — Iraj Zandi
Mercel J. Shelton, *Exec. Comm. Contact Member*

URBAN TRANSPORTATION DIVISION

Executive Committee
Ira N. Pierce, *Chairman*
Carl W. Goepfert, *Vice Chairman*
Salvatore J. Bellomo — K. C. Sinha
Edward C. Sullivan, *Secretary*
Edward F. Sullivan, *Management Group C Contact Member*

Publications Committee
Martin E. Lipinski, ***Chairman***
Michael J. Demetsky, ***Vice Chairman***
William G. Allen — Don H. Jones
William R. Hershey — Edward A. Mierzejewski
Kumares C. Sinha, *Exec. Comm. Contact Member*

PERMISSION TO PHOTOCOPY JOURNAL PAPERS

Permission to photocopy for personal or internal reference beyond the limits in Sections 107 and 108 of the U.S. Copyright Law is granted by the American Society of Civil Engineers for libraries and other users registered with the Copyright Clearance Center, 21 Congress Street, Salem, Mass. 01970, provided the appropriate fee is paid to the CCC for all articles bearing the CCC code. Requests for special permission or bulk copying should be addressed to the Manager of Technical and Professional Publications, American Society of Civil Engineers.

CONTENTS

Soil-Pipe Interaction of Heated Oil Pipelines
by Bing C. Yen, Ching H. Tsao, and R. D. Hinkle
(Pipeline Division) 1

High Head Performance of Concrete Pipe
by James W. Davidson
(Pipeline Division) 15

Permeability of Lime Stabilized Soils
by Nagih M. El-Rawi and Amir A. A. Awad
(Highway Division) 25

Tax Allocation Formulas by Stepwise Regression
by Lansford C. Bell and Russell D. Shelton
(Highway Division) 37

Soil-Pipe Interaction and Pipeline Design
by Syed Ahmed, Ralph W. McMickle, and Carl L. Brassow
(Pipeline Division) 45

→

This Journal is published bimonthly by the American Society of Civil Engineers. Publications office is at 345 East 47th Street, New York, N.Y. 10017. Address all ASCE correspondence to the Editorial and General Offices at 345 East 47th Street, New York, N.Y. 10017. Allow six weeks for change of address to become effective. Subscription price to members is $12.50. Nonmember subscriptions available; prices obtainable on request. Second-class postage paid at New York, N.Y. and at additional mailing offices. TE.

The Society is not responsible for any statement made or opinion expressed in its publications.

Superplastic Cone-Shaped Sandwich Cores
by Charles E. S. Ueng
(Aerospace Division) 59

Impact Behavior of Barriers on Nonlevel Terrain
by Hayes E. Ross, Jr. and Darrell G. Smith
(Highway Division) 69

Simplified Procedures for Estimating Trip Attractions
by Ashok Kumar
(Urban Transportation Division) 81

DISCUSSION

Proc. Paper 15954

Basic Pipe Stress Evaluation Summary, by Gerald F. Mouser (July, 1979. Prior Discussion: July, 1980).
closure 103

Load Response of Transportation Support Systems, by Lufti Raad and Jose L. Figueroa (Jan., 1980).
errata 103

Cracking in Concrete Pavements,[a] by Robert C. Deen, James H. Havens, Assaf S. Rahal, and W. Vernon Azevedo (Mar., 1980).
by Clyde N. Laughter 103

Diesel Fuel Forecasts in Virginia, by Antoine G. Hobeika and Frank Tamberrino (July, 1980).
errata 104

[a]Discussion period closed for this paper. Any other discussion received during this discussion period will be published in subsequent Journals.

15977 SOIL-PIPE INTERACTION OF OIL PIPELINES

KEY WORDS: **Corrosion; Pipelines; Powerplants; Protective coatings; Soil mechanics;** Soil-structure interaction

ABSTRACT: A study is presented analyzing the distress frequently encountered in buried heated oil pipelines due to the expansion and contraction producing soil-pipe interface shear and cyclic movements. This movement can damage the coating of the pipe and result in corrosion failure. The magnitude of the cyclic shear stress and movement depends on temperatures, soil properties, and pipeline design items such as the length of casing, bend, and straight pipe sections. Two important factors are the coefficient of horizontal subgrade reaction and the soil-pipe interface shear parameter. The interface shear parameter is unique to the heated pipeline problem and can serve as a coating performance and selection criteria. Methods to calculate pipe movements and ways to restrain such movements are analyzed. Actual field measurements of a heated oil pipeline are compared with theoretical calculations.

REFERENCE: Yen, Bing C., Tsao, Ching H., and Hinkle, R. D., "Soil-Pipe Interaction of Heated Oil Pipelines," *Transportation Engineering Journal,* ASCE, Vol. 107, No. TE1, **Proc. Paper 15977,** January, 1981, pp. 1-14

15987 HIGH HEAD PERFORMANCE OF CONCRETE PIPE

KEY WORDS: Bells; Bending stress; **Concrete pipes; Design;** Diameters; **High head; Performance; Pressure;** Prestressing; **Ring theory**

ABSTRACT: This paper deals with the manufacture and subsequent testing to 600 psi (4137 kPa) of 189-in. (4,800-mm) inside diamater prestressed concrete pipe with four layers of prestressing wire. Existing barrel design theory and a newly developed theory for determining joint ring stresses are evaluated and shown to correlate with test data.

REFERENCE: Davidson, James W., "High Head Performance of Concrete Pipe," *Transportation Engineering Journal,* ASCE, Vol. 107, No. TE1, **Proc. Paper 15987,** January, 1981, pp. 15-23

15993 PERMEABILITY OF LIME STABILIZED SOILS

KEY WORDS: Clayey soils; **Curing;** Density; Lime; **Permeability; Soil lime**

ABSTRACT: The permeability of two soils stabilized with lime when compacted at various molding water contents has been investigated in the laboratory. A poorly graded river sand and sandy silty clay were used. The effect of lime content, curing age, dry density, and type of soil on the permeability were investigated. The addition of lime reduced the permeability of the investigated sand at various moisture contents, while the permeability of the clay increased when compacted at the optimum moisture content. The permeability of all mixtures was found to decrease with curing age. There existed a molding water content for the sand-lime mixture at which the permeability reached a minimum. The permeability of the investigated sandy silty clay increased with increasing lime content at the same dry density.

REFERENCE: El-Rawi, Nagih M., and Awad, Amir A.A., "Permeability of Lime Stabilized Soils," *Transportation Engineering Journal,* ASCE, Vol. 107, No. TE1, **Proc. Paper 15993,** January, 1981, pp. 25-35

15994 TAX ALLOCATION BY STEPWISE REGRESSION

KEY WORDS: **Alligatorweed;** Distribution patterns; **Regression analysis;** Revenue; Statistical tests; **Taxes; Transportation**

ABSTRACT: A regression analysis model has been developed to derive alternate distribution formulas for statewide fuel tax revenue. The model combines predictor variables such as road mileage, population and vehicle registrations in a way that best fits the current needs of local jurisdictions. An analysis using data for Alabama's 67 counties produced distribution formulas that exhibited a significant improvement over the formula in use at the present time. An examination of statistical tests to assess the adequacy of alternate distribution formulas is also presented.

REFERENCE: Bell, Lansford C., and Shelton, Russell D., "Tax Allocation Formulas by Stepwise Regression," *Transportation Engineering Journal,* ASCE, Vol. 107, No. TE1, **Proc. Paper 15994**, January, 1981, pp. 37-44

15982 SOIL-PIPE INTERACTION AND PIPELINE DESIGN

KEY WORDS: **Deformation; Earth pressure; Failure;** Finite element method; **Pipelines;** Soil deformation; Steel pipes

ABSTRACT: The problem of steel pipe bend design with and without lateral soil restraint is studied, and the effect of backfill soil deformation on the bend design is postulated. Studies show that a finite element model utilizing nonlinear soil properties is superior to conventional earth pressure theories and can result in an economic design. The effect of backfill type and the depth of soil cover in resisting the outward radial forces at bend locations are examined. Practical design and construction recommendations are presented.

REFERENCE: Ahmed, Syed, McMickle, Ralph W., and Brassow, Carl L., "Soil-Pipe Interaction and Pipeline Design," *Transportation Engineering Journal,* ASCE, Vol. 107, No. TE1, **Proc. Paper 15982**, January, 1981, pp. 45-58

15968 SUPERPLASTIC CONE-SHAPED SANDWICH CORES

KEY WORDS: Aerospace engineering; **Cones; Cores;** Elastic properties; Energy methods; Engineering mechanics; **Projection; Sandwich structures; Shear modulus; Structural design**

ABSTRACT: A new sandwich core is formed by using the superplastic sheets and the vacuum pressure- or gas pressure-forming technique, or both. It is capable of providing opportunities for structural optimization and better bonding with the facing sheets than the conventional honeycomb core. The shear modulus of a truncated, hollow, cone-shaped core with square symmetry is determined. Energy principles are used for finding the upper and lower bounds solution. Results presented in graphic form indicate that these bounds are indeed very close. The methodology developed here is effective for providing an excellent engineering solution to the problem. The new superplastically-formed core also offers a competent approach for those who seek a more efficient metallic structural design, particularly when it is used in combination with the difussion bonding technique for weight and cost savings.

REFERENCE: Ueng, Charles E.S., "Superplastic Cone-Shaped Sandwich Cores," *Transportation Engineering Journal,* ASCE, Vol. 107, No. TE1, **Proc. Paper 15968**, January, 1981, pp. 59-68

15984 IMPACT BEHAVIOR OF BARRIERS ON NONLEVEL TERRAIN

KEY WORDS: **Automobiles; Barriers;** Guardrails; **Highways;** Impact severity; **Safety;** Slopes; **Terrain; Tests;** Vehicle trajectories

ABSTRACT: Six full-scale crash tests were conducted to evaluate the impact behavior of two widely-used roadside barriers when placed on a 6:1 side slope. Four of the six tests involved a standard W-beam rail on metal post G4(1S) system and the other two tests involved a three-cable barrier mounted on metal posts (G1 system). The tests were conducted and evaluated in accordance with national guidelines for testing of roadside appurtenances. Based on the results, it is recommended that the G4(1S) system not be placed on 6:1 or steeper side slopes. Placement of the G1 system on a 6:1 side slope is acceptable provided ample space exists between the barrier and the hazard it is shielding.

REFERENCE: Ross, Hayes E., Jr., and Smith, Darrell G., "Impact Behavior of Barriers on Nonlevel Terrain," *Transportation Engineering Journal,* ASCE, Vol. 107, No. TE1, **Proc. Paper 15984,** January, 1981, pp. 69-79

15996 PROCEDURES FOR ESTIMATING TRIP ATTRACTIONS

KEY WORDS: Forecasting; Land use zoning; **Linear regression analysis;** Models; **Transportation planning; Trip generation;** Urban transportation

ABSTRACT: For many large metropolitan areas, gross land area, stratified by broad land-use categories, such as residential, commercial, industrial, and open space, is usually the only readily obtainable data outside the central business district. Need exists for reliable techniques that can be used for trip-attraction estimation for such urban areas. This paper presents a set of equations that have been calibrated, using multiple linear regression analysis, to compute zonal person-trip attractions for various trip purposes as a function of gross land area. For each trip-purpose, equations have been further stratified by pseudo-employment density ranges and dummy variables that reflect the presence of major trip attractors capable of satisfying the trip purpose in question. For zones falling within very high density areas, equations have been calibrated as a function of zonal gross floor area. Equations have also been developed for estimating zonal nonhome-based and truck trip ends.

REFERENCE: Kumar, Ashok, "Simplified Procedures for Estimating Trip Attractions," *Transportation Engineering Journal,* ASCE, Vol. 107, No. TE1, **Proc. Paper 15996,** January, 1981, pp. 81-99

U.S. Customary-SI Conversion Factors

In accordance with the October, 1970 action of the ASCE Board of Direction, which stated that all publications of the Society should list all measurements in both U.S. Customary and SI (International System) units, the following list contains conversion factors to enable readers to compute the SI unit values of measurements. A complete guide to the SI system and its use has been published by the American Society for Testing and Materials. Copies of this publication (ASTM E-380) can be purchased from ASCE at a price of $3.00 each; orders must be prepaid.

All authors of *Journal* papers are being asked to prepare their papers in this dual-unit format. To provide preliminary assistance to authors, the following list of conversion factors and guides are recommended by the ASCE Committee on Metrication.

To convert	To	Multiply by
inches (in.)	millimeters (mm)	25.4
feet (ft)	meters (m)	0.305
yards (yd)	meters (m)	0.914
miles (miles)	kilometers (km)	1.61
square inches (sq in.)	square millimeters (mm^2)	645
square feet (sq ft)	square meters (m^2)	0.093
square yards (sq yd)	square meters (m^2)	0.836
square miles (sq miles)	square kilometers (km^2)	2.59
acres (acre)	hectares (ha)	0.405
cubic inches (cu in.)	cubic millimeters (mm^3)	16,400
cubic feet (cu ft)	cubic meters (m^3)	0.028
cubic yards (cu yd)	cubic meters (m^3)	0.765
pounds (lb) mass	kilograms (kg)	0.453
tons (ton) mass	kilograms (kg)	907
pound force (lbf)	newtons (N)	4.45
kilogram force (kgf)	newtons (N)	9.81
pounds per square foot (psf)	pascals (Pa)	47.9
pounds per square inch (psi)	kilopascals (kPa)	6.89
U.S. gallons (gal)	liters (L)	3.79
acre-feet (acre-ft)	cubic meters (m^3)	1,233

TRANSPORTATION ENGINEERING JOURNAL

SOIL-PIPE INTERACTION OF HEATED OIL PIPELINES[a]

By Bing C. Yen,[1] M. ASCE, Ching H. Tsao,[2] and R. D. Hinkle,[3] M. ASCE

(Reviewed by the Pipeline Division)

INTRODUCTION

Many utility companies operate buried pipeline networks for transporting heated fuel oil from tank farms to power generating plants. Depending on the demand of generating stations and requirements for storage capacity, the heated oil is transported intermittently between storage tanks and generating stations about 20 times/yr in a typical section of pipeline system. The intermittent flow operation requires that the fuel oil be preheated before transporting. The intermittent operation also causes periodic pipeline thermal expansion and contraction and produces soilpipe interface shear and cyclic movements which may result in damaged pipelines. High cost maintenance efforts have been necessary in recent years to repair and replace damaged pipelines.

Fig. 1 shows a typical failure of pipe and its protective coating. The "wrinkled" coating suggests that the thermal expansion and contraction induced excessive movements and cyclic shear stresses between the pipe and the surrounding soil. In this case, the "wrinkles" are orientated perpendicular to the longitudinal axis of the pipeline. In Fig. 2, the orientation of wrinkles near the pipe bend suggests lateral and radial movements of the pipe. In Figs. 1 and 2 where the coatings are wrinkled and no longer protect the pipe, corrosion-caused pipe pitting has started. Fig. 3 shows pitted areas of steel pipe that failed either in service or under hydrostatic test.

[a]Presented at the April 14–18, 1980, ASCE Convention and Exposition, held at Portland, Oreg. (Preprint 80-163).

[1]Prof., Dept. of Civ. Engrg., California State Univ., Long Beach, Calif. 90840.
[2]Prof., Dept. of Mech. Engrg., California State Univ., Long Beach, Calif. 90840.
[3]Engr., Southern California Edison Co., Rosemead, Calif.

Note.—Discussion open until June 1, 1981. To extend the closing date one month, a written request must be filed with the Manager of Technical and Professional Publications, ASCE. Manuscript was submitted for review for possible publication on April 21, 1980. This paper is part of the Transportation Engineering Journal of ASCE, Proceedings of the American Society of Civil Engineers, © ASCE, Vol. 107, No. TE1, January, 1981. ISSN 0569-7891/81/0001-0001/$01.00.

Although considerable research has been conducted on the soil-pipe interaction problem of buried pipelines, only limited nonproprietary literature is available on heated oil pipelines. A state-of-the-art survey is available (7 and references, thereto), including a survey of existing computer programs (6). However, sophisticated computer analyses are often limited by the imprecise and sometimes poorly understood soil parameters. Furthermore, it is often impractical to apply

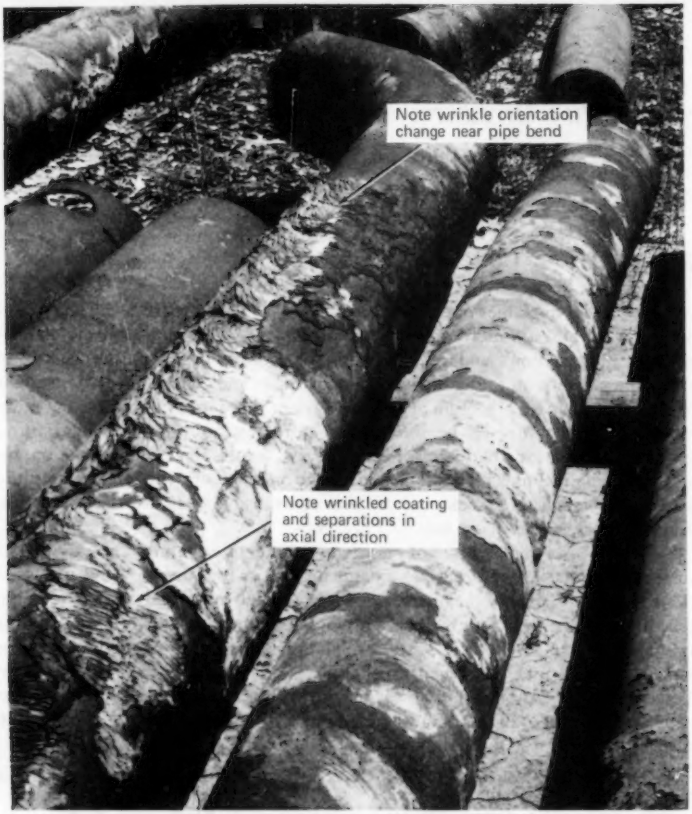

FIG. 1.—"Wrinkled" Pipe Coating Caused by Excessive Movement of Pipe to Surrounding Soil

the same level of effort for the analysis used for pipelines in a nuclear power plant to a heated-soil pipeline which may span many kilometers in length through various soil conditions. Therefore, a simplified approach compatible with the unique nature of the thermal-induced movements of heated oil pipelines has been called for by the design engineer (1) and coating manufacturers (4) in recent years.

In this article, the writers will: (1) Characterize the heated oil pipeline problem from a geotechnical engineering viewpoint; (2) analyze soil parameters pertinent

FIG. 2.—Separation of Pipe Coating in Radial Direction in Pipe Bend (note pitting at exposed pipe)

FIG. 3.—Pipe Failed at Casing Entrance (note excessive pitting at exposed pipe)

to a simplified soil-pipe interaction model for analysis and design; and (3) consider examples and compare field measurements with the theoretical analysis.

Characteristics of Heated Oil Pipelines

From a geotechnical engineering viewpoint, heated oil pipelines are characterized by the following special features:

1. Potentially, a large force can be exerted on soils at pipe bends. Due to the relatively large temperature differential between intermittent operations of the pipeline and the high internal operating pressure, the pipeline has a potential to exert large forces on the surrounding soil at pipe bends, e.g., assuming the

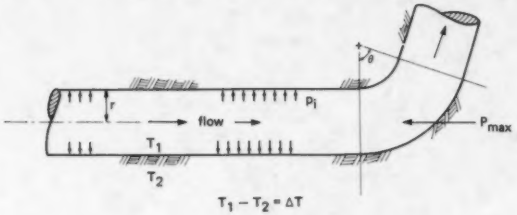

FIG. 4.—Notations at Pipe Bend

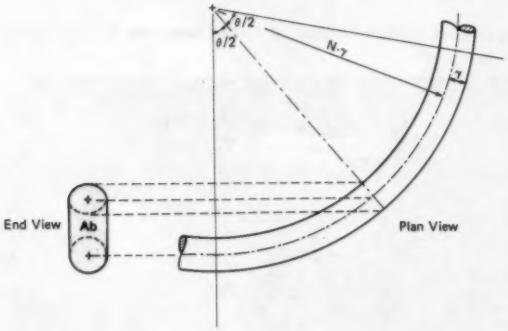

FIG. 5.—Soil Bearing Area at Pipe Bend

backfill at bends is so densely compacted that the pipe can be considered to be fully restrained (Fig. 4), the maximum axial force to be resisted by the soil at bends may be estimated by:

$$P_{max} = A_s(E\alpha\Delta T - \nu\sigma_\theta) \quad \ldots\ldots\ldots\ldots\ldots\ldots\ldots\ldots\ldots\ldots\ldots\ldots (1)$$

in which P_{max} = the maximum force to be resisted by the soil at the bend assuming a nonyield of soil; A_s = area of the steel pipe section; E = modulus of elasticity of pipe; α = thermal expansion coefficient of pipe; ΔT = temperature differential, degrees; ν = Poisson's ratio of pipe material; σ_θ = average hoop stress; $\sigma_\theta = (P_i \cdot r)/t$; and t = pipe wall thickness. For instance, for a typical 16-in. (406 mm) OD steel pipeline with wall thickness of 5/16 in. (8 mm) operated

at a temperature differential of 140° F (60° C) and an internal pressure of 1,000 psi (6.9 MN/m^2), the maximum axial force is 361 kips (1.6 MN) at a 45° bend. This is a large force to be resisted by the soils at pipe bends.

Note also that Eq. 1 is independent of pipe length, and the maximum force exerted on the soil depends only on operating temperature, pressure, and the geometry of the bend. Actually, the forces transmitted to the soil are lower because the soil at the bend is not infinitely rigid and does not fully restrain the pipeline; the actual force depends on the resistance of soil to deformation at pipe bends. The stiffer the soil at the bend, the larger the force will be. But for the time being, suffice it to say that the heated oil pipeline is capable of exerting large forces on the soil at bends and these forces increase significantly as the operating temperature increases. Under such large forces, the soil is likely to yield causing movements between the pipe and soil. This leads to the second special feature.

2. Cyclic Movements.—The cyclic movements induced by intermittent operations occur at locations where the pipeline changes direction (bends), changes in size, or terminates. These movements also cause shear stresses at soil-pipe interface. If these movements are not sufficiently restrained and the shearing stresses become excessive, the coating may be damaged. Methods to restrain the pipe movements are commonly the use of a large pipe bend radius or installation of large thrust blocks at the bend. These are expensive methods and frequently use of large pipe bends is infeasible as will be examined next.

3. Limitation of Use of Large Pipe Bend Radius.—Using thrust blocks or large radius bends to restrain the pipeline movements may be subject to practical limitations. For pipe bends, the effective soil bearing area, A_b, may be estimated as (Fig. 5):

$$A_b = \frac{\pi r^2}{2}\left(1 + \cos\frac{\theta}{2}\right) + 2Nr^2\left(1 - \cos\frac{\theta}{2}\right) \quad \ldots\ldots\ldots\ldots\ldots\ldots (2)$$

in which N = ratio of bend radius to pipe radius; and all other notations have been defined before.

In a given street corner or right-of-way, the pipeline designer is often limited by how large a bend can be used. A small N value means small soil area to restrain pipeline movement. Therefore, from a designer's viewpoint it is essential to provide a quantitative technique to estimate the pipe movements in terms of N and soil properties.

4. Cased Pipe Crossing.—Casing are generally used at locations where pipelines cross under roadways. Pipelines are supported by low-friction spacers within the casing, and therefore the pipe is not restrained by the surrounding soil. Movement and potential coating damage occur outside the casing where the surrounding soil is in contact with the pipe, e.g., Fig. 3 shows a pipeline that failed near a casing entrance. Therefore, it is essential for the engineer to be able to estimate the amount of pipe movement at the casing entrance.

Soil-Pipe Interaction

Although buried pipelines may have configurations consisting of bends, casings, straight sections, and combinations thereof, these configurations can be de-

composed into two generic elements shown in Fig. 6. A combination of these generic elements can simulate most pipeline configurations as shown in Fig. 7. Thus, other pipeline design configurations can be calculated once the mathematical model of the two generic elements are solved.

In the mathematical models the pipe bends have been replaced by a soil restraining force P. For the straight pipe section where the soil is in contact with the surrounding soil, there is a soil-pipe interface shearing force q, acting against the pipe. Within the casing, there is no contact between the pipe and soil; thus $q = 0$.

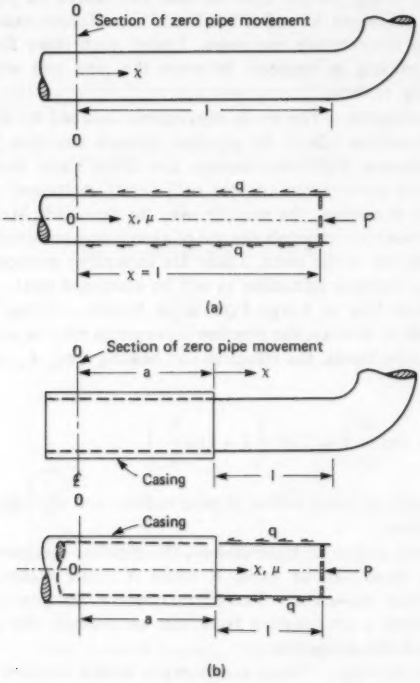

FIG. 6.—Physical and Mathematical Models: (*a*) Generic Element A; and (*b*) Generic Element B

Analysis of Generic Element A: Straight Pipe and Bend.—When the pipe heats up, the pipe expands. The soil-coating interface shear force (q) acts along the pipe to resist expansion and the pipe bend counters the expansion with force P. The stresses in the pipe wall is

$$\sigma_x = \frac{-\int_x^l q\,dx - P}{A_s}$$

at a distance x from the section of zero pipe movement . . . . . (3)

and the pipe strain is the summation of thermal-induced strain plus the strain caused by soil stresses, i.e.:

$$\epsilon_x = \frac{du}{dx} = \frac{\sigma_x}{E} + (\alpha \cdot \Delta T - \nu \cdot \sigma_0) \quad \ldots\ldots\ldots\ldots\ldots\ldots\ldots\ldots\ldots\ldots (4)$$

in which u = pipe movement at section x. Let $q = C \cdot u$, i.e., assuming the soil-pipe interface shear force is proportional to the pipe movement. It can

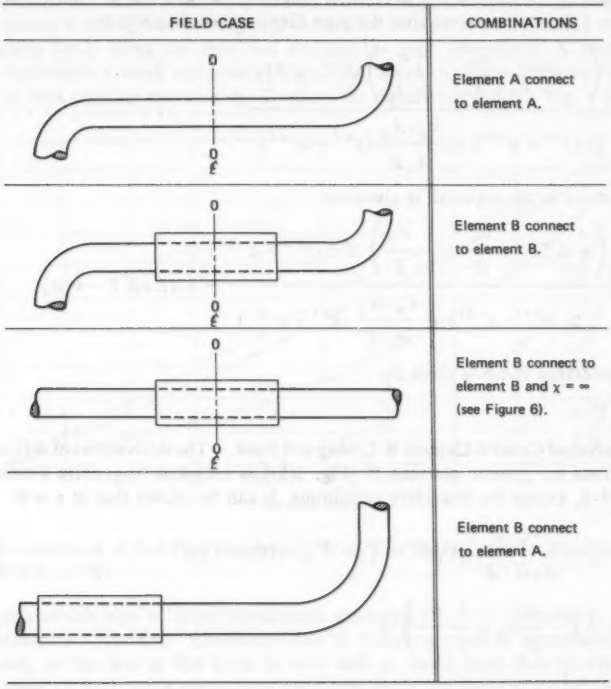

FIG. 7.—Examples Showing Pipeline Configurations by Combining Generic Elements

be shown that the differential equation describing the relationship of pipe movements is

$$\frac{d^2\mu}{dx^2} - \beta^2 \cdot u = 0 \quad \ldots\ldots\ldots\ldots\ldots\ldots\ldots\ldots\ldots\ldots\ldots\ldots\ldots\ldots (6)$$

in which β = the soil-pipe interaction parameter relating pipe property to the soil-pipe interface shear:

$$\beta = \left(\frac{C}{A_s \cdot E}\right)^{1/2} \quad \ldots\ldots\ldots\ldots\ldots\ldots\ldots\ldots\ldots\ldots\ldots\ldots\ldots\ldots\ldots\ldots (7)$$

The physical significance of β and C will be considered later. The general solution of Eq. 6 is

$$\mu_x = C_1 e^{\beta x} + C_2 e^{-\beta x} \quad \ldots\ldots\ldots\ldots\ldots\ldots\ldots\ldots\ldots\ldots\ldots\ldots\ldots\ldots\ldots\ldots (8)$$

Parameters C_1 and C_2 may be solved using boundary conditions: (1) At $x = 0$, $\mu = 0$, $C_1 + C_2 = 0$; and (2) at $x = l$, $\sigma_x = -P/A_s = (k_H \cdot A_b \cdot \mu_1)/A_s$ in which k_H = coefficient of horizontal subgrade reaction; and μ_l = pipe movement at $x = l$. It can be shown that the pipe displacement is given by:

$$\mu_x = \frac{\left(\alpha \cdot \Delta T - \nu \frac{\sigma_\theta}{E} + \frac{1}{2}\frac{\sigma_\theta}{E}\right)(e^{\beta x} - e^{-\beta x})}{\beta \cdot (e^{\beta l} + e^{-\beta l}) + \frac{k_H \cdot A_b}{A_s E}(e^{\beta l} - e^{-\beta l})} \quad \ldots\ldots\ldots\ldots\ldots\ldots\ldots\ldots\ldots\ldots (9)$$

The stress in the pipewall is given by

$$\sigma_x = \frac{\left(\alpha \cdot \Delta T - \nu \frac{\sigma_\theta}{E} + \frac{1}{2}\frac{\sigma_\theta}{E}\right) \cdot E \cdot \beta\,(e^{\beta x} + e^{-\beta l})}{\beta \cdot (e^{\beta l} + e^{-\beta l}) + \frac{k_H \cdot A_b}{A_s \cdot E}(e^{\beta l} - e^{-\beta l})} - (E\alpha\Delta T - \nu \cdot \sigma_\theta) \qquad (10)$$

The interface shear is given by

$$q_x = C \cdot \mu_x \quad \ldots\ldots\ldots\ldots\ldots\ldots\ldots\ldots\ldots\ldots\ldots\ldots\ldots\ldots\ldots\ldots (11)$$

Analysis of General Element B: Casing and Bend.—The derivations of differential equations for generic element B [Fig. 6(*b*)] is identical to generic element A, Eqs. 4–8, except for boundary conditions. It can be shown that at $x = 0$

$$C_1 + C_2 = \frac{-C \cdot a}{A_s E \cdot \beta}[(C_1 e^{\beta l} - C_2 e^{-\beta l}) - (C_1 - C_2)]$$

$$+ \left(\alpha \cdot \Delta T - \frac{\nu}{E}\sigma_\theta + \frac{1}{2}\frac{\sigma_\theta}{E}\right) \cdot a \quad \ldots\ldots\ldots\ldots\ldots\ldots\ldots\ldots\ldots\ldots (12)$$

or at $x = l$:

$$(C_1 \cdot e^{\beta l} + C_2 e^{-\beta l}) \cdot \frac{-k_H \cdot A_b}{A_s \cdot E} = \beta \cdot (C_1 \cdot e^{\beta l} - C_2 e^{-\beta l})$$

$$- \left(\alpha\Delta T - \frac{\nu}{E}\sigma_\theta + \frac{1}{2}\frac{\sigma_\theta}{E}\right) \quad \ldots\ldots\ldots\ldots\ldots\ldots\ldots\ldots\ldots\ldots (13)$$

The two unknowns, C_1 and C_2, can be obtained by solving Eq. 12 and Eq. 13 simultaneously. Once C_1 and C_2 are known, the pipe movement is

$$u_x = C_1 e^{\beta x} + C_2 e^{-\beta x} \quad \ldots\ldots\ldots\ldots\ldots\ldots\ldots\ldots\ldots\ldots\ldots\ldots\ldots\ldots\ldots\ldots (14)$$

The soil-pipe interface shear at a distance x from the casing entrance is:

$$q_x = C(C_1 e^{\beta x} + C_2 e^{-\beta x}) \quad \ldots\ldots\ldots\

the coating used, the movements may be too large for the coating to resist and damage may ensue. Therefore, $\beta 1$, (and thus the C value) is a unique criterion to measure the performance and behavior of the soil-coating-pipe interaction of hot oil pipelines.

Location of Section of Zero-Pipe-Movement.—Section 0-0 in Fig. 6 represents a location at which the pipe has no movement relative to the soil, i.e., $u = 0$. Physically, Section 0-0 could be the location: (1) Where the pipe is connected to rigid structure; or (2) a symmetrical condition with the existence of an identical bend configuration to the left of Section 0-0. Section 0-0 may be located for a straight pipe connecting different bends at which pipe movements at each bend are known: $(u)_{l_1}/l_1 = (u)_{l_2}/l_2$; and $l_1 + l_2 =$ pipeline length between the two bends. If the soil conditions (q), and bend geometry are different, iterations will be required to locate Section 0-0 using initially assumed displacements at each bend.

Influence of Pipe Bend Radii and Coefficient of Soil Horizontal Subgrade Reaction.—A large bend radius (large multiplier, N) will increase the effective

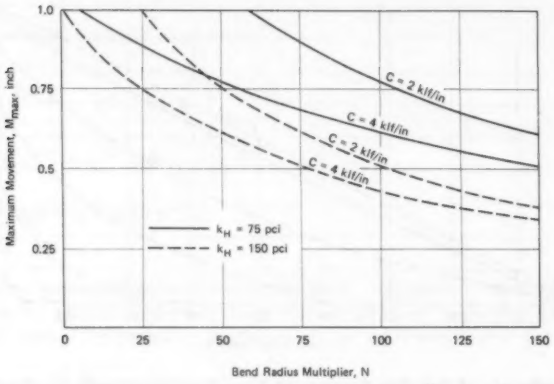

FIG. 9.—Influence of N and C on Maximum Pipe Movements

soil bearing area. Higher coefficient of subgrade reaction, k_H, will also increase the soil resistance at a bend. Fig. 9 shows the influence of both N and k_H on the maximum pipe movement for a 16-in. (406-mm) OD steel pipe with $l = 500$ ft (152.4 m) heated to a temperature differential of 140° F (60° C). Note that the greater the frictional resistance (C-value) between soil and coating, the smaller is the pipe movement. The greater is the soil horizontal subgrade reaction coefficient (k_H) at the bend, the smaller is the pipe movement. A relationship such as this can be used to assess the cost-effectiveness of selection trench backfill soil and compaction requirements, because the soil type and density influence the C and k_H values. In addition, for a given coating and soil type, the pipe movement can be estimated by increasing bend radius. Thus, with proper choice of coating and appropriate design and construction, information such as Fig. 9 may be used to limit the potential pipeline movements without damage to the coating. However, for the time being, little is known on the

coating integrity when it is subjected to the thermal induced cyclic movements during the design life of the pipeline.

From a geotechnical engineering viewpoint, k_H depends on soil type, density, and depth of pipe burial. It also varies with soil deformation and strength (2). Since heated oil pipelines are characterized by a low operating frequency (about 20 times/yr) of cyclic loading acting on a generally sandy trench backfill of shallow depths (2 m–3 m), k_H can be estimated from nonlinear, drained stress-strain relationship of sands. The range shown in Fig. 9 represents the estimated values of concrete sands as backfill compacted in a trench about 2.5 m deep (8).

The C value is coating dependent and also varies with soil type, density, and operating temperature. Modified direct shear tests on heated samples of

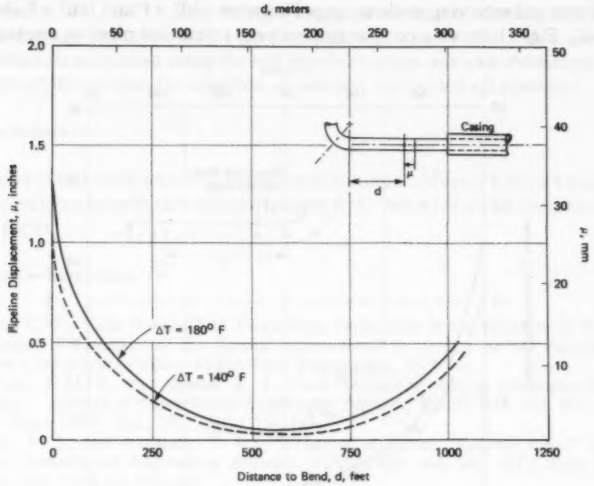

FIG. 10.—Influence of Casing for 1,000 ft Pipe at Two Operating Temperatures

a given coating against sands were conducted (8). The range of C values (105 kN/cm^3–210 kN/cm^3) is partly from results of such tests and partly from field average coating wrinkle spacing, u (note that $C = q/\mu$). It is emphasized that these C values are preliminary and indicate only an order of magnitude because of the many limitations associated with testing coating using a direct shear device. A PCSI (Pipe-Coating-Soil Interaction) tester is being developed (9) to determine C and to evaluate pipe coating performances at elevated temperatures.

Influence of Casing.—Since the pipe within casing is not subjected to shearing resistance like the pipe buried in a trench, pipe movements near the casing entrance as well as near bends are locations of high damage potential. Fig. 10 shows this phenomenon at two different operating temperatures. Fig. 10 represents a 16-in. (406-mm) steel pipe buried 10 ft (3 m) with $N = 42$; $k_H = 150$ pci (0.27 N/cm^3); and $C = 2$ Klf/in. (115 N/cm^2). If a coating is

known to be subjected to damage when the cyclic movements exceed 0.5 in. (13 mm), a pipeline designed from Fig. 10 will be subjected to failure within the reach of about 100 ft (30.5 m) from the bend. Fig. 10 also shows that pipe failure can be expected at the casing entrance if the operating temperature differential exceeds 180° F (82° C).

Comparison with Field Data

A 16-in. (406-mm) OD steel pipe with a 90° bend and $N = 42$ but no casing was instrumented to monitor pipe movements (9). The soil cover ranged from 7 ft–10 ft (2 m–3 m) at the bend area with backfill ranging from concrete sands to silty sands. Temperature at the bend was not exactly known but the temperature at delivery and receiving stations ranged between 150° +F and 160° +F (66° +C–71° +C). Fig. 11 shows a comparison between calculated pipeline displacements

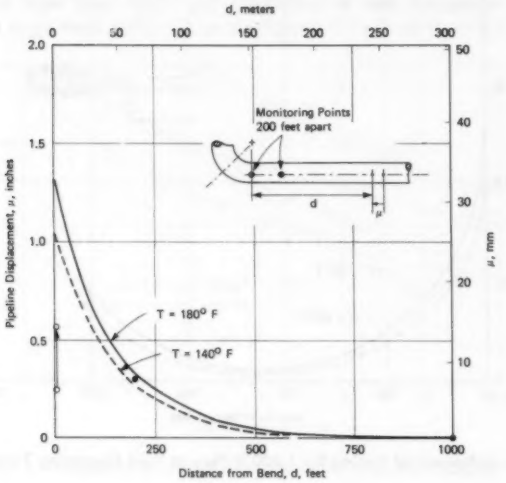

FIG. 11.—Comparison between Calculated Pipe Movement Profile and Measured Field Data

and field measured data. Detailed analysis is given in Ref. 9. Considering many uncertainties that involve soil properties, construction procedures, and pipeline operations, the comparison as shown in Fig. 11 is considered satisfactory and generally substantiate the soil-pipe interaction analysis.

Conclusions

Based on field observations of damaged pipe, soil-pipe interaction analysis, and field measurements, the following conclusions appear to be appropriate:

1. The expansion and contraction of heated oil pipelines produce soil-pipe

interface shear and cyclic movements. The magnitude of the interface shear and movements depends on soil properties and pipeline design such as length of straight pipe sections, bend radius, and casing length.

2. Excessive interface shear and movements may damage protective coatings and expose the pipeline and lead to corrosion-induced failures.

3. The interface shear and pipe movements can be estimated using the soil-pipe interaction equations which have two principal parameters. One is the soil coefficient of horizontal subgrade reaction, k_H. The other parameter appears to be unique to heated oil pipeline problems. It is the interface shear parameter, C, and its related relative stiffness parameter β. Parameter C measures the coating resistance to pipe movement at elevated temperatures. The interface shear parameter is coating dependent and more research is needed.

4. Increase of k_H and C values will decrease pipe movements thereby decreasing pipeline damage potential. For a given pipeline geometry and soil conditions, the movements calculated using the soil-pipe interaction analysis showed promise to be one of the criteria for selection of coatings for heated oil pipelines.

Acknowledgment

Portions of this work were funded by the Southern California Edison Company. Their permission to publish is acknowledged. R. L. Allen reviewed the manuscript of this paper.

Appendix I.—References

1. Argent, C. T., "The Role of Soil Assessment Techniques in the Selection of Pipeline Coatings," *Proceedings of the Second International Conference on the Internal and External Protection of Pipes*, BRHA Fluid Engineering, 1977.
2. Audibert, J. M. E., and Nyman, K. J., "Soil Resistance Against Horizontal Motion of Pipes," *Journal of Geotechnical Engineering Division*, ASCE, Vol. 103, No. GT10, Proc. Paper 13303, Oct., 1977, pp. 1119–1143.
3. Krizek, R. J., and McQuade, P. V., "Behavior of Buried Concrete Pipe," *Journal of the Geotechnical Engineering Division*, ASCE, Vol. 104, No. GT7, Proc. Paper 13899, July, 1978, pp. 815–837.
4. Lange, M., discussion of "The Corrosion Protection of Underground Pipelines by Plastic Tape Pipeline Coatings," by G. M. Harris, *Proceedings of the Second International Conference on the Internal and External Protection of Pipes*, 1977, pp. x–13.
5. Ligon, J. B., and Mayer, G. R., "Friction Resistance of Buried Pipeline Coatings Studied," *Pipeline and Gas Journal*, Feb., 1975, pp. 33–35.
6. Strauss, S. D., and O'Keefe, W., "Piping for Nuclear Plants," *Power*, June, 1978, pp. S1–S24.
7. Wang, L. R. L., and O'Rourke, "State-of-the-Art of Buried Lifeline Earthquake Engineering," *Current State of Knowledge of Life-Line Earthquake Engineering*, ASCE, Aug., 1977, pp. 252–266.
8. Yen, B. C., "Soil-Pipe Interaction of Heated Oil Pipeline," Report to Southern California Edison Company, Dec., 1978, pp. 1–89.

Appendix II.—Notation

The following symbols are used in this paper:

A_b = effective bearing area at pipe bend, L^2;
a = length of casing measured from zero pipe movement, L;

C = soil-pipe interface shear parameter, F/L^2;
C_1, C_2 = coefficients for determining pipe movements, L;
E = modulus of elasticity of the pipe F/L^2;
k_H = coefficient of horizontal subgrade reaction, F/L^3;
l = pipe length from zero movement to pipe bend;
N = ratio of bend radius to pipe radius;
P_i = pipe internal pressure, F/L^2;
P_{max} = maximum force to be resisted by soil at bend in x direction, F;
P = soil reaction force at bend to pipe expansion in x direction, F;
q = interface shear resistance per unit length of pipe, F/L;
r = radius of pipe, L;
t = thickness of pipe wall, L;
μ_x = pipe movement at location x, L;
α = coefficient of thermal expansion, L/L/degree of temperature;
β = soil-pipe interaction parameter, $1/L$;
δ = apparent friction angle between soil and coating, degree;
ΔT = temperature differential between hot oil and ambient soil, degree;
γ = unit weight of soil, F/L^3; and
ν = Poisson's ratio, dimensionless.

TRANSPORTATION ENGINEERING JOURNAL

HIGH HEAD PERFORMANCE OF CONCRETE PIPE[a]

By James W. Davidson,[1] A. M. ASCE

(Reviewed by the Pipeline Division)

INTRODUCTION

The performance limits of concrete pipe, specifically prestressed concrete cylinder pipe (PCCP), are continually being extended to higher and higher internal pressure heads. In order to withstand these heads, pipe cores must be heavily prestressed during manufacture, and steel spigot rings must be carefully analyzed. This all requires that the stresses in the pipe core and spigot ring be accurately predicted from manufacture through joining through pressurization.

Core prestress, which often requires multiple layers or wraps of prestressing wire in heavily prestressed pipe, causes the core to deflect radially inward. This induces initial residual longitudinal bending stresses in the steel spigot ring. When pipe are joined, the spigot ring is compressed radially inward as the gasket and ring contact the much stiffer bell, also inducing longitudinal bending stresses. Under internal pressure, the pipe core and joint expand radially but not uniformly, because of the difference in stiffness in the joint area, thus causing additional bending stresses.

THEORY

The theory presented in this paper is based on the assumption that the joints and barrel parts of the pipe core can be modeled as a relatively flexible spigot attached to a pipe barrel, restrained from excessive outward radial deflection under internal pressure by a rigid bell attached to another pipe barrel. An example of this is shown in Fig. 1; the bell is on the right and the spigot is on the left.

---

[a]Presented at the April 2–6, 1979, ASCE Convention and Exposition, held at Boston, Mass.

[1]Mgr., Research and Development, Hitco, 1600 West 135th St., P.O. Box 1097, Gardena, Calif. 90249.

Note.—Discussion open until June 1, 1981. To extend the closing date one month, a written request must be filed with the Manager of Technical and Professional Publications, ASCE. Manuscript was submitted for review for possible publication on April 23, 1979. This paper is part of the Transportation Engineering Journal of ASCE, Proceedings of the American Society of Civil Engineers, © ASCE, Vol. 107, No. TE1, January, 1981. ISSN 0569-7891/81/0001-0015/$01.00.

An earlier version of the theory was developed by Gordon Robertson of Ameron, and appears in a proprietary unpublished paper. Tests of 108-in. (2,740-mm) inside diameter (ID) prestressed concrete cylinder pipe were conducted and it was found that the theory needs to account for the radial spigot ring restraint produced by the bell part of the joint. The 189-in. (4,800-mm) ID PCCP tests reported in the paper verify the expanded theory. A computer program has been written to solve the complex equations at multiple locations along the total pipe.

The loads that act to produce stress and deformation in the spigot result from prestressing load, radial gasket load, internal water pressure, external earth loads, and radial restraint load acting through the raised flat portion of the spigot ring that is in contact with the bell ring. Calculation of the latter load requires a knowledge of the pressure induced radial deflections of the bell and spigot at their point of contact.

The method of analysis used to determine the response of the joint components to the imposed loads is based on the theory of beams on elastic foundation

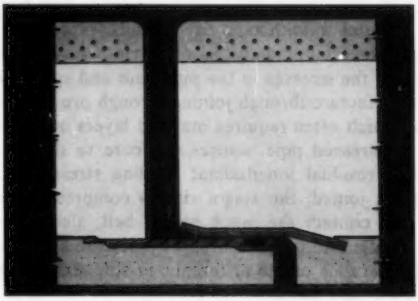

FIG. 1.—Typical Prestressed Concrete Cylinder Pipe Joint Configuration

(2). This theory, as applied to pipe, assumes that a longitudinal element of a relatively thin pipe under axially-symmetric loading may be regarded as a beam on elastic foundation, with the elastic supports along the beam being provided by circular elements of pipe. For simplicity, a pipe wall longitudinal element of unit width is analyzed.

To account for discontinuity in the pipe wall longitudinal element at the bell or spigot ends, the beam is "cut" at the junction of the end and barrel. The parts are then analyzed separately for deflections and rotations at the cut caused by known external loading along the beam, and unknown continuity moments and shears at the cut. By equating deformations at the cut, the continuity moments and shears can be determined. Knowing these values and the response to external loading, final deflections and stresses can be calculated in the end and in the barrel.

The short bell end of the pipe, which has an embedded steel bell ring and is nearly as thick as the barrel, is analyzed as a rigid beam of constant thickness. The spigot end of the pipe is analyzed as a flexible beam, also of constant thickness, with no credit given for the mortar lining.

The purpose of this paper is to report on tests of large diameter PCCP carried out to verify existing pipe design theory (1) and a new unified theory, based in part on a "beam on elastic foundation" analogy, developed for predicting pipe core and steel spigot ring stresses from manufacture to pressurization.

Two 189-in. (4,800-mm) ID lengths of PCCP with four layers of prestressing wire were pressurized to up to 1,386 ft (422 m) of head or 600 psi (4,137 kPa). The spigot ring in the joint between the two pipes was strain-gaged, as were each layer of prestressing wire on both pipe. Strain-gage data showed good correlation with predicted values.

Manufacture

Overall test pipe design dimensions were: (1) ID = 189 in. (4,800 mm); (2) core thickness = 15 in. (381 mm); (3) overall length = 10 ft, 4-1/2 in. (3.16 m); (4) spigot length = 6-1/4 in. (159 mm); and (5) bell length = 5-3/4 in. (146 mm). A typical PCCP joint is shown in Fig. 1.

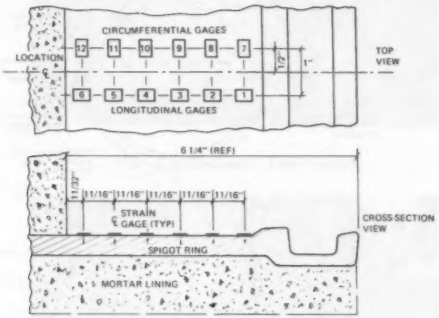

FIG. 2.—Strain-Gage Locations on Steel Spigot Ring (1 in. = 25.4 mm)

Four layers of 1/4-in. (6.35-mm) diam., American Society for Testing and Materials, ASTM A648 Class III prestressing wire were applied at a tensile load of approx 8,900 lb (4,036 kg), producing 3,430 psi (23.6 MPa) of prestress in the pipe core. After each layer of prestressing wire was applied, strain gages were attached to the wire and strain readings were taken to determine the effect of applying successive layers of wire on the previously applied layers.

The strain-gaged spigot ring had 1/16-in. (1.59-mm) gages along its length oriented in the longitudinal and circumferential directions, as shown in Fig. 2. They were read before and after each layer of wire was applied.

Gages on the prestressing wire and spigot ring were located at four points around the pipe circumference, as shown in Fig. 3.

Typical plots of longitudinal and circumferential spigot strains for actual test data and values predicted by the new theory are shown in Fig. 4. Stresses can be assumed to be 28 times microstrain.

Predicted average change in prestressing wire strain due to an additional layer of wire being applied was 216 microstrain. Test values averaged 201 microstrain, which was within 7% of the predicted value.

A few data points in Fig. 4 that were not consistent with the others were due to bad strain-gage readings caused by problems in maintaining even resistance

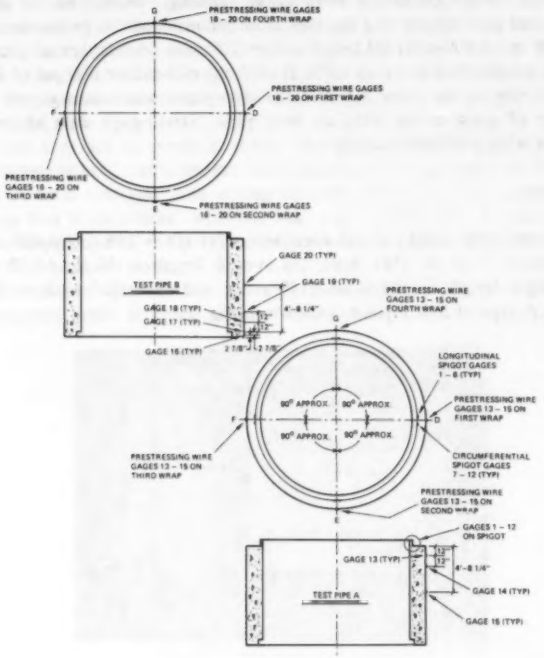
PRESTRESSING WIRE GAGES 18 – 20 ON FOURTH WRAP
PRESTRESSING WIRE GAGES 18 – 20 ON FIRST WRAP
PRESTRESSING WIRE GAGES 18 – 20 ON THIRD WRAP
PRESTRESSING WIRE GAGES 18 – 20 ON SECOND WRAP
GAGE 20 (TYP)
GAGE 19 (TYP)
TEST PIPE B
GAGE 18 (TYP)
GAGE 17 (TYP)
GAGE 16 (TYP)
4'-8 1/4"
12"
12"
2 7/8"
2 7/8"
PRESTRESSING WIRE GAGES 13 – 15 ON FOURTH WRAP
LONGITUDINAL SPIGOT GAGES 1 – 6 (TYP)
PRESTRESSING WIRE GAGES 13 – 15 ON FIRST WRAP
90° APPROX.
90° APPROX.
90° APPROX.
90° APPROX.
CIRCUMFERENTIAL SPIGOT GAGES 7 – 12 (TYP)
PRESTRESSING WIRE GAGES 13 – 15 ON THIRD WRAP
PRESTRESSING WIRE GAGES 13 – 15 ON SECOND WRAP
GAGES 1 – 12 ON SPIGOT
GAGE 13 (TYP)
12"
12"
4'-8 1/4"
GAGE 14 (TYP)
TEST PIPE A
GAGE 15 (TYP)

FIG. 3.—Strain-Gage Locations Around Pipe Circumference (1 in. = 25.4 mm; 1 ft = 304.8 mm)

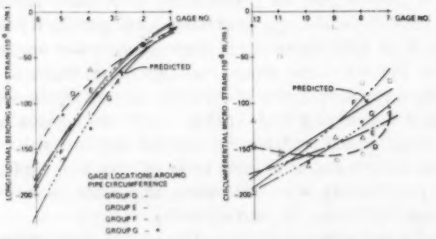

FIG. 4.—Typical Longitudinal Bending and Circumferential Strains Induced in Steel Spigot Ring from a Layer of Prestressing Wire (1 in./in. = 1 mm/mm)

in the gage attachment to the gage meter following each application of each layer of prestressing wire.

Pressure Test

A diagram of the pressure test setup is shown in Fig. 5. Pipe A, with the strain-gaged spigot ring, is on the bottom.

An inside displacement tube, leaving a 1-in. (25-mm) clearance between its outside diameter and the pipe's inside diameter, was used to minimize end thrust in the bulkheads of the test setup. Special floating ring bulkhead sealing components were used to approximately match adjacent pipe joint stiffness on the top and bottom bulkheads. Details are shown in Fig. 6.

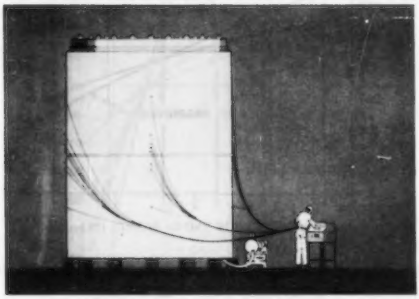

FIG. 5.—Pressure Test Setup

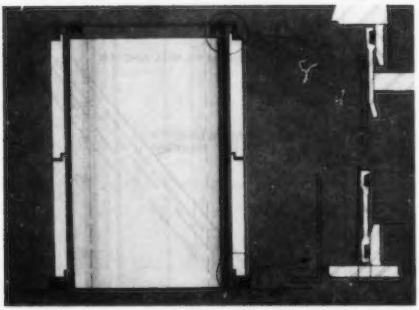

FIG. 6.—Detail Diagram Showing Components of Displacement Tube Bulkhead Parts

Predicted versus actual longitudinal bending strains in the spigot after being joined to the bell, assuming a 200-lb/in. (35.7-kg/cm) gasket load are plotted in Fig. 7.

Predicted versus actual values of tensile strain in the prestressing wires versus internal pressure is plotted for selected gages in Fig. 8. These pertain to the first full pressure cycle. The predicted values are conservative.

Predicted versus actual longitudinal bending strains in the steel spigot ring due to internal pressure are plotted in Fig. 9 for up to 450 psi (3,100 kPa) of internal pressure.

At slightly over 450 psi (3,100 kPa), yielding of the spigot ring occurs. This is shown quite dramatically in Fig. 10. In this figure, the predicted yield strain plot is not a set value because there are residual strains in the spigot due

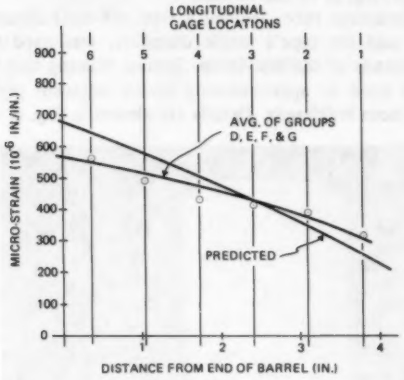

FIG. 7.—Predicted Versus Actual Longitudinal Bending Strain in Steel Spigot Ring Due to Joining (1 in./in. = 1 mm/mm; 1 in. = 25.4 mm)

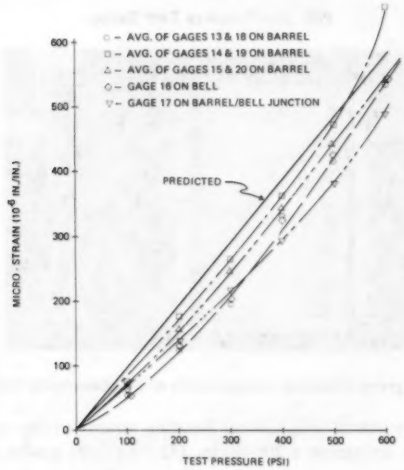

FIG. 8.—Predicted Versus Actual Prestressing Wire Strains Due to Pressure (1 in./in. = 1 mm/mm; 1 psi = 6.8948 kPa)

to manufacture and joining that are present prior to pressure tests. At the 600-psi (4,137-kPa) pressure level, excessive spigot yielding occurred. This was clearly evident after the test pipes were pulled apart and there was seen a pronounced bulge in the spigot ring.

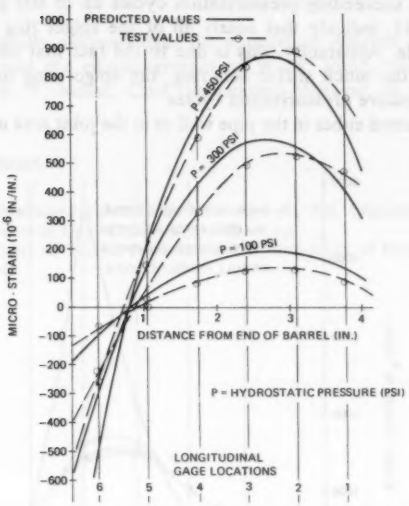

FIG. 9.—Predicted Versus Actual Longitudinal Bending Strains in Steel Spigot Ring Due to Internal Pressure (1 in./in. = 1 mm/mm; 1 psi = 6.8948 kPa)

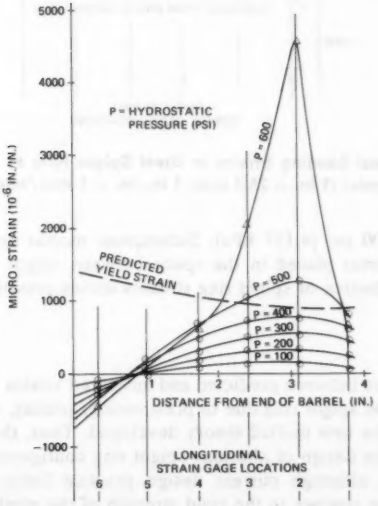

FIG. 10.—Longitudinal Bending Stresses in Steel Spigot Ring Due to Internal Pressure (1 in. = 25.4 mm; 1 in./in. = 1 mm/mm; 1 psi = 6.8948 kPa)

Interestingly, succeeding pressurization cycles up to 600 psi (4,137 kPa), as shown in Fig. 11, indicate that nearly all of the spigot ring yielding occurred in the first cycle. Apparently, this is due to the fact that once the spigot ring yielded out to the much stiffer bell ring, the spigot ring had no more room to yield in successive pressurization cycles.

No leaks occurred either in the pipe wall or in the joint area up to the maximum

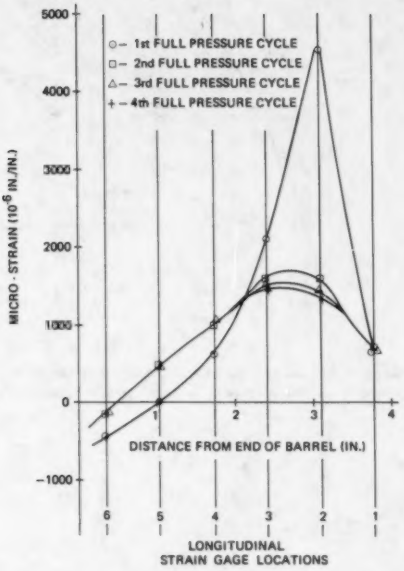

FIG. 11.—Longitudinal Bending Strains in Steel Spigot Ring at 600 psi (4,137 kPa) for Four Pressure Cycles (1 in. = 25.4 mm; 1 in./in. = 1 mm/mm)

test pressure of 600 psi (4,137 kPa). Subsequent mortar grouting of the test pipe joint with mortar placed in the space between spigot ring and bell ring showed further reduction of spigot ring stresses during pressurization.

Conclusions

A good correlation between predicted and measured strains in the prestressing wire and in the steel spigot ring due to prestressing, joining, and pressurization appears to verify the new unified theory developed. Thus, the new theory may be safely used in the design of alternate spigot ring configurations.

It is noted that although current design practice limits steel spigot ring longitudinal bending stresses to the yield strength of the steel, such a limitation is not necessary. After a spigot ring yields and contacts the bell ring, no more yielding can take place, and the joint should even be tighter because of yielding.

Acknowledgment

The writer gratefully acknowledges the support of Ameron who sponsored the test program and the encouragement of W. R. Dana, Vice President of Engineering and K. F. Miller, Civil Engineering Manager, in the preparation of this report.

Appendix I.—References

1. *The Design of Prestressed Concrete Cylinder Pipe PC-100,* Engineering Library No. 1–3, Ameron, Monterey Park, Calif., July, 1975.
2. Hetenye, M., *Beams on Elastic Foundation,* The University of Michigan Press, Ann Arbor, Mich., 1946.

TRANSPORTATION ENGINEERING JOURNAL

PERMEABILITY OF LIME STABILIZED SOILS

By Nagih M. El-Rawi[1] and Amir A. A. Awad[2]

(Reviewed by the Highway Division)

INTRODUCTION

Many soil types can be stabilized economically with lime. Soil-lime mixtures may be used as a sub-base or base course for roads, airfields, parking lots, highway shoulders, and similar applications (1,2). Soil stabilization with lime has a good prospect in Iraq as limestone deposits are available in a number of areas throughout the country and the weather is suitable for this type of stabilization (3,4).

The improvements in the engineering properties of a soil as lime is added are attributed to two basic reactions (2):

1. Colloidal-type reactions which occur almost immediately and result in immediate changes in soil plasticity, workability, and swell properties (5). It involves one of the following: (1) Ion exchange of calcium for the ion carried by the soil; (2) depression of the double layer on the soil colloids as a result of the increased cation concentration in the pore water; and (3) expansion of the double layer of the soil colloids from the high pH of lime.
2. Pozzolanic reactions between the lime with the available reactive alumina or silica in the soil, or both.

When lime is added to a fine grained soil, it generally increases the plasticity index of low plasticity soils and decreases the plasticity of cohesive soils. They become friable and easy to work (6,7). Lime reduces the maximum dry density and increases the optimum moisture content of clayey soils at a given compactive effort (4,7,8). The swelling characteristic of the soil is reduced and the shrinkage limit is increased when lime is added (6). The strength properties of Iraqi soils are improved when stabilized with lime (9,10,11).

[1]Asst. Prof., Dept. of Civ. Engrg., Coll. of Engrg., Univ. of Baghdad, Baghdad, Iraq.
[2]Asst. Instr., Inst. of Tech., Baghdad, Iraq.

Note.—Discussion open until June 1, 1981. To extend the closing date one month, a written request must be filed with the Manager of Technical and Professional Publications, ASCE. Manuscript was submitted for review for possible publication on April 3, 1980. This paper is part of the Transportation Engineering Journal of ASCE, Proceedings of the American Society of Civil Engineers, © ASCE, Vol. 107, No. TE1, January, 1981. ISSN 0569-7891/81/0001-0025/$01.00.

Permeability.—Permeability is a measure of the ease with which a fluid passes through a material. It is one of the fundamental engineering properties of a soil. It enters into almost all seepage, settlement, and stability calculations.

The coefficient of permeability is used to indicate the permeability of soils (12,13). The coefficient of permeability for a given soil depends on particle diameter, properties of the pore fluid, the void ratio, the shape and arrangements of the pores and of the soil particles, and the amount of undisolved gas in the pore water (14,15,16,17).

The permeability of compacted soils varies with the molding water content. On dry side of optimum moisture content the permeability is high due to the flocculant soil structure and the low density. A marked decrease in permeability accompanies the increase in molding water content on the dry side of the optimum.

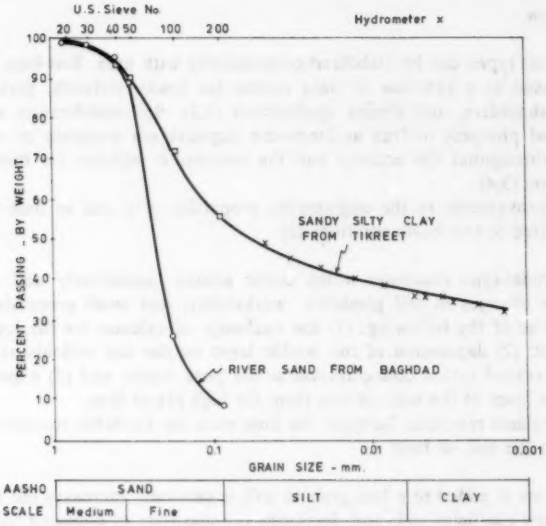

FIG. 1.—Grain Size Distribution

The permeability reaches a minimum at or slightly above the optimum moisture content, after which a slight increase in permeability occurs. The large decrease in permeability with increasing molding water content on the dry side of the optimum is caused by the orientation of the clay-size particles. Wet of optimum, the permeability increases slightly because the effects of a decreasing dry density more than offset the effects of the particle orientation (2,14,16,18).

When lime is added to a clayey soil, the soil becomes flocculated and the permeability increases. In granular soils, the lime reduces the void ratio and the permeability.

The purpose of this paper is to investigate the validity of this hypothesis. The effect of lime on the permeability of two compacted Iraqi soils was

investigated. The effects of such factors as lime content, molding moisture content, and curing age on the coefficient of permeability were investigated.

Materials Used

Soils.—Two soils were used, i.e., a poorly graded fine river sand from Baghdad which is typical of Iraqi river sands, and a sandy silty clay from Tikreet. Fig. 1 shows the grain size distribution of the two soils. Some of the properties

TABLE 1.—Soil Properties

Variable (1)	Sample Number 1 (2)	Sample Number 2 (3)
Location	Baghdad	Tikreet
Unit weight of solids	2.66	2.69
Atterberg limits		
liquid limit, in percent	—	28
plastic limit, in percent	—	18
plasticity index, in percent	N.P.	10
Soil description	poorly graded, gray, fine, river sand	reddish-brown sandy silty clay

TABLE 2.—Chemical Analysis of Lime

Oxide (1)	By weight, in percent (2)
CaO	64.96
SO_3	7.58
MgO	0.71
Al_2O_3	0.64
SiO_2	0.53
Na_2O	0.32
Fe_2O_3	0.16
Loss on ignition	24.70

of the soils are given in Table 1.

Lime.—Hydrated lime manufactured from limestone deposits from Heet area was used throughout this investigation. Table 2 gives the chemical analysis of the lime used.

Water.—Ordinary drinking water was used to mold specimens at various moisture contents. Distilled water was used for the permeability tests.

Compaction.—The standard Proctor compaction hammer and mold was used to prepare 4 in. (10.1 cm) diam by 4.6 in. (11.7 cm) high specimens of the river sand. The soil was compacted in three layers with 25 blows/layer. The height of fall was 12 in. (30 cm) using a 5.5 lb (2.5 kg) drop hammer.

Smaller specimens with 2.8 in. (7.1 cm) diam and 1.1 in. (2.8 cm) high using

a model hammer of 1.8 lb (0.82 kg) with drop height 8 in. (20 cm), were prepared of the sandy silty clay. The compactive effort was equivalent to that of standard Proctor compaction test. It was observed that the maximum dry density using the model hammer was 5% less than that of the standard Proctor test. The optimum moisture content of the raw soil was about the same as shown in Fig. 2.

Specimen Preparation.—The required amount of lime (percent of the dry weight of the soil) was mixed with the oven dried pulverized soil. Water for the compaction was than added. After compaction the specimens and the molds were wrapped in cellophane paper and sealed with paraffin wax and stored in a curing room at 100% relative humidity. After the curring and after the wax had been removed, the permeability was determined using the compaction cylinder as part of the permeameter to reduce the disturbance along the edges of the specimens if they are removed from the compaction cylinder.

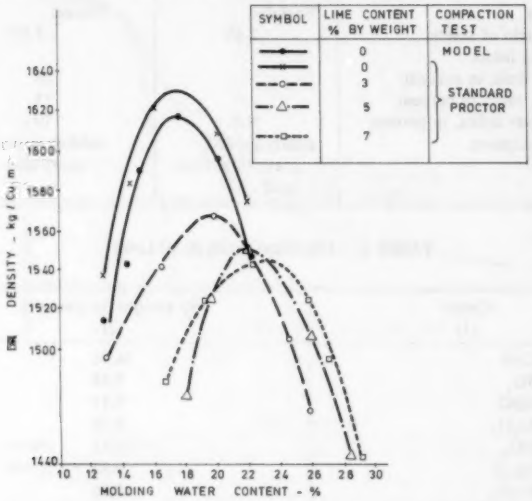

FIG. 2.—Effect of Lime Content on Compaction Properties of Soil from Tikreet

Permeability Tests.—The compaction cylinder was used as permeameter as mentioned before. A falling head permeability test was used throughout this investigation. The clayey soil specimens were subjected to a pressure of up to 5 kg/cm^2 for 6 h before the start of the tests to saturate the specimens (19). The tests were carried out according to British Standards No. 1377-1975 and at room temperature of 25°C. The values reported were the average of three tests.

Results

River Sand.—The maximum dry density of the compacted river sand increased with increasing lime content as shown in Fig. 3(*a*). This was expected since

the river sand was uniformly poorly graded.

The permeability tests on the samples which were investigated just after the addition of lime were carried out 2 h after the molding. This time was needed to saturate the samples.

Immediate Tests.—The following results were obtained from the tests carried out 2 h after molding:

1. The permeability was relatively high on the dry side of the optimum water content. It decreased with increasing molding water content reaching a minimum

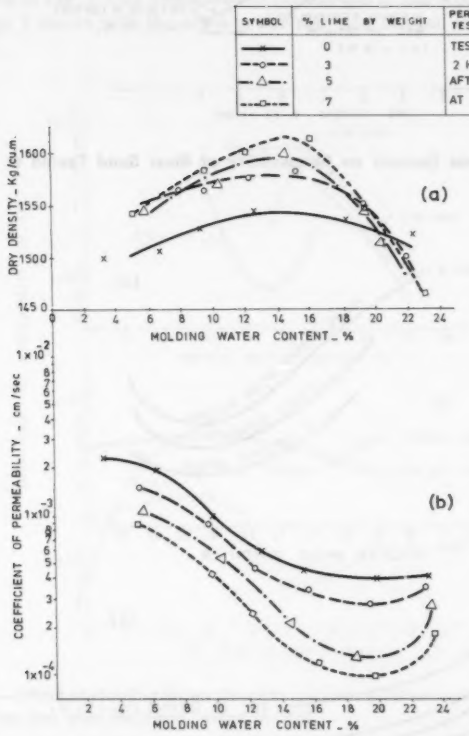

FIG. 3.—Effect of Molding Water Content and Lime Content on Permeability of River Sand

value slightly wet of optimum, after which the permeability increased as shown in Fig. (3*b*).

2. The permeability decreased with the increasing lime content for all investigated water contents as shown in Fig. 3(*b*) and 4. The lime acted as a filler plugging the voids and reduced the flow channels in the mixture.

3. The specimens molded on the dry side of the optimum had a higher

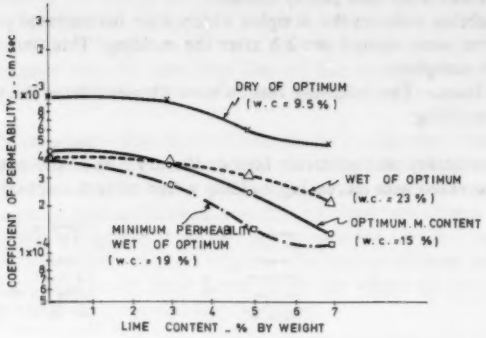

FIG. 4.—Effect of Lime Content on Permeability of River Sand Tested at 25°C 2 h after Molding

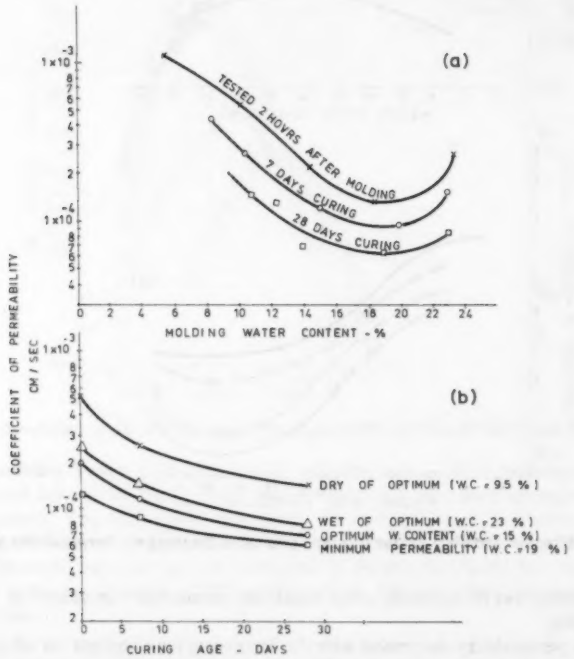
(a)
TESTED 2 HOVRS AFTER MOLDING
7 DAYS CURING
28 DAYS CURING
MOLDING WATER CONTENT - %
COEFFICIENT OF PERMEABILITY
CM / SEC
(b)
DRY OF OPTIMUM (W.C = 9.5 %)
WET OF OPTIMUM (W.C. = 23 %)
OPTIMUM W. CONTENT (W.C. = 15 %)
MINIMUM PERMEABILITY (W.C. = 19 %)
CURING AGE - DAYS

FIG. 5.—Influence of Curing Age on Permeability of River Sand +5% Lime by Weight at Different Molding Water Content when Tested at 25°C

permeability than the specimens prepared wet of optimum as indicated in Fig. 4. There is a certain molding water content that produces a minimum permeability for all investigated lime contents. This water content was 19%, which is 4% higher than the optimum water content for this soil-lime mixture.

Cured Specimens.—For the soil-lime specimens which were cured at 100% humidity and at 25°C, the following results were obtained:

1. The permeability was reduced with curing age at all molding water contents as shown in Fig. 5. One hypothesis to explain this is that when the lime hydrates with age it reacts with the silica in the soil, and the gel will grow with curing

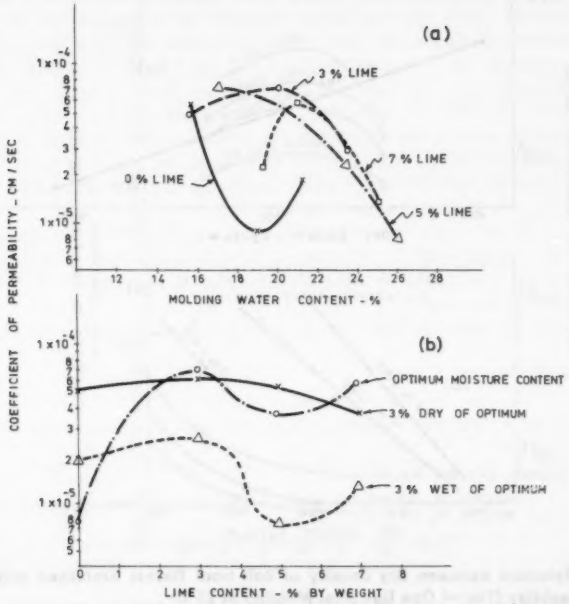

FIG. 6.—Effect of Molding Water Content and Lime Content on Permeability of Tikreet Soil (One Day after Molding) Tested at 25°C

age filling the voids. The decrease in permeability could also be due to the precipitation of calcium carbonate in the voids as the ionized calcium reacts with the dissolved carbon dioxide in the water.

2. There exists a molding water content at which the permeability is a minimum regardless of curing age. This molding water content is about 4% higher than the optimum moisture content as shown in Fig. 5(*a*).

Sandy Silty Clay.—When lime was added to the clayey soil, the maximum dry density decreased and the optimum moisture content increased with increas-

ing lime content as shown in Fig. 2. This agrees with other results reported in the literature (2,4,9). The permeability tests on the compacted clayey soil-lime mixture gave the following results:

1. The permeability of the compacted soil without lime decreased with increasing molding water content. It reached a minimum at a water content slightly on the wet side of the optimum moisture content. The permeability increased when the water content was increased further as shown in Fig. 6(*a*). This agrees well with the results reported from other tests in the literature.

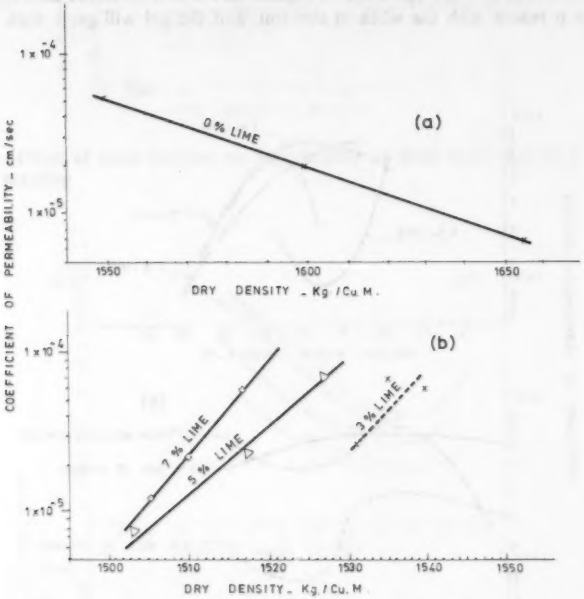

FIG. 7.—Relations between Dry Density of Soil from Tikreet Stabilized with Lime and Permeability (Tested One Day after Molding at 25°C)

The density was low dry of optimum and the soil is flocculated, thus the permeability is high. As the molding moisture content increased the density increased and the soil particles become more oriented resulting in a less permeable soil. When the moisture content increased further (wet of optimum), although the soil particles are well oriented (dispersed structure), the permeability increases as shown in Fig. 6(*a*). This is due to the low density wet of optimum.

2. When lime was added, the soil became flocculated. When gel formed around the soil particles, the soil particles grew in size and the voids in the mixture increased compared with raw soil. Therefore the permeability of the soil-lime mixture was higher than that of the original clayey soil without lime as shown in Fig. 6(*a*).

3. At 3% and 7% lime there was a molding water content at which the permeability reached a maximum. This molding water content was identical to the optimum moisture content for that soil-lime mixtures as shown in Figs.

4. Fig. 6(*b*) indicates that lime content did not affect much the permeability of soil-lime mixtures dry of optimum. This is probably because the soil already has a flocculated structure. The largest effect of the lime on permeability occurred at the optimum moisture content. The coefficient of permeability of specimens one day after molding increased with the addition of lime up to 3% where the permeability reached a maximum, after which the permeability decreased at 5% lime. It increased again at 7% lime. The effect of lime on the compressive strength showed a similar pattern with a maximum at 3% lime (10,11). Specimens

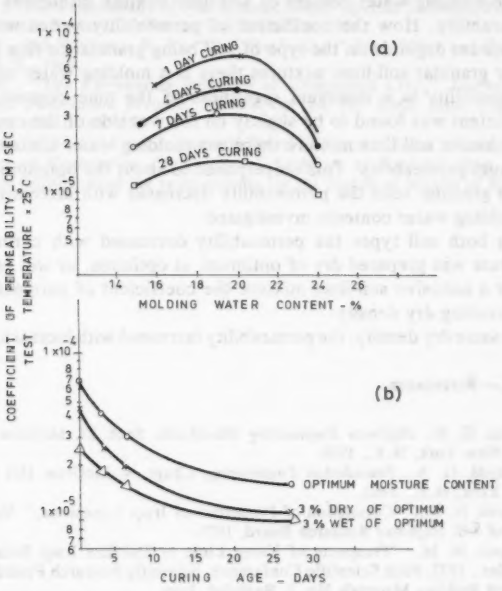

FIG. 8.—Influence of Curing Age and Molding Water Content on Permeability of Soil from Tikreet +3% Lime

which were compacted at wet of optimum moisture content behaved in a similar manner to that compacted at optimum.

5. For compacted soil without lime the coefficient of permeability decreased with increasing dry density as should be expected. When lime was added, the permeability increased with increasing dry density. Fig. 7 indicates a linear trend at 0%, 5%, and 7% lime. At the same dry density the permeability increased with increasing lime content, probably due to the increased flocculation at higher lime contents.

6. The permeability of soil-lime mixture decreased with curing age for all moisture contents tried as shown in Fig. 8.

7. At 3% lime the permeability reached a maximum slightly wet of the optimum molding water content for all curing ages as shown in Fig. 8(*a*).

Conclusions

The following conclusions may be drawn, limited to the soils and test conditions investigated:

1. The permeability characteristics of soil-lime mixture depends on the type of soil. For granular soils the permeability decreases with the addition of lime while for cohesive soils the permeability is increased.
2. The molding water content of soil-lime mixture influences the coefficient of permeability. How the coefficient of permeability varies with the molding water content depends on the type of soil being granular or fine grained.
3. For granular soil-lime mixtures there is a molding water content at which the permeability is a minimum regardless of the lime content. This molding water content was found to be slightly on the wet side of the optimum.

For cohesive soil-lime mixture there is a molding water content that produces a maximum permeability. This corresponds to about the optimum water content.

4. For granular soils the permeability decreases with increasing lime content at all molding water contents investigated.
5. For both soil types the permeability decreased with curing age whether the mixture was prepared dry of optimum, at optimum, or wet of optimum.
6. For a cohesive soil-lime mixture the coefficient of permeability increased with increasing dry density.

At the same dry density, the permeability increased with increasing lime content.

Appendix.—References

1. Woods, K. B., *Highway Engineering Handbook*, Sect. 21, McGraw Hill Book Co., Inc., New York, N.Y., 1960.
2. Leonards, G. A., *Foundation Engineering*, Chapt. 4, McGraw Hill Book Co., Inc., New York, N.Y., 1962.
3. El-Rawi, N. M., "Correlation of Properties of Iraqi Limestone," *Highway Research Record 447*, Highway Research Board, 1973.
4. El-Rawi, N. M., "Prospects of Using Lime to Stabilize Iraqi Soils," presented at the Mar., 1972, First Scientific Conference, Scientific Research Foundation, Engineering and Building Materials No. 2, Baghdad, Iraq.
5. Thompson, M. R., "Lime-treated Soils for Pavement Construction," *Journal of the Highway Division*, ASCE, Vol. 94, No. HW2, Proc. Paper 6249, Nov., 1968, pp. 191–217.
6. Mateous, M., "Soil-lime Research at Iowa State University," *Journal of the Soil Mechanics and Foundation Division*, ASCE, Vol. 90, No. SM2, Proc. Paper 3847, Mar., 1964, pp. 127–153.
7. Marks, B. D., and Haliburton, T. A., "Effects of Sodium Chloride and Sodium Chloride-lime Admixtures on Cohesive Oklahoma Soils," presented at the 1970, 49th Annual Meeting of the Highway Research Board.
8. Ladd, C. C., Moh, Z. C., and Lambe, T. W., "Recent Soil-lime Research at the Massachusetts Institute of Technology," presented at the Jan., 1960, 39th Annual Meeting of the Highway Research Board.
9. El-Rawi N. M., and Najem-El-Dean, A., "Use of pH values to Find the Lime Content Required to Stabilize Iraqi Soils," *Al-Muhandis*, Vol. 15, No. 1, Serial No. 45, Baghdad, Iraq, Nov., 1971.

10. Sabbagh, M. Y., "Effect of Lime on Strength of Iraqi Soils," thesis presented to the College of Engineering, University of Baghdad, at Baghdad, Iraq, in July, 1973, in partial fullfillment of the requirements for the degree of Master of Science.
11. Said, N. K., "Effect of Methods of Compaction on Strength of Soil-lime Mixtures," thesis presented to the College of Engineering, University of Baghdad, at Baghdad, Iraq, in June, 1974, in partial fulfillment of the requirements for the degree of Master of Science.
12. Taylor, D. W., *Soil Mechanics*, John Wiley and Sons, Inc., New York, N.Y., 1948.
13. Harr, M. E., *Groundwater and Seepage*, McGraw Hill Book Co., Inc., 1962.
14. Michaels, A. S., and Lin, C. S., "Permeability of Kaolinite," *Industry and Engineering Chemistry*, Vol. 46, 1954.
15. Michaels, A. S., and Lin, C. S., "Effects of Counter Electro-Osmosis and Sodium Ion Exchange on the Permeability of Kaolinite," *Industry and Engineering Chemistry*, Vol. 47, 1955.
16. Lambe, T. W., "The Permeability of Fine Grained Soils," *Special Technical Publication No. 163*, American Society for Testing and Materials, 1954.
17. Lambe, T. W., and Whitman, R. V., "*Soil Mechanics*," John Wiley and Sons, Inc., New York, N.Y., 1969.
18. Lambe, T. W., "The Engineering Behavior of Compacted Clay," *Journal of Soil Mechanics and Foundation Division*, ASCE, Vol. 84, No. SM2, Proc. Paper 1655, May, 1958, pp. 1655-1–1655-35.
19. Awad, A. A. A., "Effect of Lime on Permeability of Compacted Soils," thesis presented to the College of Engineering, University of Baghdad, at Baghdad, Iraq, in Apr., 1977, in partial fulfillment of the requirements for the degree of Master of Science.

TRANSPORTATION ENGINEERING JOURNAL

TAX ALLOCATION FORMULAS BY STEPWISE REGRESSION

By Lansford C. Bell,[1] M. ASCE and Russell D. Shelton[2]

(Reviewed by the Highway Division)

INTRODUCTION

A significant source of operating capital for city and county road programs is statewide gasoline or motor fuel tax revenues. A portion of the statewide revenue is typically distributed to a county, city, or other local municipality according to its population, road mileage, surface area, traffic volume, or some combination of these or other variables.

In 1979, legislation was introduced in 25 states to increase a statewide gasoline tax (7). Some of the legislation introduced in 1979 contained provisions for altering the distribution formulas that provide revenue to local road programs. A bill containing provisions to alter Alabama's distribution formula was considered and then rejected by committee action during the 1979 legislative session. Similar proposals in a number of other states have been reported to the writers.

Revenue distribution formulas have evolved over the years as the result of political compromise with little or no attempt at rational analysis. Many distribution formulas are outdated in that they were established at a time when there was a pressing need to construct new roads in rural areas to facilitate transporting agricultural products into urban market centers. Today, however, a great percentage of local road expenditures go toward roadway maintenance, bridge replacement and repair, and safety improvements.

A previous research project conducted at Auburn University (3) compiled data on the current condition of Alabama's secondary or county road system. The research results cited a need for a \$0.04/gal increase in the statewide gasoline tax, assuming the counties were to continue receiving 55% of all collected revenue. It became apparent during the course of the research, however, that

[1]Assoc. Prof., Dept. of Civ. Engrg., Auburn Univ., Auburn, Ala. 36830.
[2]Grad. Research Asst., Dept. of Civ. Engrg., Auburn Univ., Auburn, Ala. 36830.

Note.—Discussion open until June 1, 1981. To extend the closing date one month, a written request must be filed with the Manager of Technical and Professional Publications, ASCE. Manuscript was submitted for review for possible publication on March 28, 1980. This paper is part of the Transportation Engineering Journal of ASCE, Proceedings of the American Society of Civil Engineers, © ASCE, Vol. 107, No. TE1, January, 1981. ISSN 0569-7891/81/0001-0037/\$01.00.

revenue generated by the tax increase would not coincide with the critical needs of the counties if the additional revenue was distributed according to formulas being considered by the state legislature at that time.

A second research project was therefore initiated to develop a formula that best allocated revenue generated by an increase in statewide gasoline tax to Alabama's 67 county road departments. Six variables thought to be predictors of county revenue need were initially selected for possible inclusion in the formula. Stepwise regression techniques were then applied to the data to select the optimum combination of variables and their respective percentages in the formula. Presented herein is an examination of the procedure used to determine proposed allocation formulas and assess their adequacy.

Motor Fuel Tax Allocation Formulas

Specific allocation formulas are used in 35 states to allocate motor fuel tax revenue to county road programs. Specific formulas are used in 33 states to allocate motor fuel tax revenue to cities or other municipalities. The most common variables used in motor fuel allocation formulas are shown in Table 1 (9). It should be noted that most states combine two or more variables in their formula and many states allocate some portion of revenue equally to all counties or municipalities.

TABLE 1.—Variables Used in Distribution of Statewide Motor Fuel Receipts

Variable used to determine part or all of statewide distribution (1)	Number states using variable as part of a distribution formula to counties (2)	Number of states using variable as part of a distribution formula to cities and municipalities (3)
Road miles	15	14
Population	13	23
Vehicle registration or license fees	13	3
Land area	11	—
Revenue	4	5
Need	4	—
Vehicle miles	2	—
Property values	1	2
Farm products sold	1	—
Linear feet of bridges	1	—

A workable tax allocation formula should ideally possess the following characteristics:

1. Variable data should be readily available or inexpensive to tabulate.
2. Variable data should not be subject to manipulation by the local jurisdictions.
3. The formula should not be unnecessarily complex. Linear combinations of variables should be employed unless it can be shown that more complex

expressions result in a higher correlation with revenue need.

4. The formula should be compatible with the purpose for which the tax or tax increase is imposed.

To the writers' knowledge, the only comprehensive investigation of motor fuel allocation formulas was performed in the state of Washington (5,10,11,12). This investigation was conducted by the University of Washington and the State College of Washington using funds provided by the Washington legislature. The research resulted in a formula that distributed revenue to 39 of the state's 41 counties as follows: 10% equally; 30% on the basis of vehicle registration; 30% on the basis of trunk mileage multiplied by the prorated estimated annual cost per trunk mile; 30% on the basis of trunk mileage multiplied by a prorated money need factor. The estimated cost per trunk mile and the money need factor are updated periodically.

The state of Washington has apparently achieved the desired level of coordination between university researchers and a political advisory committee. Recent correspondence from Washington highway officials indicates, however, that changes to achieve a greater degree of formula simplicity are being contemplated.

Multiple Linear Regression

Method.—Multiple linear regression analysis can be used to predict, or estimate the value of one dependent variable from known values of other independent variables. The method involves the assumption of a linear relationship of the form

$$Y = \alpha + \beta_1 X_1 + \beta_2 X_2 + \ldots \beta_k X_k + \epsilon \quad \ldots\ldots\ldots\ldots\ldots\ldots\ldots\ldots (1)$$

in which Y = a linear function of k predictor variables X_1, X_2, ..., X_k. The coefficients α, β and the error term, ϵ, are never known exactly. The researcher therefore postulates a prediction or regression equation of the form:

$$\hat{Y} = a + b_1 X_1 + b_2 X_2 + \ldots + b_k X_k \quad \ldots\ldots\ldots\ldots\ldots\ldots\ldots\ldots (2)$$

in which $\hat{Y}$ = the predicted value of Y; and the regression coefficients a and b = estimates of α and β. The overall goal of regression analysis is to obtain values for the regression coefficients and then perform statistical tests to evaluate the adequacy of the model.

Stagewise regression is a procedure by which a large set of predictor variables can be narrowed down by eliminating variables that do not make significant contributions to the regression equation. Forward elimination, backward elimination, and stepwise regression are techniques for successively examining combinations of predictor variables and then revising the variable set according to predetermined statistical tests.

Fuel Tax Allocation Model.—Consider the case where highway revenue need can be accurately determined or estimated for n counties or political jurisdictions within a state. Assume data defining population, road mileage and other possible need predictors are also available for each county. Regression techniques could then be used to determine which variables in what relative proportion should be included in a linear equation to best distribute fuel tax revenue throughout the state.

An obvious question to be asked is "why not distribute revenue according to need if data reflecting need can be compiled?" The answer is simply that formulas involving predictor variables such as those shown in Table 1 are simple, acceptable to the public and not subject to political manipulation or debate. Revenue need is, however, somewhat subjective and may be a function of local priorities. The need variable employed in the regression analysis should ideally be calculated using weighting factors, priorities or guidelines approved by a state legislative committee, county associations or other designated organizations.

Computer Software.—Multiple regression analysis computer programs are available at most large computing facilities. The BMDP Biomedical Computer Programs (4), the SPSS Statistical Package for the Social Sciences (6), and the SAS Statistical Analysis System (2) are each capable of performing regression analysis and stagewise variable selection. The use of these program packages and their relative merits are also examined in Ref. 13.

Proposed Allocation Formula for Alabama Counties

Model Variables.—Alabama's current fuel tax distribution formula, enacted in 1967, allocates 55% of all statewide \$0.07/gal gasoline tax revenue to the

TABLE 2.—Variables Used in Regression Analysis

Variable (1)	Description (2)
POPL	County population, 1978 estimate
MILE	Miles of county roads, 1978
AREA	Square miles of county land area
VEHR	Total number of vehicles registered in a county, 1978
TRUCKR	Total number of trucks registered in a county, 1978
MTLS	Thousands of tons of timber, coal and other bulk materials mined in a county, 1978
NEED (dependent variable)	\$13,000 times miles of road in need of immediate resurfacing plus cost associated with all bridges in need of immediate replacement

67 counties such that 45% of the counties' share is distributed equally and 55% is distributed on the basis of population. Previous research indicated that legislation proposing an increase in statewide gasoline tax should include an improved allocation formula.

As a first step in deriving a distribution formula for the additional revenue, six predictor variables, defined in Table 2, were identified. The variables POPL, MILE, AREA and VEHR are the variables most commonly used in other states. The variables TRUCKR and MTLS were included because local haulers of timber, coal and other bulk materials have apparently accelerated road deterioration in many counties. Data for each variable were then compiled from various state agencies.

The dependent variable, NEED, was determined from data compiled in a 1979 questionnaire survey of county engineers conducted as part of the research

described in Ref. 3. It was felt that any increase in tax revenue would be spent primarily on resurfacing and bridge replacement. The value of the need variable was therefore computed as $13,000 times the number of miles of road in need of immediate resurfacing plus the cost associated with all bridges in need of immediate replacement.

Defining need in this manner results in a $307,000,000 total revenue requirement for all counties. This $307,000,000 estimated revenue requirement would be generated in about 5 yr if the current $0.07/gal gasoline tax was raised to $0.11/gal.

Regression Analysis.—The regression analysis model can now be stated as an equation to estimate need as a function of six predictor variables:

$$\text{NEED} = a + b_1(\text{POPL}) + b_2(\text{MILE}) + b_3(\text{AREA}) + b_4(\text{VEHR}) + b_5(\text{TRUCKR}) + b_6(\text{MTLS}) \quad \ldots (3)$$

in which NEED = the estimated revenue requirement for a given county; and the coefficients a, b_1, b_2, ... b_6 are to be determined by regression analysis.

To obtain an equation in terms of only those variables that contribute significantly to the prediction of revenue need, variable data were entered into the BMDP1R stepwise regression computer program. Variables are entered or removed by performing partial F tests which determine if H_o:$\beta_i = 0$ should be rejected at some stage in the variable selection procedure. When H_o cannot be rejected it is giving the same information as some other predictor variable in the formula. The level of significance at which a variable is entered or removed is determined by the program user. A significance level of $\alpha = 0.05$ was used herein. For additional information relating to statistical tests, variable selection and program controls the reader is referred to Ref. 1, 4, 8, and 13.

An initial program execution produced the regression equation:

$$\text{NEED} = \$552{,}320 + 20.1(\text{VEHR}) + 3{,}590(\text{MILE}) \quad \ldots (4)$$

in which NEED = the predicted allocation to a given county in units of dollars.

Removing VEHR from the data set in an attempt to obtain a formula in terms of the five remaining variables results in the regression equation:

$$\text{NEED} = \$750{,}180 + 125(\text{TRUCKR}) + 2{,}960(\text{MILE}) \quad \ldots (5)$$

And finally, removing TRUCKR from the data set in an attempt to formulate an equation in terms of POPL, MILE, AREA, and MTLS results in:

$$\text{NEED} = \$415{,}420 + 14.10(\text{POPL} + 3{,}840(\text{MILE}) \quad \ldots (6)$$

It is interesting to note that MTLS and AREA were not selected for entry into Eqs. 4–6. There is therefore a 95% confidence that these variables do not contribute significantly to the estimation or prediction of need.

Formula Adequacy.—Two standard statistical parameters can be calculated to assess formula adequacy or compare a proposed allocation formula with one in current use. The standard error of the estimate measures the amount that actual need varies from need as predicted by the regression equation. Standard errors associated with Eqs. 4–6 were calculated as $2,430,000, $2,440,000, and $2,450,000, respectively. These values can be interpreted to mean that if $307,000,000 was distributed to 67 counties using Eq. 4, then the allocation

would vary from actual need by $2,430,000 for an average county.

The standard error of the estimate can be used to compare a regression formula to a formula in current use or to other formulas under consideration by a state legislature. Regression Eq. 6 is compared to two such formulas in Table 3. It can be seen that the standard error of the regression equation is significantly less than the standard error of Alabama's current allocation formula.

A second statistic that assesses the overall adequacy of a regression equation is the multiple coefficient of determination, or R^2. Values of R^2 associated with Eqs. 4–6 were within a range of 0.43–0.45 indicating that only 43%–45% of the variation in need can be explained by the regression equation. This could be interpreted as justification for distributing a portion of fuel tax revenues according to documented need when it can be accomplished without political bias or data manipulation.

TABLE 3.—Standard Error of Alternate Allocation Formulas

Allocation formula (1)	Variables (relative weights), as a percentage (2)	Standard error, in millions of dollars (3)
Regression equation	9 (equal distribution) 17 (by population) 74 (by road mileage)	2.45
Traditional 1/3 formula (considered in previous Alabama legislation—not enacted)	33 (by population) 33 (by road mileage) 33 (by land area)	2.81
Alabama's current formula	45 (equal) 55 (by population)	3.38

Eqs. 4–6 employ different variable combinations but produce standard test statistics that are approximately equal because the variables TRUCKR, VEHR, and POPL are highly correlated.

Conclusion

Statewide fuel tax revenues are typically distributed to local jurisdictions on the basis of population, road miles, registered vehicles, and other variables for which data are readily available. Many states are considering legislation to increase statewide fuel taxes but little or no attention has been given to the adequacy of current or proposed allocation formulas.

Multiple linear regression analysis is well suited to the derivation of simple fuel tax allocation formulas that best distribute statewide revenue to local political jurisdictions. Although arbitrarily defined in the analysis performed herein, the dependent variable NEED should ideally be structured with input from legislative advisory committees or county associations.

Six variables that were thought to be related to current county highway needs in Alabama were identified and a regression analysis performed. Three gasoline tax allocation formulas were obtained that would be appropriate for distributing

revenue generated from a proposed increase in Alabama's statewide gasoline tax.

The degree of improvement associated with an allocation formula derived by regression techniques is best measured by the standard error of the estimate. For a total allocation of $307,000,000 to Alabama counties and the assumed definition of need, a typical regression equation improves the error in allocation to an average county by ($3,380,000–$2,450,000) or $930,000.

Acknowledgments

This research was supported in part by a grant from the Auburn University Engineering Experiment Station.

Appendix I.—References

1. Afifi, A. A., and Azen, S. P., *Statistical Analysis: A Computer Oriented Approach*, Academic Press, Inc., New York, N.Y., 1972.
2. Barr, A. J., et. al., *A Users Guide to SAS 76*, SAS Institute Inc., Raleigh, N.C., 1976.
3. Bell, L. C., "An Assessment of Alabama's Secondary Road System," Association of County Commissions of Alabama, Montgomery, Ala., Apr., 1979.
4. Dixon, W. J., ed., *Biomedical Computer Programs: P Series*, University of California Press, Berkeley, Calif., 1979.
5. Goff, H., "Cost Factor Study," Report Prepared for Washington State Association of Counties, 1978.
6. Nu, N. H., *SPSS: Statistical Package for the Social Sciences*, McGraw-Hill Book Co., Inc., New York, N.Y., 1975.
7. Reed, M. F., "What's Happening to State Highway Finance?," Highway Users Federation, Washington, D.C., July, 1979.
8. Shelton, R. D., Jr., "Development of a Distribution Formula for the Allocation of Fuel Tax Revenue Using Regression Techniques," thesis presented to Auburn University, at Auburn, Ala., in 1980, in partial fulfillment of the requirement for the degree of Master of Science.
9. *Highway Statistics 1977*, United States Department of Transportation, Federal Highway Administration, Washington, D.C.
10. "County Gas Tax Allocation Study," Washington State University, College of Engineering Research Division, Report Prepared for the Joint Committee on Highways, Pullman, Wash., 1954.
11. "Continuation Study of County Gas Tax Fund Allocation," Washington State University, College of Engineering Research Division, Report Prepared for the Joint Committee on Highways, Pullman, Wash., 1956.
12. "Cost Factor Adjustment," Washington State University, College of Engineering Research Division, Report Prepared for the Joint Committee on Highways, Pullman, Wash., 1965.
13. Younger, M. S., *Handbook for Linear Regression*, Duxbury Press, North Scituate, Mass., 1979.

Appendix II.—Notation

The following symbols are used in this paper:

a = constant in regression equation;
b = coefficient in regression equation;
X = independent variable;

Y = dependent variable in linear model;
$\hat{Y}$ = dependent variable in regression equation;
α = constant in linear model;
β = coefficient in linear model; and
ϵ = error term in linear model.

Subscripts

k = number of predictor variables used in regression equation.

TRANSPORTATION ENGINEERING JOURNAL

SOIL-PIPE INTERACTION AND PIPELINE DESIGN[a]

By Syed Ahmed,[1] A. M. ASCE, Ralph W. McMickle,[2] and Carl L. Brassow,[3] A. M. ASCE

(Reviewed by the Pipeline Division)

INTRODUCTION

The sizing of straight segments of buried pipelines is based on conventional analysis methods. The line is first sized to react to internal pressure using the well-known relationship for hoop stresses:

$$\sigma_H = \frac{Pr}{t} \quad \ldots \ldots \ldots

in degrees Fahrenheit or degrees Celsius; and μ = Poisson's ratio.

For designs with high temperature differentials, the critical stress is usually the principal shear stress (τ_{max}) which is obtained from the relationship:

$$\tau_{max} = \frac{\sigma_H + \sigma_L}{2} \quad \ldots \ldots \ldots

$$F = PA + A_s(E\alpha\Delta T - \mu\sigma_H) \quad \ldots\ldots\ldots\

since the moments and shears associated with movement large enough to significantly decrease the resultant end force would yield critical pipe stresses.

From Fig. 2 it is apparent that the resistance to the thrust force at a bend is reacted by a combination of the structural strength of the pipe as well as the backfill soil resistance. Since the mobilization of soil resistance depends on pipe movement, insufficient lateral movement of a very rigid pipe may not take advantage of the available backfill resistance. On the other hand, excessive lateral movements may cause a failure of the backfill and the eventual separation of the pipe from the surrounding soil. Continued use of the pipeline under these circumstances may overstress the pipe bend structurally.

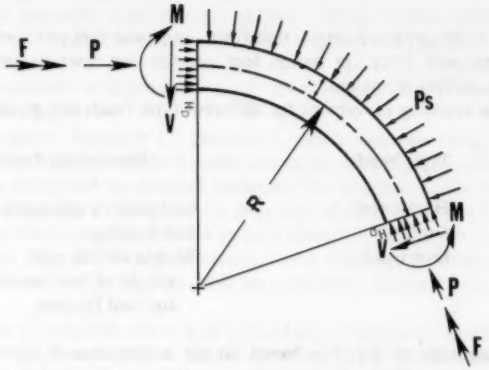

FIG. 2.—Free Body Diagram of Pipe Bend with Movement

This study makes reference to horizontal bends but the conclusions apply equally to overbends and sagbends.

Analytical Model

A finite-element approach was used to analyze the pipe-soil interaction. The computer program described by Radhakrishnan and Jones (6) was adapted to the problem in the following manner.

1. It was recognized that the actual radial force shall vary along the length of the bend in a three dimensional manner. However, a two-dimensional analysis on a 1-ft long section of the bend subjected to maximum radial force per foot was considered satisfactory. The weight of steel and the weight of oil in the 1-ft long section of the pipe bend were combined and divided by the total volume of the 1-ft long pipe section to arrive at a density of a material which was a mathematical equivalent of the previously mentioned two components. Other parameters were assigned to this mathematically equivalent ficticious material consistent with the nonlinear model described in the following paragraphs. The cross section of the pipe was idealized by a number of straight line segments since the program does not incorporate curved lines. The pipe-soil interaction

force (P_s) calculated was distributed equally among the nodes of the finite-element mesh within the pipe sections. A typical finite-element mesh is shown in Fig. 3; the arrows identify the nodes carrying the pipe soil interaction force, P_s.

2. The soil enveloping the pipe bend was modeled as a continuum of one material by assigning parameters representative of their type determined by laboratory testing. The nonlinearity of the stress-strain relationship was modeled by hyperbolic transformation as suggested by Kondner and Zelasko (4) and defined by the following relation:

$$\frac{\epsilon}{(\sigma_1 - \sigma_3)} = a + bE; \quad R_f = \frac{(\sigma_1 - \sigma_3)f}{(\sigma_1 - \sigma_3)\,ult} \quad \ldots\ldots\ldots\ldots\ldots\ldots (6)$$

in which ϵ = strain; σ_1 and σ_3 = major and minor stresses respectively; R_f = the failure ratio of stress difference at failure to the ultimate asymptotic value of the hyperbolic stress strain curve; and a and b = the intercept and slope respectively of the straight line represented by the first part of Eq. 6.

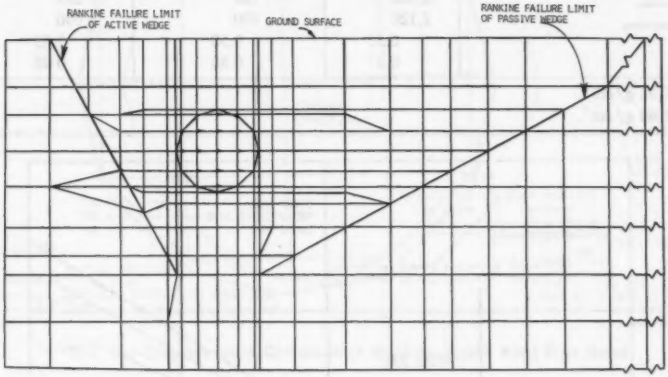

FIG. 3.—Finite Element Mesh of 42-in. (1,067 mm) Pipe Bend

The confining pressure dependency of the stress-strain modulus was modeled in line with Janbu (3), and Duncan and Chang's (2) research as stated by the following relation:

$$E = kPa\left(\frac{\sigma_3}{Pa}\right)^n \quad \ldots\ldots\ldots\ldots\ldots\ldots\ldots\ldots\ldots\ldots\ldots\ldots\ldots\ldots (7)$$

in which E = initial, unloading, or reloading modulus; K = primary loading, unloading, or reloading modulus number; Pa = atmospheric pressure; σ_3 = minor principal stress; and n = the modulus exponent. All the parameters used in the analysis are summarized in Table 1.

The state of stress in the finite-element mesh was studied by utilizing a $\bar{p}$-$\bar{q}$ diagram. The parameters $\bar{p}$ and $\bar{q}$ are functions of effective principal stresses $\bar{\sigma}_1$ and $\bar{\sigma}_3$ as shown in Fig. 4.

The boundaries of the soil continuum were established at a sufficient distance

away from the pipe such that the influence of the radial force on the soil continuum was not affected by them. A relatively small grid (elements) was used in the vicinity of the pipe to closely determine the effect of movement on the backfill nearest to the source of the radial force.

TABLE 1.—Soil Continuum (Backfill) Parameters

Variable (1)	Dense sand (2)	Medium dense sand (3)	Loose sand (4)
Unit weight	120 pcf[a]	100 pcf[b]	100 pcf[b]
Poisson's ratio before failure	0.30	0.30	0.30
Poisson's ratio near failure	0.49	0.49	0.49
Coefficient of lateral earth pressure at rest	0.38	0.43	0.50
Friction angle	38°	35°	30°
Cohesion	0	0	0
$K_{loading}$	2,000	720	295
$K_{unloading}$	2,120	900	1,090
n	0.55	0.50	0.65
R_f	0.87	0.80	0.90

[a] 1.92 g/cm^3.
[b] 1.60 g/cm^3.

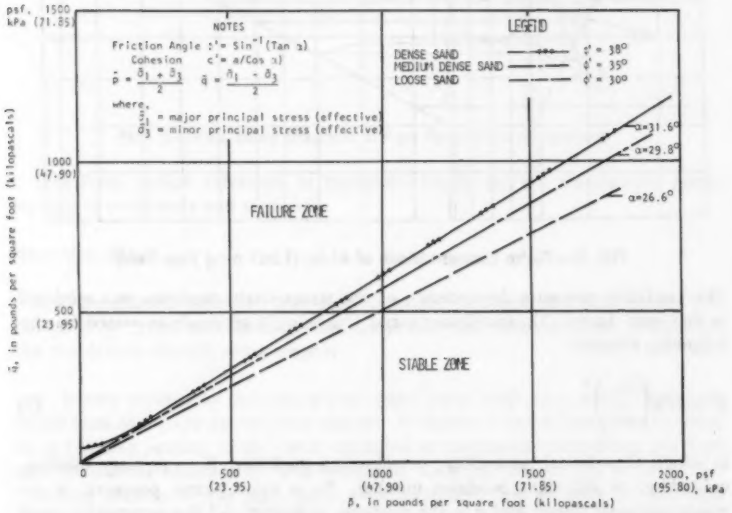

FIG. 4.—Soil Backfill Failure Envelopes

The computer program generates and solves several simultaneous equations for each grid or mesh element under the selected nonlinear constitutive stress-strain relationship in order to calculate stresses and displacements in the soil

backfill continuum. The stresses and displacements obtained for various pipe sizes, radial forces, soil cover, and backfill types were studied to derive the conclusions presented in the following sections.

Effect of Backfill Type

The effect of backfill on the outward radial movement is illustrated by considering three states of sand denseness, namely dense sand, medium dense sand, and loose sand. Their associated properties are given in Table 1, and their failure envelope determined by laboratory tests are depicted in Fig. 4.

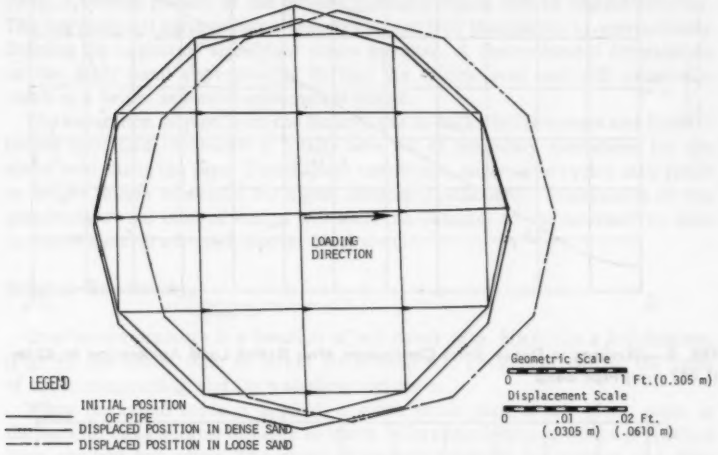

FIG. 5.—Displacement Comparison of 42-in. (1,067 mm) Pipe Bend

A 42-in. (1,067 mm) diam steel pipe bend of 120 ft (36.6 m) radius and 6 ft (1.83 m) of soil cover carrying crude oil at a design pressure of 600 psi (4,134 kPa) was considered to develop an outward radial force of 8,000 lb/ft (116,721 N/m) of the bend. Two types of soil backfill were studied, namely a dense sand and a loose sand, the resulting outward movement of the pipe bend is depicted in Fig. 5 where the displacement scale is magnified five times in relation to the geometric scale. The maximum radial displacements were calculated to be 0.09 in. (2.29 mm) and 0.93 in. (23.62 mm) for the dense sand and loose sand backfill continuums, respectively.

The displacements are directly related to the stresses in any soil continuum. In general, the stresses in the soil backfill elements on the inside of the bend radius will reduce (active case) from the at rest condition (no radial force development), while the stresses in the backfill elements on the outside of the bend will increase (passive case).

The state of stress in the finite-element mesh elements exhibiting a passive case is shown in Fig. 6 and Fig. 7 for the dense and loose sand continuums, respectively, for a single load cycle. In contrast with the dense sand continuum,

the state of stress in a number of elements in the region of significant passive pressure plots above the failure envelope for loose sand continuum for the same radial force, thus indicating unstable conditions. The maximum radial displacement for loose sand was calculated to be more than ten times that

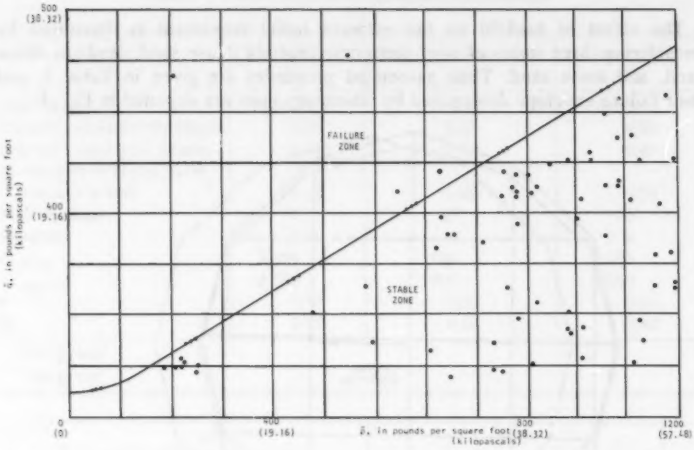

FIG. 6.—Stresses in Dense Sand Continuum after Radial Load Application in 42-in. (1,067 mm) Pipe Bend

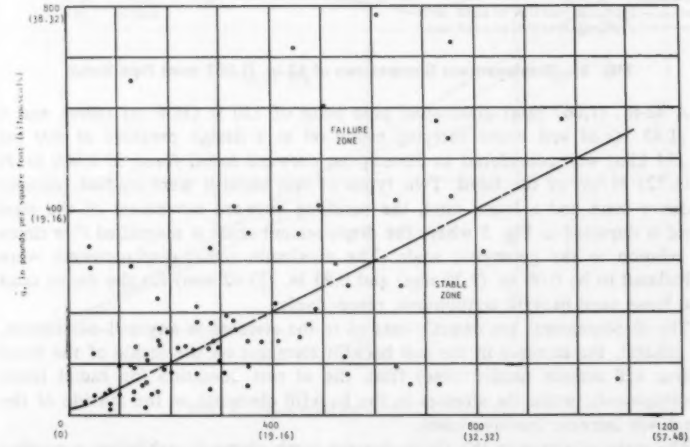

FIG. 7.—Stresses in Loose Sand Continuum After Radial Load Application in 42-in. (1,067 mm) Pipe Bend

of the dense sand. The conclusions about the backfill instability depend on the backfill type alone and are independent of the pipe-bend diameter.

It was observed that the region of significant stress increase was 1–2 diam in front and below the pipe for both dense and loose sand continuums. With reference to Fig. 3 where Rankine passive wedge extends 1 diam below the pipe bottom and intersects the ground surface at approximately 4 diam away from the pipe, it is evident that the region of significant passive pressure development is overestimated when compared with finite-element procedures. If the passive wedge slope were to be drawn such that the wedge intersects the bottom of the pipe, i.e., intersecting the ground at approximately 2 diam away, a critical portion of the passive pressure region will be underestimated. The conventional earth pressure theories do not lend themselves to appropriately defining the region of significant stress increase. A finite-element formulation on the other hand appropriately defines the critical area and will eventually result in a better and more economical design.

The separation of pipe from the backfill due to high displacements and backfill failure condition represents a totally new set of boundary conditions for the stress analysis in the pipe. Under these conditions, successive cycles may result in fatigue failure especially for highly stressed components. Recognition of this possibility at the time of design will alert the designer to use alternatives such as better backfill material, anchor blocks, etc.

Effect of Soil Cover

Overburden pressure is a function of soil cover [Fig. 8(*a*)]. On a $\bar{p}$-$\bar{q}$ diagram (Fig. 4), the initial state of stress for a deep soil cover will plot to the right of the corresponding plot for a shallow soil cover.

When the radial force is applied, a given stress path at any given point in the backfill has a shorter distance to travel before the failure envelope is reached for a shallow soil cover. The mode of backfill behavior for shallow and deep soil covers is schematically represented in Figs. 8(*b*) and 8(*c*).

Analyses were performed for two cases of 16-in. (406 mm) pipe with a 60-ft (18.3-m) bend radius under different soil cover and density conditions. The results were: Case I—3 ft (0.92 m) soil cover, a dense sand backfill, and a radial force of 3,700 lbf/ft (53,984 N/m); and Case II—10 ft (3.05 m) soil cover, a medium dense sand backfill, and a radial force of 4,000 lbf/ft (58,361 N/m). Fig. 9 shows a comparison of displacements for the aforementioned two cases during the first cycle of loading; the displacement scale is magnified 17 times to illustrate the displacement mode. The zone of significant passive pressure development was found to extend approximately 1 diam–3 diam in front and under the pipe for both cases. It extended up to the surface for Case I and up to 3 diam above the pipe for Case II. The results of the analysis showed that even though radial force was approximately equal, the state of stress in a relatively large number of critical elements in the dense sand continuum (which is stronger of the two continuums) plotted above the failure envelope indicated a widespread failure region compared with the medium dense sand where only a few isolated elements of local failure were observed. In the writers' opinions, the comparatively larger displacements and the unstable conditions in the dense sand backfill are the result of the shallow soil cover. As a corollary,

this conclusion also suggests that a stronger backfill continuum is not a replacement for an adequate soil cover.

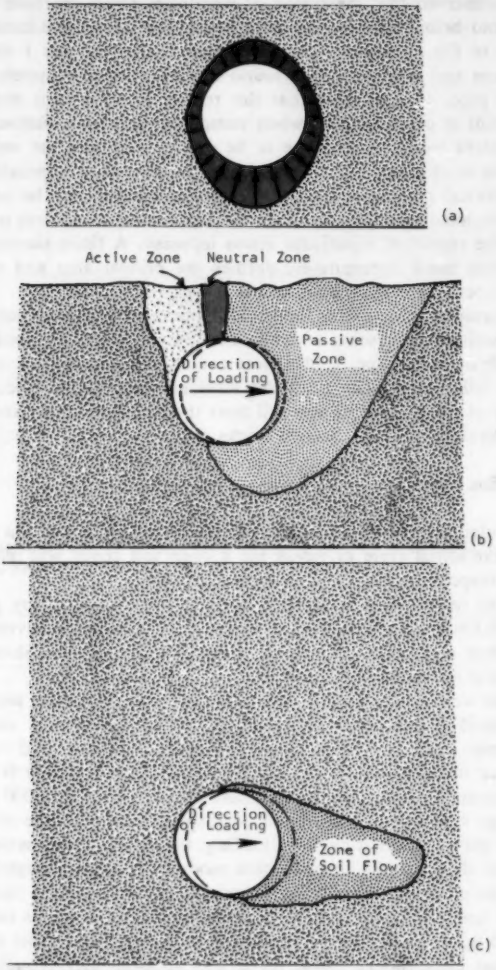

FIG. 8.—Schematic Backfill Behavior: (*a*) At Rest; (*b*) Shallow Soil Cover; and (*c*) Deep Soil Cover

A shallow soil cover may cause pipe overbends to lift out of the ground. Determination of the optimum thickness of soil cover and the suitable backfill type is necessary to make the design cost effective.

PRACTICAL APPLICATION

From a practical application standpoint, the pipe-soil interaction force (P_s) should be computed using Eq. 5 and compared with the appropriate soil resistance available for given subsurface conditions. If the available passive resistance is not adequate, the designer should consider a more sophisticated finite-element analysis to compute the pipe bend movement and the resulting stresses (Fig. 2) for a proper design. Alternatively, an appropriate combination of backfill type and soil cover can be achieved by the finite-element analysis considered in this paper to allow for very small bend movement and design conditions approaching a fully restrained condition (Fig. 1).

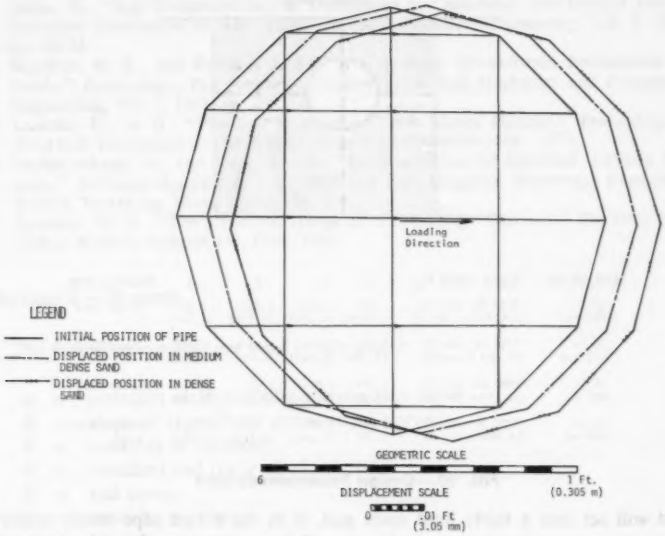

FIG. 9.—Displacement Comparison of 16-in. (406 m) Pipe Bend

Based on this analysis, design recommendations similar to those shown in Fig. 10 developed for this study, should be formulated which would allow tolerable bend movement and design conditions approaching a fully restrained condition (Fig. 1).

It is recognized that achievement of a high quality of compaction is not construction expedient especially if the bends are located in difficult access areas. Furthermore, achievement of the desired compaction level closest to the pipe which is the most critical area is very difficult. As an alternative to compaction, we selected a sample of concrete sand with 15% cement added and mixed it with sufficient water to produce a pumpable slurry. The resulting slurry was left to stand for at least 7 days in triaxial test molds that were about 6 in. (152.4 mm) high and with a 3-in. (76.2-mm) diam to allow the removal

of excess water. Subsequently, these samples were tested in a manner similar to the testing of dense sand (Fig. 4). The resulting failure envelope indicated the cement stabilized sand to be stronger than the dense sand. In our judgement a cement stabilized sand will exhibit bonding or cohesion of particles more than a compacted sand and its angle of internal friction will also be higher thus making it a stronger overall material. Consequently, the dense-sand backfill can be replaced by a sand stabilized with about 15% cement. This alternative should be construction expedient since sand, cement, and water can be combined in a conveniently located mixing plant and pumped in-place by means of common grout pumps and attenuated pipes; no compaction equipment will be required at the site of the bends. It should be pointed out here that the cement stabilized

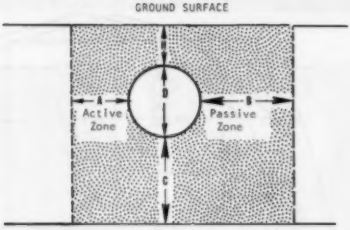

DIAMETER (D)	RADIAL FORCE (P_S)	H	C	A	B	BACKFILL TYPE
42 in. (1067 mm)	8000 lb per ft. (116,721 n per m)	6ft. (1-83m)	3.5ft. (1.07m)	1.75ft. (0.53m)	7.0ft. (2.14)	Dense Sand
36 in. (914 mm)	4750 lb per ft. (69,303 n per m)	4.5ft. (1.37m)	3.0ft. (0.92m)	1.50ft. (0.46m)	6.0ft. (1.82m)	Dense Sand
16 in. (406 mm)	2300 lb per ft. (33,557 n per m)	4.5ft. (1.37m)	3.0ft. (0.92m)	1.0ft. (0.31m)	2.7ft. (0.82m)	Dense Sand
16 in. (406 mm)	3700 lb per ft. (53,984 n per m)	10.0ft. (3.05)	3.0ft. (0.92m)	1.0ft. (0.31m)	2.7ft. (0.82m)	Medium Dense Sand

FIG. 10.—Design Recommendations

sand will set into a fairly hard mass and, if in the future pipe bends require uncovering, some breaking and chipping of the cement stabilized backfill will be required. For a given project and conditions, various sand-cement ratios should be experimented with to determine the most cost effective mixture.

Conclusions

1. When designing buried pipelines, the pipe-soil interaction force, P_s, required to restrain a bend segment should be computed and compared with the available soil resistance calculated by conventional methods. If P_s is larger than available resistance, use of finite-element procedure and nonlinear soil properties will result in an economical design.
2. Use of finite-element technique and the nonlinear soil properties permit delineation of the zone requiring select backfill which is smaller than suggested by conventional theories. This can result in design and construction cost savings.
3. For a given pipe-soil interaction force, an increase in the depth of soil

cover is the most practical method of achieving the higher backfill resistance.

4. A compacted sand backfill can be replaced by a pumpable cement-sand slurry for construction expediency without any loss in the backfill strength.

Appendix I.—References

1. Audibert, J. M. E., and Nyman, K. J., "Soil Restraint Against Horizontal Motion of Pipes," *Journal of the Geotechnical Engineering Division*, ASCE, Vol. 103, No. GT10, Proc. Paper 13303, Oct., 1977, pp. 1119–1142.
2. Duncan, J. M., and Chang, C. Y., "Nonlinear Analysis of Stress and Strains in Soils," *Journal of the Soil Mechanics and Foundation Division*, ASCE, Vol. 96, No. SM5, Proc. Paper 7513, Sept., 1970, pp. 1629–1653.
3. Janbu, N., "Soil Compressibility as Determined by Oedometer and Triaxial Tests," European Conference on Soil Mechanics and Foundation Engineering, Vol. 1, 1963, pp. 19–25.
4. Kondner, R. L., and Zelasko, J. S., "A Hyperbolic Stress-Strain Formulation for Sands," *Proceedings*, Pan American Conference on Soil Mechanics and Foundation Engineering, Vol. I, 1963, pp. 289–324.
5. Luscher, U., et al., "Pipe-Soil Interaction, Trans-Alaska Pipeline," *Proceedings of the ASCE Conference on Pipelines in Adverse Environments*, Jan., 1979.
6. Radhakrishnan, N., and Jones, W. H., "Documentation for Modified U-Frame Program," *Technical Report k-76-1*, United States Army Engineer Waterways Experiment Station, Vicksburg, Miss., June, 1976.
7. Spangler, M. G., "The Structural Design of Flexible Pipe Culverts," *The Iowa State College Bulletin*, Bulletin 153, Dec., 1941.

Appendix II.—Notation

The following symbols are used in this paper:

a = intercept of Hyperbolic stress-strain curve;
b = slope of Hyperbolic stress-strain curve;
E = modulus of elasticity;
F = resultant end force on pipe bend;
H = soil cover;
K = modulus number;
n = modulus exponent;
P = internal pressure of pipeline fluid;
Pa = atmospheric pressure;
Ps = pipe-soil interaction force;
$\bar{p}$ = horizontal axis of $\bar{p}$-$\bar{q}$ diagram;
$\bar{q}$ = vertical axis of $\bar{p}$-$\bar{q}$ diagram;
R = bend radius;
r = pipe radius;
t = pipe wall thickness;
α = coefficient of thermal expansion;
ΔT = temperature differential;
ϵ = strain;
μ = Poisson's ratio;
σ_H = hoop stress;
σ_L = longitudinal stress;

σ_1 = total major principal stress;
σ_3 = total minor principal stress;
$\bar{\sigma}_1$ = effective major principal stress;
$\bar{\sigma}_3$ = effective minor principal stress; and
τ_{max} = maximum shear stress.

TRANSPORTATION ENGINEERING JOURNAL

SUPERPLASTIC CONE-SHAPED SANDWICH CORES[a]

By Charles E. S. Ueng,[1] M. ASCE

(Reviewed by the Aerospace Division)

INTRODUCTION

The applications of sandwich construction are increasing steadily. In addition to aerospace vehicle structures, sandwich panels are also widely used in housing, transportation, and packaging industries to take advantage of the high strength-to-density and high stiffness-to-density ratios. Traditionally, sandwich cores appear in hexagonal cell shape and with vertical walls, which are often referred to as a honeycomb. The use of aluminum foil to manufacture such a honeycomb practically dominates all important structural applications of sandwich panels. There are several disadvantages associated with the manufacturing and application of such honeycomb cores: (1) It involves expensive and complicated tooling facilities; (2) the core is bonded to facing sheets only by the edge lines of the core; and (3) the same geometrical configuration is used for all applications and no possibility is provided for optimization studies.

A new method using superplastic alloy sheets and gas-forming techniques developed at the Georgia Institute of Technology (1) can eliminate all these drawbacks. In this new process, different core configurations can be obtained by heating the superplastic sheet to a critical temperature, applying gas pressure, or vacuum pressure, or both, and allowing the sheet to collapse gently onto a die having the desired geometry. Thus, through a change or a modification of the die, a core of different projection shape and positional symmetry becomes possible, which can be studied experimentally and analytically for optimization purposes depending on the load environment and application. By using truncated projections, the top surfaces are available for bonding instead of edges only. Shapes like hollow truncated cones, hollow truncated square or hexagonal

[a]Presented at the October 22–26, 1979, ASCE Annual Convention and Exposition, held at Atlanta, Ga. (Preprint 3694).

[1]Prof., School of Engrg. Sci. and Mechanics, Georgia Inst. of Tech., Atlanta, Ga. 30332.

Note.—Discussion open until June 1, 1981. To extend the closing date one month, a written request must be filed with the Manager of Technical and Professional Publications, ASCE. Manuscript was submitted for review for possible publication on November 1, 1979. This paper is part of the Transportation Engineering Journal of ASCE, Proceedings of the American Society of Civil Engineers, © ASCE, Vol. 107, No. TE1, January, 1981. ISSN 0569-7891/81/0001-0059/$01.00.

pyramids, etc., arrayed in square, hexagonal, etc., symmetry patterns, are just some examples from the possible configurations. Optimization studies undertaken include, e.g., the maximization of the shear modulus of the core (2,3,4,5), and the analysis of configuration for least weight (6,7). In this paper, procedures for the determination of upper and lower bounds of shear modulus for a hollow, truncated, cone-shaped core (see Fig. 1) with a simple, square array symmetry, are reported.

Properties of Superplastic Materials

The most important characteristic of superplastic materials is their exceptional stability in uniaxial tensile deformation. Extremely large elongation up to 4,850% has been reported recently in the literature for superplastic alloy Pb-62% Sn eutectic without fracture or necking, by Langdon and his associates (8). This extreme extensibility is often referred to as "superplasticity." It is in contrast with most metals and metallic alloys where necking or breaking usually occurs in the range between 5% and 50% elongation in a tension test. This extremely large elongation can take place at low load and slow strain rate with a temperature of about half the absolute melting point without appreciable strain hardening.

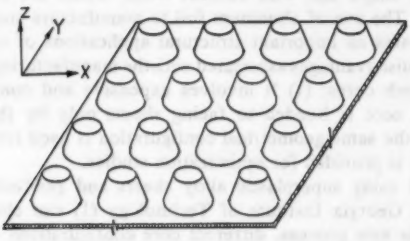

FIG. 1.—Sandwich Core Consisting of Truncated, Hollow, Cone-Shaped Projections

The essential microstructural condition is an extremely fine grain size, which under the correct conditions of temperature and strain rate deforms largely by grain boundary sliding and not by the more usual slip and grain deformation processes. After deforming superplastically, a relatively simple anneal restores the normal grain size and the normal metallic properties.

The unusual superplastic property described here can provide a simple and relatively inexpensive method of producing complex shapes through various forming processes. It has been reported that a 30% savings in weight and 50% in cost are possible when superplastic forming is combined with the diffusion bonding technique in various aerospace structures (9).

Shear Modulus

For efficient sandwich structures, the core must be light weight and strong in carrying the loadings, particularly the transverse shear. Therefore, the determination of the shear modulus of the core is one of the most important

tasks. In order to simplify the analysis, the following assumptions are made: (1) The complete core structure is made up of identical projections, placed with square symmetry where the number of such projections in a given panel is large enough that any local, or boundary effect, or both, can be ignored; (2) the effect of the small radius at the corners of a core projection due to manufacturing is negligible; (3) the wall thicknesses at different locations in the projections are the same, and are small in comparison with other dimensions such as the width, height, or depth; (4) buckling or warping of the inclined walls in the core projections is excluded from consideration; and (5) the core is assumed to behave in a linearly elastic fashion.

Kelsey, Gellatly, and Clark (10) made a theoretical and experimental study of the shear modulus of foil honeycomb cores. Simple expressions for upper and lower limits were obtained by application of the unit displacement and unit load methods (11) in conjunction with simplifying assumptions as to the strain and stress systems respectively, in the core. Chang and Ebcioglu (12) studied a similar problem. They adopted an approach which corresponds to the unit displacement method from equilibrium consideration. It can be proved that the results obtained in Ref. 12 correspond to the upper limit solution presented in Ref. 10.

Using energy theorems (11), let the direction of the applied force be denoted by subscript 1 and the direction normal to it (in the horizontal xy-plane) by subscript 2. The shear stresses along directions 1 and 2 can be expressed for the shear strains as

$$\begin{bmatrix} \gamma_1 \\ \gamma_2 \end{bmatrix} = \begin{bmatrix} f_{11} & f_{12} \\ f_{21} & f_{22} \end{bmatrix} \begin{bmatrix} \tau_1 \\ \tau_2 \end{bmatrix} \quad \ldots\ldots\ldots\ldots\ldots\ldots\ldots\ldots\ldots\ldots\ldots\ldots\ldots\ldots (1a)$$

$$\text{or} \quad [\gamma] = [f]\,[\tau] \quad \ldots\ldots\ldots\ldots\ldots\ldots\ldots\ldots\ldots\ldots\ldots\ldots\ldots\ldots\ldots\ldots (1b)$$

in which $[f]$ = the flexibility matrix. Conversely, one has

$$[\tau] = [k]\,[\gamma] \quad \ldots\ldots\ldots\ldots\ldots\ldots\ldots\ldots\ldots\ldots\ldots\ldots\ldots\ldots\ldots\ldots\ldots\ldots (2)$$

in which $[k]$ = the stiffnes matrix; and $[f] = [k]^{-1}$. It should be noted that all practical tests of the effective shear properties of cores are limited to the determination of what is effectively a single direct flexibility f_{11}, i.e.

$$G_{\text{eff}} = \frac{1}{f_{11}} = k_{11} - \frac{k_{12}^2}{k_{22}} \quad \ldots\ldots\ldots\ldots\ldots\ldots\ldots\ldots\ldots\ldots\ldots\ldots\ldots\ldots\ldots (3)$$

Upper Bounds.—Applying the principle of virtual work to the true state, i, and the virtual state, j, one obtains

$$\mathbf{k}_{ij} = \int_v \{\sigma_i\}^T \{\bar{\epsilon}_j\}\, dv \quad \ldots\ldots\ldots\ldots\ldots\ldots\ldots\ldots\ldots\ldots\ldots\ldots\ldots\ldots\ldots (4)$$

in which $\mathbf{k}_{ij}$ = the required force applied at j to produce unit displacement at i, while all other displacements are zero. The variable $\{\sigma_i\}$ represents the actual stresses due to unit displacement at i, with all others zero; the variable $\{\bar{\epsilon}_j\}$ represents the virtual strains due to unit displacement at j; and the superscript T denotes the transpose. It should be noted here that the "unit displacements" used here are the unit overall shear strains γ_1 and γ_2 of the core as a whole.

For the hollow, truncated cone-shaped core with a square symmetry (see Fig. 2), the stiffness can be expressed as

$$\mathbf{k}_{ij} = \int_o^{2\pi} \frac{Gt\gamma_{i\theta}\gamma_{j\theta}(2b + d_1 \cos\beta)\, d_1\, d\theta}{2S^2 d_1 \sin\beta}; \quad (i,j = 1,2) \ldots\ldots\ldots\ldots (5)$$

in which b, t, d_1, β, and S are parameters describing the dimensions of the core; G = the shear modulus of the core material in bulk; and $\gamma_{i\theta}$ = the shear strain in the wall at θ due to unit strain γ_i on the core as a whole.

Taking into account only the shear stresses in the plane of the inclined wall,

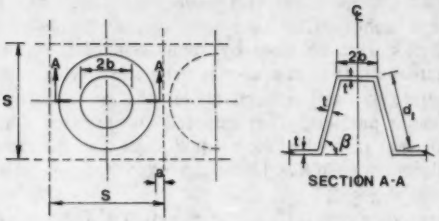

FIG. 2.—Unit Projection of Truncated, Hollow, Cone-Shaped Core

the shear strain component of inclined wall due to a unit overall shear strain, γ, of the core in the i direction is

$$\gamma_{i\theta} = \sin\theta \sin\beta \ldots\ldots\ldots\ldots (6a)$$

Similarly, the shear strain component of the inclined wall due to a unit overall shear strain, γ, of the core in the j direction is

$$\gamma_{j\theta} = \cos\theta \sin\beta \ldots\ldots\ldots\ldots (6b)$$

Substitution of Eqs. 6*a* and 6*b* into Eq. 5 yields

$$[k] = \frac{\pi Gt(2b + d_1 \cos\beta)\sin\beta}{2S^2} \begin{bmatrix} 1 & 0 \\ 0 & 1 \end{bmatrix} \ldots\ldots\ldots\ldots (7)$$

Then from Eq. 3, the effective shear modulus of the core in either xz- or yz-plane by the unit displacement method, can be expressed as

$$G_d = \frac{\pi Gt(2b + d_1 \cos\beta)\sin\beta}{2S^2}; \quad 0 < \beta < \frac{\pi}{2} \ldots\ldots\ldots\ldots (8a)$$

$$G_d = \frac{\pi Gtb}{S^2}; \quad \beta = \frac{\pi}{2} \ldots\ldots\ldots\ldots (8b)$$

Lower Bounds.—The flexibility coefficients can be expressed in a similar way as

$$\mathbf{f}_{ij} = \int_v \{\bar{\sigma}_i\}^T \{\epsilon_j\}\, dv \ldots\ldots\ldots\ldots (9)$$

which is analogous to Eq. 4. The lower bound of the effective shear modulus

can be obtained by using the unit load method. The "unit loads" used here are the unit shear stresses τ_1 and τ_2 acting on the core projection. The resulting shear flows developed in the curved wall of the projections due to τ_1 and τ_2 can be computed from the conditions of equilibrium within the core. Assuming that the shear stress is constant for points at the same elevation over the curved wall, it can be shown that $\mathbf{f}_{ij}$ for a core of this particular shape can be written in the form

$$\mathbf{f}_{ij} = \int\int \frac{q_{i\theta}\, q_{j\theta}\, dA}{GtS^2\, d_1 \sin\beta}; \quad (i,j = 1,2) \quad \ldots\ldots\ldots\ldots\ldots\ldots\ldots\ldots \quad (10)$$

in which $dA = (b + \xi \cos\beta)\, d\theta\, d\xi$ (see Fig. 3); and $q_{i\theta}$ = the shear flow in the curved wall at θ and at an elevation, $\xi \sin\beta$, from the top area of the core

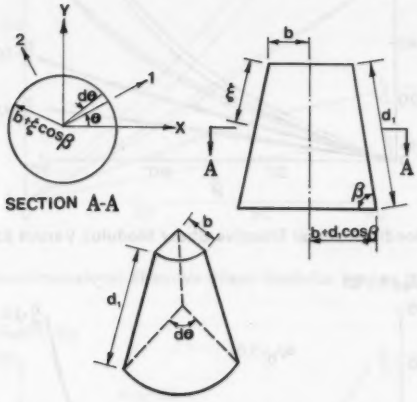

FIG. 3.—Side-View and Sections of Unit Projection

due to a unit shear stress, τ_i, acting on the core. These shear flows can be expressed as

$$q_{1\theta} = \frac{S^2 \sin\theta}{\pi(b + \xi\cos\beta)} \quad \ldots\ldots\ldots\ldots\ldots\ldots\ldots\ldots\ldots\ldots\ldots\ldots \quad (11a)$$

and $$q_{2\theta} = \frac{S^2 \cos\theta}{\pi(b + \xi\cos\beta)} \quad \ldots\ldots\ldots\ldots\ldots\ldots\ldots\ldots\ldots\ldots\ldots\ldots \quad (11b)$$

Substitution of Eq. 11 into Eq. 10 yields

$$[f] = \frac{S^2 \ln\left(1 + \dfrac{d_1}{b}\cos\beta\right)}{\pi G t d_1 \sin\beta\cos\beta} \begin{bmatrix} 1 & 0 \\ 0 & 1 \end{bmatrix}; \quad \text{if} \quad 0 < \beta < \frac{\pi}{2} \quad \ldots\ldots\ldots \quad (12a)$$

and $$[f] = \frac{S^2}{\pi G b t} \begin{bmatrix} 1 & 0 \\ 0 & 1 \end{bmatrix}; \quad \text{if} \quad \beta = \frac{\pi}{2} \quad \ldots\ldots\ldots\ldots\ldots\ldots\ldots \quad (12b)$$

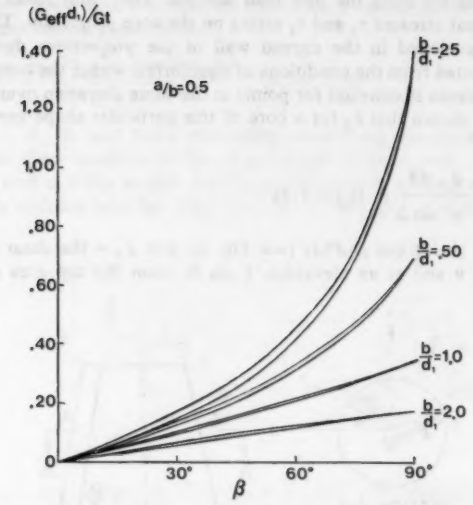

FIG. 4.—Nondimensional Effective Shear Modulus Versus β; $a/b = 0.5$

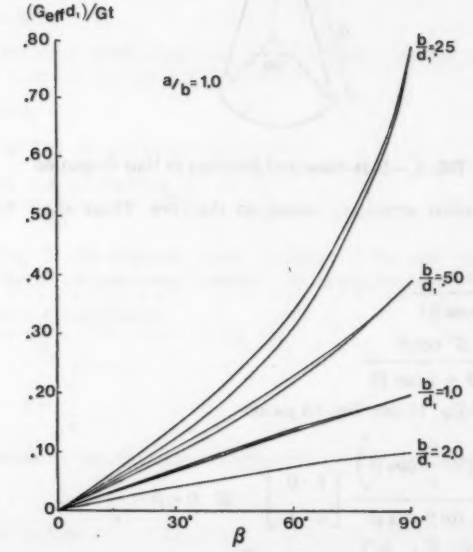

FIG. 5.—Nondimensional Effective Shear Modulus Versus β; $a/b = 1.0$

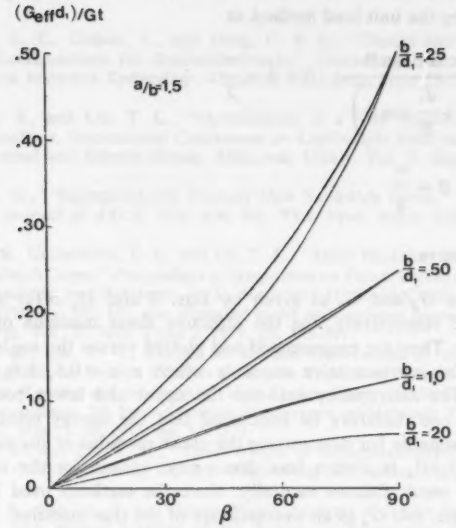

FIG. 6.—Nondimensional Effective Shear Modulus Versus β; $a/b = 1.5$

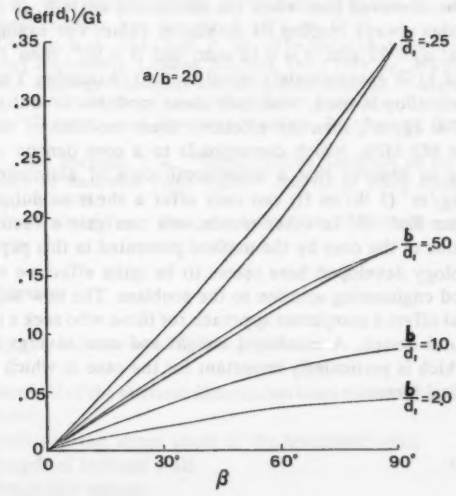

FIG. 7.—Nondimensional Effective Shear Modulus Versus β; $a/b = 2.0$

The effective shear modulus for the same core in xz- or yz-plane can now be calculated by the unit load method as

$$G_l = \frac{G\pi t d_1 \cos\beta \sin\beta}{S^2 \ln\left(1 + \frac{d_1}{b}\cos\beta\right)}; \quad 0 < \beta < \frac{\pi}{2} \quad \ldots\ldots\ldots\ldots\ldots\ldots \quad (13a)$$

$$G_l = \frac{G\pi bt}{S^2}; \quad \beta = \frac{\pi}{2} \quad \ldots\ldots\ldots\ldots\ldots\ldots\ldots\ldots\ldots\ldots \quad (13b)$$

Analysis of Results

The variables G_d and G_l as given by Eqs. 8 and 13, offer an upper and a lower bound respectively, for the effective shear modulus of the core in xz- or yz-plane. They are programmed and plotted versus the angle β, as shown in Figs. 4–7 for representative cases in which $a/b = 0.5$, 1.0, 1.5 and 2.0, respectively. The discrepancy between the upper and lower bound curves is very small. It can therefore be concluded that the energy principles used in this study are suitable for determining the shear modulus of the sandwich core. The ratio of G_l/G_d is always less than unity, except for the case in which $\beta = \pi/2$. This result follows naturally, since the methods used lead to G_l as an underestimate, and G_d as an overestimate of the true modulus. In the special case, $\beta = \pi/2$, the equality of the two results indicates that the statically-equivalent stress system is also kinematically compatible, so that the two methods yield an identical result and the analysis is exact. From the representative curves shown, it can be observed that when the inclination angle β, is equal to $\pi/2$, the shear modulus always reaches its maximum value. For example, let $a = 3$ mm; $b = 6$ mm; $d_1 = 12$ mm; $t = 0.10$ mm; and $\beta = 90°$; then Fig. 4 gives a value for $(G_{\text{eff}} d_1)/Gt$ approximately equal to 1.40. Assuming Titanium 6%A1, 4%V superplastic alloy is used, with bulk shear modulus $G = 41$ GPa and bulk density $\gamma = 4{,}500$ kg/m^3, then the effective shear modulus of the core, G_{eff}, turns out to be 483 MPa, which corresponds to a core density of 90 kg/m^3. It is interesting to observe that a honeycomb core of aluminum foil with a density of 80 kg/m^3 (5 lb/cu ft) can only offer a shear modulus of 228 MPa (33,000 psi) from Ref. 13. In other words, one can gain a factor of two for the shear modulus of the core by the method presented in this paper.

The methodology developed here seems to be quite effective and useful for providing a good engineering solution to the problem. The new superplastically-formed core also offers a competent approach for those who seek a more efficient metallic structural design. A combined weight and cost savings can therefore be achieved, which is particularly important for the case in which the structural weight is a critical factor.

Acknowledgment

This research was supported by a grant from the National Science Foundation, ENG-75-17968, with Charles A. Babendreier, Program Director.

Appendix I.—References

1. Underwood, E. E., Gomez, A., and Ueng, C. E. S., "Design and Fabrication of New Core Configurations for Sandwich Panels," *Proceedings*, 4th Inter-American Conference on Materials Technology, Caracus, Venezuela, June 29–July 4, 1975, p. 531.
2. Ueng, C. E. S., and Liu, T. L., "Optimization of a New Lightweight Sandwich Core," *Proceedings*, International Conference on Lightweight Shell and Space Structures for Normal and Seismic Zones, Alma-Ata, USSR, Vol. 2, Sept. 13–16, 1977, pp. 375–383.
3. Ueng, C. E. S., "Superplastically Formed New Sandwich Cores," *Transportation Engineering Journal of ASCE*, Vol. 104, No. TE4, Proc. Paper 13869, July, 1978, pp. 437–447.
4. Ueng, C. E. S., Underwood, E. E., and Liu, T. L., "Shear Modulus of Superplastically Formed Sandwich Cores," *Proceedings of Symposium on Future Trends in Computerized Structural Analysis and Synthesis*, A. K. Noor and H. G. McComb, Jr., eds., Oct. 30–Nov. 1, 1978, pp. 393–397; also appeared in the *International Journal of Computers and Structures*, Vol. 10, Nos. 1 and 2, 1979, pp. 393–397.
5. Ueng, C. E. S., Liu, T. L., Crooks, R. E., and Underwood, E. E., "Fabricacion Pruebas y Analisis de Nuevos Diseños Core para Paneles de Estructura Sandwich," ("Fabrication, Testing and Analysis of New Design Cores for Structural Sandwich Panels"), *Proceedings*, 5th Inter-American Conference on Materials Technology, São Paulo, Brazil, Nov. 5–10, 1978, pp. 531–535.
6. Ueng, C. E. S., and Liu, T. L., "Least-Weight of Superplastically-Formed Cores," *Advances in Civil Engineering Through Engineering Mechanics*, ASCE, May, 1977, pp. 440–443.
7. Ueng, C. E. S., and Liu, T. L., "Least-Weight Analysis of a New Sandwich Core," *Proceedings*, 14th Annual Meeting of the Society of Engineering Science, Lehigh University, Bethlehem, Pa., Nov. 14–16, 1977, pp. 273–283.
8. Ahmed, M. M. I., and Langdon, T. G., "Exceptional Ductility in the Superplastic Pb-62% Sn Eutectic," *Metal Transactions A*, Vol. 8A, 1977, pp. 1832–1833.
9. Weisert, E. D., and Stacher, G. W., "Fabricating Titanium Parts with SPF/DB Process," *Metal Progress*, Vol. 111, No. 3, 1977, pp. 33–37.
10. Kelsey, S., Gellatly, R. A., and Clark, B. W., "The Shear Modulus of Foil Honeycomb Core," *Aircraft Engineering*, London, England, Oct., 1958, pp. 294–302.
11. Argyris, J. H., "Energy Theorems and Structural Analysis," *Aircraft Engineering*, London, England, Vol. 26, Oct.–Nov., 1954; Vol. 27, Feb.–Mar., 1955; see also Argyris, J. H., *Energy Theorems and Structural Analysis*, Butterworth, London, England, 1960.
12. Chang, C. C., and Ebcioglu, I. K., "Effect of Cell Geometry on the Shear Modulus and on Density of Sandwich Panel Cores," *Journal of Basic Engineering*, ASME, Dec., 1961, pp. 513–518.
13. *Mechanical Properties of Hexcel Honeycomb Materials*, TSB120, Hexcel, Dublin, Calif., 1974 (revision).

Appendix II.—Notation

The following symbols are used in this paper:

a = one half of the shortest distance between two neighboring unit projections;
b = radius of the upper circle of the truncated cone;
d_1 = length of inclined wall;
$\mathbf{f}_{ij}$ = flexibility matrix;
G = shear modulus of bulk material;
G_{eff} = effective or equivalent shear modulus of core;

G_d, G_l = shear moduli of the core, by unit-displacement method and unit-load method, respectively;
$\mathbf{k}_{ij}$ = stiffness matrix;
S = base length of unit projection;
t = thickness of the wall;
β = inclined angle of the wall;
γ = shear strain;
$\{\bar{\epsilon}_j\}$ = virtual strains due to unit displacement at j; and
$\{\sigma_i\}$ = actual stresses due to unit displacement at i.

TRANSPORTATION ENGINEERING JOURNAL

IMPACT BEHAVIOR OF BARRIERS ON NONLEVEL TERRAIN[a]

By Hayes E. Ross, Jr.,[1] M. ASCE and Darrell G. Smith[2]

(Reviewed by the Highway Division)

INTRODUCTION AND SCOPE

Impact behavior of a roadside or median barrier is dependent on a number of factors, including size and spacing of posts, size and mounting height of rail or beam, offset of beam from posts, soil conditions, and roadside conditions between the edge of the traveled way and the barrier. Little is known about the effects of this last factor although it may have the greatest influence on performance. In general, barriers have been designed and tested for flat terrain conditions even though roadside and median barriers are commonly placed on side slopes, in depressed medians, in ditch bottoms, etc.

At the inception of this study, trips were made to several states to survey current barrier placement practices and to solicit input from various state transportation personnel. It was found that there are four basic conditions for which roadside and median barriers are typically placed on nonlevel terrain. These are shown in the photographs of Figs. 1–4. First, barriers used to shield bridge piers, overhead sign bridge supports, or other rigid objects in depressed medians or on side slopes are often placed as near to the object as the barrier design permits. In many cases this places the barrier on the side slope, as shown in Fig. 1. Secondly, barriers used to shield bridge abutments or other rigid objects near the shoulder are often flared away from the shoulder and

[a]Presented at the October 22–26, 1979, ASCE Annual Convention and Exposition, held at Atlanta, Ga.

[1]Research Engr. and Prof., Texas Transportation Inst., Texas A&M Univ., College Station, Tex. 77843.

[2]Research Assoc., Texas Transportation Inst., Texas A&M Univ., College Station, Tex. 77843.

Note.—Discussion open until June 1, 1981. To extend the closing date one month, a written request must be filed with the Manager of Technical and Professional Publications, ASCE. Manuscript was submitted for review for possible publication on November 20, 1979. This paper is part of the Transportation Engineering Journal of ASCE, Proceedings of the American Society of Civil Engineers, © ASCE, Vol. 107, No. TE1, January, 1981. ISSN 0569-7891/81/0001-0069/$01.00.

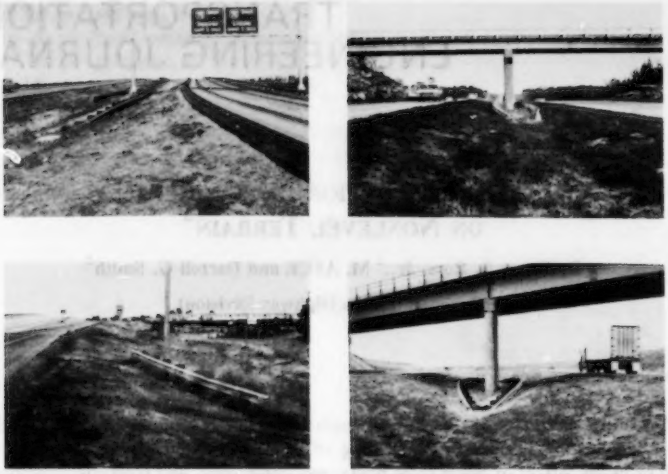

FIG. 1.—Barriers Shielding Rigid Objects

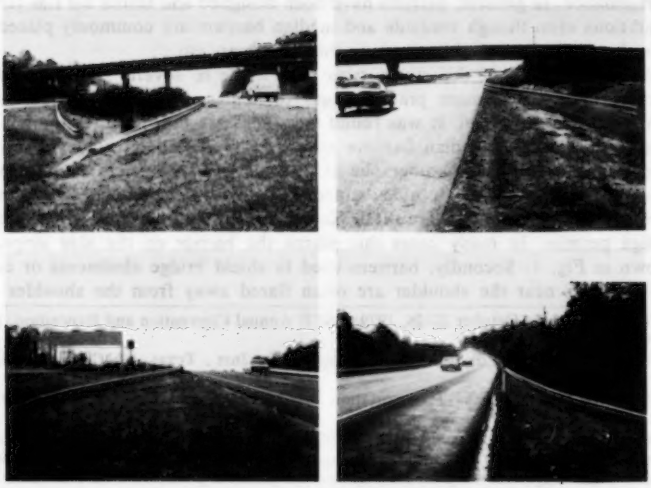

FIG. 2.—Flared Barriers

terminated. As a consequence a portion of the barrier is placed on the side slope, as shown in Fig. 2. Thirdly, roadside barriers are sometimes placed on "barn roof" sections in high-fill areas. Typically, the roadside is composed of a shoulder, then a relatively flat sloped embankment (usually a 6:1 slope) which may extend up to 20 ft (6.1 m) laterally, and finally, a relatively steep embankment (usually 2:1 or steeper). In this case, the barrier is placed on the 6:1 slope to shield the steeper embankment. This is shown in Fig. 3. The last condition, which is not as common as the other conditions mentioned, involves median barriers used to prevent crossover head-on accidents that are placed on stepped or depressed medians. This is shown in Fig. 4.

To gain insight on behavior of typical barriers on nonlevel terrain, two roadside barriers were evaluated through a full-scale crash test program. These were the G1 system and the G4(1S) system. (Designations are consistent with those

FIG. 3.—Barrier on Barn Roof Section

contained in Ref. 4.) The G1 system consists of three steel cables mounted on "weak" posts, while the G4(1S) system consists of a standard steel W-beam mounted on "strong" posts. Selection of these systems was based on four factors: (1) Both are operational (as per Ref. 1); (2) both are widely used; (3) both are used to varying degrees on nonlevel terrain conditions; and (4) the G1 barrier is a "flexible" system which may undergo considerable lateral movement on impact, while the G4(1S) barrier is a "semi-rigid" system and will displace much less than the G1 system for a given set of impact conditions.

Selection of a 6:1 slope was based on an evaluation of previous research involving computer simulation of vehicle trajectory on side slopes (see Appendix F of Ref. 4). The reference work showed that a vehicle could possibly vault a typical roadside barrier placed near the shoulder on slopes steeper than approx 10:1 to 8:1. It was concluded that a 6:1 slope would be in the critical range

for lateral barrier offsets up to approx 12 ft (3.66 m) from the edge of the shoulder.

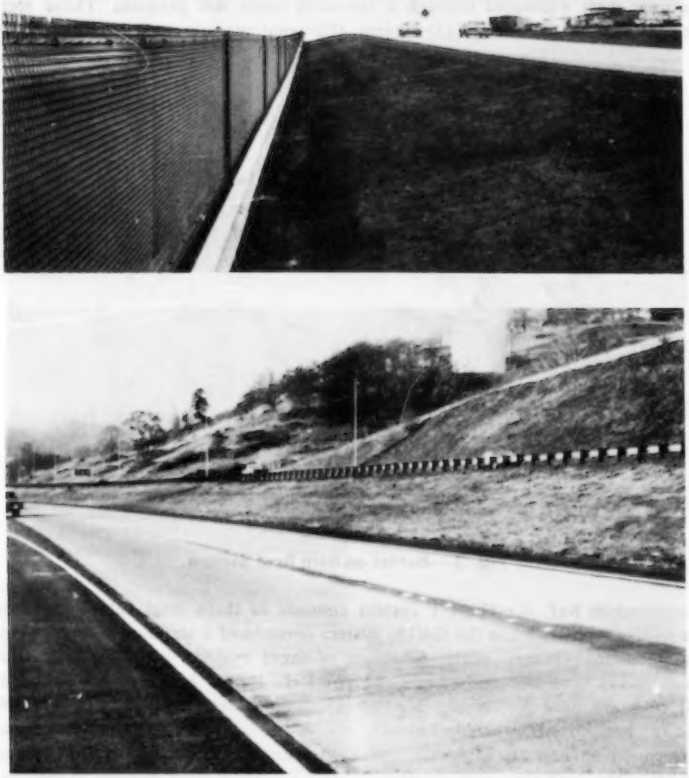

FIG. 4.—Median Barriers

This paper was condensed from a report to the Federal Highway Administration (FHWA) (6).

Test Conditions and Evaluation Criteria

Test Site.—The test site, shown in Fig. 5, was designed to represent a common roadside section defined by the road surface itself, a shoulder, a side slope, and a back slope. The road surface consisted of an existing concrete surface (airport apron). An 8-ft (2.4-m) shoulder area was cut on a 15:1 slope, and a 12-ft (3.7-m) side slope was cut on a 6:1 slope. A 3-ft–4-ft (0.9-m–1.2-m) ditch bottom was added to aid in drainage and a 4:1 back slope returned the configuration to the original ground level. The existing horizontal concrete surface

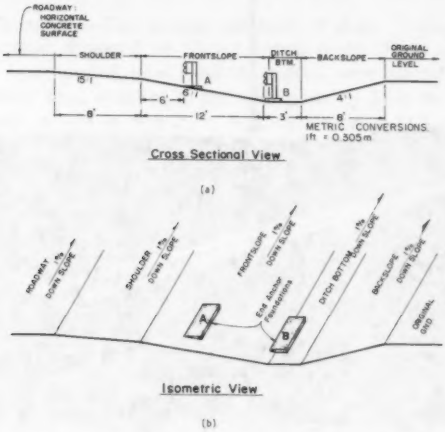

FIG. 5.—Test Site Geometry

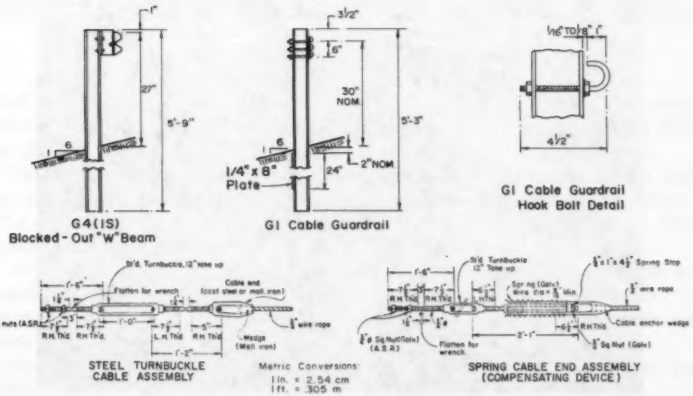

FIG. 6.—Roadside Barrier Systems and Details

has a downgrade slope parallel to the rail of 1% and the test slopes were constructed to parallel this drainage pattern.

The length of the installed roadside barrier was 200 ft (61.0 m) in each case, excluding the rigid anchors on both ends. Two sets of anchor foundations were installed, one locating the face of the guardrail 6 ft (1.8 m) from the edge of the shoulder (installation A) and the other locating it 12 ft (3.7 m) from the shoulder (installation B).

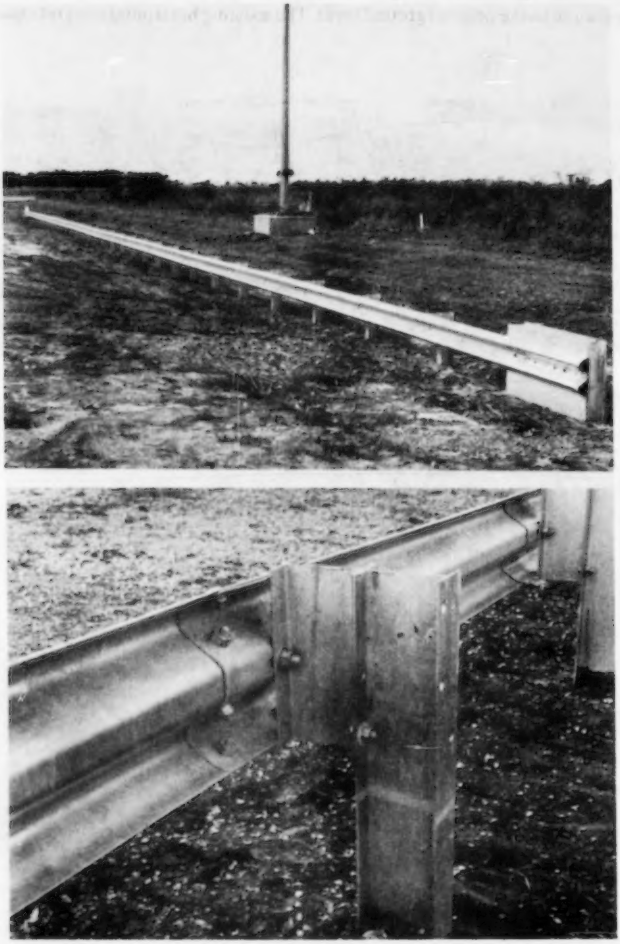

FIG. 7.—G4(1S) Barrier Installed on 6:1 Slope

Description of Barrier Systems.—Reference should be made to Fig. 6 for details of the two barrier systems described in the following.

G4(1S) Blocked-Out W-Beam.—This system consisted of a standard 12-gage steel W-beam mounted on W6 × 8.5-steel posts. The blockout was a W6 × 8.5, 14-in. (35.6-cm) long steel block which was bolted to the steel post. The top of the rail was 27 in. (68.6 cm) above ground level at the post. The posts were spaced 6.25 ft (1.91 m) center-to-center, and they were set 42 in. (106.7 cm) in an 18-in. (45.7-cm) diam drilled hole and then backfilled with a well-graded base material. This roadside barrier system, which was used in tests 1–4, is shown in Fig. 7.

G1 Cable Guardrail.—This system consisted of three 3/4-in. (1.9-cm) diam pretensioned cables mounted on S3 × 5.7-steel posts. The top cable was 30 in. (76.2 cm) from ground level, and the cables were spaced 3 in. (7.6 cm) apart. The cables were attached to the steel posts by 5/16-in. (0.79-cm) diam steel hook bolts. A 1/4 in. × 8 in. × 24 in.- (0.64 cm × 20.3 cm × 61.0 cm-)

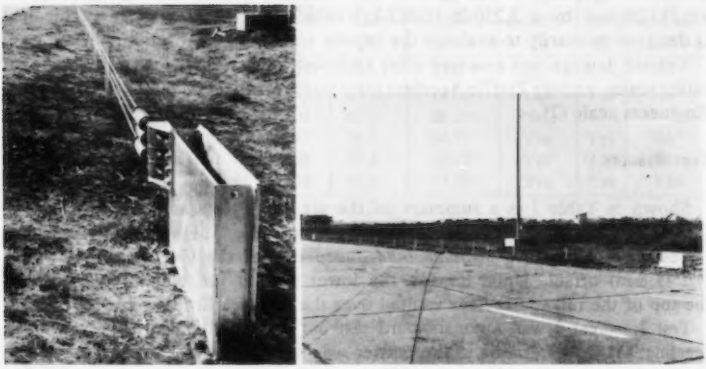

FIG. 8.—G1 Cable Rail Installed on 6:1 Slope

steel bearing plate was welded to the back flange of each post. The posts were spaced 16 ft (4.9 m) apart center-to-center, and they were driven 29.5 in. (74.5 cm) into the soil.

Cables were attached to the downstream end anchor by turnbuckles, and the upstream end of each cable was attached to a spring-compensating device. The cables were pretensioned to approx 1,000 lb (454 kg) before the test. This system, used in tests 5 and 6, is shown in Fig. 8.

Evaluation Criteria.—Ref. 5 states that three appraisal factors are to be considered for the test of a longitudinal barrier: (1) Structural adequacy; (2) impact severity; and (3) vehicle trajectory hazard. In summary, criteria for each appraisal factor are:

Structural Adequacy.—The test article shall redirect the vehicle; thus the vehicle shall not penetrate or vault over the installation.

Impact Severity.—Where the test article functions by redirecting the vehicle, the maximum vehicle acceleration (50 m/sec average) measured near the center

of mass should be less than the following values:

Maximum Vehicle Accelerations (g's)

Lateral	Longitudinal	Total	Remarks
3	5	6	Preferred
5	10	12	Acceptable

These rigid body accelerations apply to impact tests at 15° or less.

Vehicle Trajectory Hazard.—After impact, the vehicle trajectory and final stopping position shall intrude a minimum distance into adjacent traffic lanes.

Two tests are recommended (5) to evaluate a roadside barrier along its "length of need" (excludes end treatments). A strength test in which the barrier is impacted at 60 mph (96.5 km/h) by a 4,500-lb (2,043-kg) vehicle encroaching at 25°, is recommended. The primary purpose of this test is to evaluate the *structural adequacy* of the barrier. The second test involves a 60 mph (96.5 km/h) impact by a 2,250-lb (1,022-kg) vehicle encroaching at 15°. This test is designed primarily to evaluate the *impact severity* of the barrier.

Vehicle damage was assessed after each test in accordance with two national rating scales, namely Traffic Accident Data scale (7) and the Society of Automotive Engineers scale (2).

Test Results

Shown in Table 1 is a summary of the six crash tests and results obtained therefrom.

Test 1.—This was a *structural adequacy* test of the G4(1S) system for a 6-ft (1.8-m) offset. Upon impact, the lower part of the bumper just cleared the top of the rail and the car vaulted over the rail with little redirection.

Test 2.—Test 2 was a nonstandard test but was conducted for two primary reasons: (1) To determine if the barrier was structurally adequate for a lower encroachment angle (15° versus 25°); and (2) to provide data for validating and updating barrier computer simulation programs (to be used later to supplement the crash test program). The car was contained and smoothly redirected. However, the car would have crossed adjacent traffic lanes, thereby posing a potential trajectory hazard.

Test 3.—This was a *structural adequacy* test of the G4(1S) system for a 12-ft (3.7-m) offset. Upon impact, the vehicle began to redirect. However, the combined action of lateral, longitudinal, and vertical loads on the rail and right front wheel snagging on support posts resulted in a complete fracture of the rail. The right front wheel and portions of the wheel assembly were torn free of the vehicle. The vehicle penetrated the rail and came to rest approx 90 ft (27.5 m) beyond the point of impact just behind the barrier. It is noted that post and rail material properties were in compliance with recommended standards.

Test 4.—This was an *impact severity* test of the G4(1S) system for a 12-ft (3.7-m) offset. The car was contained and smoothly redirected. However, the car would have crossed adjacent traffic lanes, thereby posing a potential trajectory hazard.

Test 5.—This was a *structural adequacy* test of the G1 system for a 6-ft (1.8-m) offset. The car was contained and smoothly redirected and there was no trajectory hazard. Maximum dynamic deflection of the cables was 9.5 ft (2.9 m).

Test 6.—This was an *impact severity* test of the G1 system for a 6-ft (1.8-m) offset. The car was contained and smoothly redirected, decelerations were below

TABLE 1.—Summary of Crash Test Results[a]

Test number (1)	Barrier type (2)	Barrier offset, in feet[b] (3)	Vehicle weight, in pounds (4)	Impact speed, in miles per hour (5)	Impact angle, in degrees (6)	Adherence to Performance Specifications[c]		
						Structural adequacy? (7)	Impact severity? (8)	Exit angle? (9)
1	G4(1S)	6.0	4,500	62.83	25.0	No[d]	N/A	—[d]
2	G4(1S)	6.0	4,500	63.30	14.75	Yes	Yes	No[e]
3	G4(1S)	12.0	4,500	62.9	26.25	No[f]	N/A	—[f]
4	G4(1S)	12.0	2,300	58.2	14.75	Yes	Yes	No[e]
5	G1	6.0	4,500	59.6	24.75	Yes	N/A	Yes
6	G1	6.0	2,250	58.4	17.25	Yes	Yes	Yes

[a] All barriers tested were placed on a 6:1 side slope.
[b] Distance from outer edge of shoulder to face of barrier.
[c] See Section V-A for analysis of performance specifications.
[d] Vehicle vaulted over barrier.
[e] Subjective evaluation.
[f] Vehicle penetrated through fractured rail element.
Note: N/A = Not Applicable; 1 ft = 0.305 m; 1 lb = 0.454 kg; and 1 mph = 1.609 km/h.

suggested limits, and there was no trajectory hazard. Maximum dynamic deflection of the cables was 4.2 ft (1.3 m).

Conclusions

Conclusions drawn as a result of the six tests reported herein are:

1. The G4(1S) roadside barrier system does not satisfy *structural adequacy* requirements when placed on a 6:1 slope at offsets up through 12 ft (3.7 m). In other words, the barrier, when placed as stated, will not contain and redirect a 4,500 lb (2,043 kg) automobile impacting at 60 mph (96.5 km/h) and an encroachment angle of 25°.
2. The G4(1S) system, when placed on a 6:1 slope and a 6-ft (1.8-m) offset, will contain and smoothly redirect a 4,500 lb (2,043 kg) automobile impacting at 60 mph and an encroachment angle of 15°. Although not proven by the test, it is the writers' opinion that the G4(1S) system will satisfy *impact severity*

requirements when placed on a 6:1 slope and a 6-ft (1.8-m) offset.

3. The G4(1S) system satisfies *impact severity* requirements when placed on a 6:1 slope at a 12-ft (3.7-m) offset. In other words, the barrier, when placed as stated, will contain and smoothly redirect a 2,250-lb (1,022-kg) automobile with tolerable decelerations when impacting at 60 mph (96.5 km/h) and an encroachment angle of 15°.

4. Post-impact vehicle trajectory was less than desirable following the G4(1S) tests in which the vehicle was redirected, i.e., in tests 2 and 4. Results of these two tests could be interpreted to mean that a *vehicle trajectory hazard* existed; i.e., after impact, trajectory of the vehicle would pose a hazard to traffic in adjacent lanes.

5. The G1 roadside barrier system, when placed on a 6:1 slope at a 6-ft (1.8-m) offset, satisfied all three performance specifications for a roadside barrier. When compared to the G4(1S) system, improved performance of the G1 system is attributed to the 30-in. (76.2-cm) mounting height of the top cable [versus 27 in. (68.6 cm) for the W-beam]. The cables remained at essentially the same height following impact, while the W-beam in the G4(1S) system rotated backward and downward, creating a ramp for the vehicle.

Recommendations

Results of limited tests reported herein form a basis for the *tentative* recommendations which follow.

1. Roadside or median barriers utilizing the standard W-beam, mounted 27 in. (68.6 cm) above ground, should not be placed on 6:1 or steeper slopes for offsets up to 12 ft (3.7 m). Offset is the lateral distance from the shoulder's edge to the face of the barrier. When placed within these boundaries the barrier cannot be expected to contain and redirect an automobile leaving the shoulder at 60 mph (96.5 km/h) with an encroachment angle equaling or exceeding 25°. In other words, the barrier will not meet current performance specifications regarding "structural adequacy" (5). Barrier performance for offsets greater than 12 ft (3.7 m) is unknown and therefore no recommendation can be made regarding placement beyond this distance. Trajectory analysis (4) indicates that an errant automobile with the aforementioned encroachment conditions would strike the barrier at or below the normal or level terrain impact height for offsets greater than 12 ft (3.7 m). It must be noted that the G4(1S) system *did* contain and redirect an automobile at 6-ft (1.8-m) and 12-ft (3.7-m) offsets for a 60-mph (96.5-km/h), 15° encroachment angle. Statistics have shown that approx 80% of all errant vehicles leave the travel way at an angle of 15° or less. Barrier systems now in place on 6:1 slopes utilizing a 27-in. (68.6-cm) W-beam can thus be expected to contain and redirect a large majority of errant vehicles.

2. The G1 roadside barrier system is acceptable for placement on side slopes 6:1 or flatter. However, care must be exercised in its placement to insure an adequate distance behind the barrier for displacement during impact. A lateral displacement of approx 10 ft (3.1 m) can be expected if the barrier is impacted by a full-size car traveling at 60 mph (96.5 km/h) encroaching at 25°. Therefore, the barrier should be placed 10 ft (3.1 m) or more laterally from rigid objects.

Tests (3) have shown the G1 system will contain and redirect an automobile when placed approx 18 in. (45.7 cm) from embankments with slopes as steep as 2:1 even though the barrier may deflect 10 ft (3.1 m) or more. However, in the absence of test data or other supporting information, it is recommended that the G1 system be placed 10 ft (3.1 m) or more laterally from embankments or drop-offs with slopes steeper than 2:1.

Acknowledgments

Research reported in this paper was sponsored by the FHWA under Contract DOT-FH-11-9343. The writers are grateful to the FHWA for their permission to publish this work. Morton S. Oskard of the FHWA served as technical contract manager, and his guidance and cooperation were appreciated. The contents of this paper reflect the views of the writers who are responsible for the facts and the accuracy of the data presented herein. The contents do not necessarily reflect the official views or policy of the Department of Transportation. This paper does not constitute a standard, specification, or regulation.

Appendix.—References

1. Bruce, R. W., Hahn, E. E., and Iwankiw, N. R., "Guardrail/Vehicle Dynamic Interaction," *Report No. FHWA-RD-77-29*, Federal Highway Administration, Mar., 1976.
2. *Collision Deformation Classification, Recommended Practice J224a*, Society of Automotive Engineers, New York, N.Y., 1973.
3. Graham, M. D., et al., "New Highway Barriers: The Practical Application of Theoretical Design," *Highway Research Record 174*, 1967.
4. *Guide for Selecting, Locating, and Designing Traffic Barriers*, American Association of State Highway and Transportation Officials, Washington, D.C., 1977.
5. "Recommended Procedures for Vehicle Crash Testing of Highway Appurtenances," *Transportation Research Circular No. 191*, Transportation Research Board, Washington, D.C., Feb., 1978.
6. Ross, H. E., Jr., and Smith, D. G., "Impact Behavior of Roadside Barrier on Nonlevel Terrain—Crash Test Study," *Research Report 3659-1*, Texas Transportation Institute, Texas A&M University, College Station, Tex., Apr., 1979.
7. "Vehicle Damage Scale for Traffic Accident Investigators," *Traffic Accident Data Project Bulletin No. 1*, National Safety Council, Chicago, Ill., 1971.

TRANSPORTATION ENGINEERING JOURNAL

SIMPLIFIED PROCEDURES FOR ESTIMATING TRIP ATTRACTIONS

By Ashok Kumar[1]

(Reviewed by the Urban Transportation Division)

INTRODUCTION

Estimates of trips produced from and attracted to a traffic analysis zone are essential in a conventional four-step (trip generation, trip distribution, mode split, and route split) urban transportation modeling system (UTMS). This paper addresses the problems associated with obtaining reliable estimates of trips attracted to a traffic analysis zone. Usually, rich data sets are available to estimate the trips produced from a traffic zone; e.g., origin-destination (O-D) surveys conducted at home, Special Fourth Count United States Bureau of Census Data Tabulations (24), census tract level population and household estimates prepared by the National Planning Data Corporation (12), aerial photographs, etc. However, basic data pertaining to variables needed to estimate trips attracted to a traffic zone are usually either lacking or difficult to obtain.

Variables commonly used to estimate trips attracted to a zone are: (1) Gross floor area; (2) employment; and (3) gross land area. Statistical techniques such as regression analysis and cross classification analysis to correlate these variables to trip attraction are well-documented in two publications of the Federal Highway Administration (7,20) and in a paper by Shuldiner (16). The major problem in estimating trip attractions lies not in the use of these statistical techniques but in assembling the data for the base year model calibration. The year model validation is undertaken as a part of the continuing 3-C process and the forecast year for which design traffic is to be estimated.

[1]Sr. Transportation Planner, Northeast Ohio Areawide Coordinating Agency, 1501 Euclid Ave., Cleveland, Ohio 44115.

Note.—Discussion open until June 1, 1981. To extend the closing date one month, a written request must be filed with the Manager of Technical and Professional Publications, ASCE. Manuscript was submitted for review for possible publication on November 14, 1979. This paper is part of the Transportation Engineering Journal of ASCE, Proceedings of the American Society of Civil Engineers, © ASCE, Vol. 107, No. TE1, January, 1981. ISSN 0569-7891/81/0001-0081/$01.00.

Data Problems

Problems related to data assembly in the base year, or model validation year, are mostly due to budgetary constraints on staff and data processing. In some states the employment data by type of Standard Industrial Classification Code (SIC) and street addresses can be obtained from the state bureau of employment services or the bureau of workmen's compensation, or both. There are commercially available data sources such as the listings compiled by Dun and Bradstreet, but the completeness of these listings remains to be seen.

Despite the advances made in setting up the Dual Independent Map Encoding (DIME) File (5) for matching (ADMATCH) the street addresses to census tract blocks (CTB) and subsequent compression of these blocks to traffic zones, very few large metropolitan areas have been able to use the employment listings aforementioned to estimate employment by traffic zone. A manual matching of these listings to traffic zones proves to be impractical, if the study area is large. Compilation of gross floor area data (obtainable from Sanborn Maps and the county auditor's office) at the traffic zone level for the entire cordon area is also cumbersome and impractical.

The only readily obtainable data are the gross land area, secured from sources such as the county auditor's office; zoning maps prepared by cities, townships and villages; United States Geological Survey (USGS) aerial maps and LANDSAT photographs (6). These data can also be measured and summarized by traffic zones by inexperienced staff.

Problems related to data assembly for the forecast year are even greater. Large scale urban development models like Projective Land Use Model (PLUM) (2) and EMPIRIC Activity Allocation Model (2) are available in the transportation planning literature for forecasting future year zonal population and employment. But, these models are not suitable for forecasting future growth and change for those metropolitan areas which are experiencing losses in population and employment in the central city. To this writer's knowledge, no satisfactory mathematical models have been developed which can reflect decline, shift, and growth in population and employment at the traffic zone level for such urban areas.

The Northeast Ohio Areawide Coordinating Agency (NOACA), the metropolitan planning organization (MPO) for the greater Cleveland area, faced similar problems when charged with the responsibility of updating the areawide comprehensive, land-use and transportation plans as mandated by the Department of Housing and Urban Development, Federal Highway Administration, Urban Mass Transportation Administration and Environmental Protection Agency. The comprehensive transportation and land-use plan developed in the 1960's as a part of the 3-C process using a mathematical growth allocation model called Direct Trip Allocation Model (10,19) was found to be unsatisfactory in replicating the base year (1975) traffic flows and land-use changes from 1963 (the year when O-D surveys were undertaken) to 1975.

It was decided to adopt a different approach to forecast future land-use changes. Local planners working together with the agency staff favored using a process for allocating the future growth based upon the suitability analysis of land available for development/redevelopment. Full documentation of this procedure can be found in Refs. 13, 15.

Briefly, the method is as follows: available land is judged on the basis of such attributes as (1) Development site limitations like drainage problems and excessive slopes; (2) infrastructure availability like sewer and water connections; (3) site attractiveness like locale and quality of educational system; (4) environmental limitations to development like wetlands, poor-air quality/airport noise zones; (5) transportation accessibility expressed in terms of nearness to a limited access highway interchange, to mass transit facilities, and to an airport; and (6) development proclivity.

TABLE 1.—Suitability Attribute Weightings Assumed in Developing Trend Extended Land Use Plan

Attribute (1)	Land Use Allocation Category					
	High density residential (2)	Medium density residential (3)	Low density residential (4)	Light industry (5)	Heavy industry (6)	Commercial (7)
Flood plains	X	X	X	X	X	X
Poor drainage	−2	−4	−4	−3	−2	−3
Steep slope	−1	0	0	X	X	X
Sewer service	R	R	0	R	R	R
Water service	R	R	0	R	R	R
Local alternatives	+3	+5	+3	+1	0	+4
Community service	+3	+4	+2	+1	+1	+3
Protected areas	X	X	−1	X	X	X
Air/noise pollution	−4	−4	−4	0	0	−2
Access to interstate highway	+3	+2	0	R	+4	+5
Access to dense arterial network	+4	+2	+1	R	R	R
Access to rail	−1	−1	0	+3	R	0
Access to airport	0	0	0	+2	+1	+1
High growth potential	+3	+3	0	+3	+1	+4
Industrial growth potential	0	0	−1	+5	+3	+2

Note: + = Desirable attribute for development. − = Undesirable attribute for development. X = Restricted. If present, an attribute having a weighting of X implies that future development in that land use category cannot occur, even if other desirable attributes are present. R = Required. If absent, an attribute having a weighting of R implies that future development in that land use category cannot take place, even if other desirable attributes are present.

The degree to which an attribute influences development varies from one land use to another. After extensive examination with local planners, weightings for each of the attributes for each land-use type were established (see Table 1). A series of overlays were used to map the attribute data. The area within the attribute outlines was shaded in. The attributes were mapped in the negative direction; i.e., all positive suitability attributes were shaded where they were absent and all negative suitability attributes were shaded where they were present.

This provided all-negative attribute maps. The reason for this procedure is that after overlaying attribute maps, windows of development are identifiable. A computerized version of this process is now available through the Ohio Department of Natural Resources (14).

The future land-use allocation process can be summarized as follows: based upon historical data on measured land-use inventories and the corresponding population and employment for the inventory years, a relationship between population, employment, and acres consumed by residential, commercial, and industrial land uses was established. Projected regional population and employment changes by 5-yr increments up to the year 2000 were converted into land-use acreage requirements. Using windows of development identified by suitability analysis, land-use acreage requirements were allocated. Finally, zonal boundaries were overlayed to summarize the land-use changes by 5-yr increments.

Research Objectives

Recognizing that assembling employment data at the zonal level is difficult if not impossible, it was decided to investigate the possibility of developing acceptable statistical relationships between person-trip attractions and the amount of gross land area available for residential, commercial, industrial, and open space uses. Employment categories included in calculating commercial and industrial land-consumption are shown in Table 2.

It was further decided to express the amount of residential land use by number of households rather than by acres of residential land use because compilation of household data usually poses no problem. It was also decided to express the amount of commercial and industrial land use for zones falling within very high land-use intensity areas such as the central business district (CBD) in terms of amount of gross floor area rather than by gross land area, because mixed land uses are found in the same building.

Research Methodology

Several studies on trip-generation analysis (e.g., Refs. 7, 20), have indicated that the number of trips generated from a parcel of land depends upon: (1) The amount; (2) the location; and (3) the type of land use. Researchers have attempted to identify the most prudent way to express these variables in correlating trips generated from a given parcel of land: the amount of land (gross land area, gross floor area, number of employees); location (CBD, central city, residential areas, distance from the CBD, regional accessibility); and type of land use (manufacturing, retail trade, services, finance, insurance, and real estate, wholesale trade, transportation and public utilities, institutional land use).

Studies done by Black (4) indicate that the best statistical relationships are obtained when non-residential trip generation is based upon floor area for commercial land use, upon employment for manufacturing (industrial) use, and upon land area for public buildings, public open spaces and transportation. Nakkash and Grecco (11) showed that using a dummy variable to indicate the location of a zone in the central or noncentral areas gave significantly better results than using a gravitational-type regional access measure. Kolifarth and Shuldiner (9) showed that manufacturing land-use trip generation rates varied

TABLE 2.—Detailed Land Use Categories Included Under General Industrial, Commercial, Retail, Office, and Open Space Land Use Variables Used in Regression Analysis

Industrial land use (1)	Commercial land use (2)	Retail land use[a] (3)	Office space[b] (4)	Open space (5)
Ordnance & accessories	Personal services	Shopping centers	Office buildings—general uses	Public parks & zoological gardens
Lumber & wood products, except furniture	Business services	Super markets	Federal government—offices & buildings	Golf courses
Furniture & fixtures (household or office furniture)	Automobile repair & service	Other food stores	State government—offices & buildings	Outdoor drive-in theaters
Stone, clay and glass products	Miscellaneous repair	Drug stores	County government—offices & buildings	Racetracks
Primary metal industries	Financial, insurance & real estate	Department stores	City government—offices & buildings	Football & baseball stadiums
Fabricated metal products	Medical & health services	Other general merchandise stores		Fairgrounds
Machinery, except electrical	Other professional services	Apparel & accessories stores		Other outdoor amusement centers
Electrical machinery, equipment, supplies	Eating & drinking establishments	Furniture, home furnishings & appliances		Other public open space not classified previously
Professional, scientific & controlling instruments	Gasoline service stations	Motor vehicle & vehicle accessories		Agriculture
Transportation equipment	Indoor theaters, auditoriums, field houses	Lumber, building materials		Forests
Miscellaneous industries	Other indoor recreation centers	Other retail stores		Fisheries
Mining and quarrying	Wholesalers with stocks in warehouses			
Food & kindred products (meat, dairy, etc.)	Storage warehouses			
Tobacco products	Yard storage			
Textile mill products	Railroad terminals			
Apparel & other finished products made from fabrics	Railroad yards			
Paper & allied products	Local & interurban mass transportation stations			
Petroleum refining & related industries	Motor freight transportation—terminals			
	Water transportation—terminals			
	Air transportation—terminals			
	Pipeline transportation substa-			

TABLE 2.—*Continued*

(1)	(2)	(3)	(4)	(5)
Rubber products (tires, tubes, etc.)	tions Communication			
Leather products	Utilities—substations			
Miscellaneous—nondurable (toys, pens, etc.)	Educational institutions & schools Hospitals Other medical & health buildings Cultural centers			

[a]Retail land use classification is used only in estimating home based shop attractions (HBSHPA). For other trip purposes, such as, home based work (HBW), home based other (HBO), home based social recreation (HBSRC) and truck trip ends estimation, retail land use is lumped with commercial land use.

[b]Office space classification is used only in estimating trip attractions to the CBD. For other locations, office land use is lumped with commercial land use classification.

significantly when manufacturing land-use types were stratified by detailed two-digit standard industrial classification (SIC) codes (17) and the amount of land use was expressed in gross land area. However, when trip rates were derived using the number of employees working within each detailed manufacturing SIC codes, no significant variation was found.

Building upon the research findings aforementioned and keeping in perspective the data limitations, it was decided to develop the relationships between person trip-attractions and gross land area stratified by generalized land-use types and by some locational variable. Stratification of traffic analysis zones by location is essential in developing trip-attraction rates by land area.

During the early phase of this study, scatter plots between zonal home-based person work trip attractions and the amount of industrial and commercial land use within that zone were developed. Scatter plots were also developed after stratifying the zonal data by a pseudo-employment density measure, where pseudo-employment density is defined as the ratio between zonal home-based person work trip attractions and the amount of zonal non-residential acreage (industrial plus commercial acreage). Correlations were found to be much higher after stratifying the data by pseudo-employment density. Details of this analysis can be seen in Ref. 23.

Trip generation rates as a function of land area for different land-use types have also been compiled by the Institute of Transportation Engineers (21) and the Maricopa Association of Governments Transportation Planning Office (22). The trip rates developed by these organizations are useful in specific trip-generator analysis, but cannot be readily used for the conventional four-step modeling process. The reasons are: (1) Only vehicular trips ends are estimated; (2) no differentiation is made between home-based and nonhome-based trip orientation and trip purpose; and (3) trip rates are not stratified by location type. It will

be shown later that trip rates do vary substatially by location within the study area.

For this study, pseudo-employment density measures as a locational variable was selected after considering other measures such as residential density (number of households per residential acre), gravitational accessibility, and distance from the CBD. The Cleveland metropolitan area is a multi-nucleus region with well-defined CBD in Cleveland, Lorain, Painesville, and Elyria. Therefore, a simple locational variable such as the distance from the CBD is not applicable. Gravitational access measure was found to give similar stratification patterns as pseudo-employment density and residential density. However, gravational access measure is much more difficult to compute compared to residential and employment densities and hard to comprehend by non-quantitative planning professionals and decision makers. The accessibility measure, therefore, was dropped from further consideration. Except for school person trip attraction, pseudo-employment density was found to give much superior statistical correlations. For school person trip attractions, residential density was found to be a better stratifying variable.

Trip attraction rates were developed for seven different trip purposes, namely: (1) Home-based work attractions; (2) home-based other attractions (such as personal business, medical, dental, eat meal); (3) home-based social recreation attractions; (4) home-based school attractions; (5) home-based shop attractions; (6) nonhome-based trip ends; and (7) truck trip ends. For large metropolitan areas it is essential to stratify the travel by so many trip purposes because trip length frequency distributions and mean trip lengths associated with these purposes are found to be statistically different. Combining some of these trip purposes can bias the friction factors calibrated for gravity models and subsequent trip distribution. Stratification of travel by trip purpose also aids in the selection of causal variables in statistical analysis.

Table 3 shows the relative distribution of trip ends by trip purpose and land-use type at the trip destination for the Chicago region (1). This table clearly shows, as expected, that school trips are predominantly attracted to institutional land use, while social recreational trips can be attracted to residential, open space, and commercial land use.

Using pseudo-employment density as the stratifying variable, it was necessary to determine the range of values of this variable; i.e., strata over which trip attraction rates were statistically different. A dummy variable technique covered by Suits (18) is especially useful in this type of analysis. Suppose one wishes to test the hypothesis that truck trip rates based upon industrial land acreage vary significantly for suburbs (pseudo-employment density 0.1–20 employees/nonresidential acre), central city (20.1–40.0 employees/nonresidential acre), and the CBD (40.1+ employees/nonresidential acre). Note that these values are for illustrative purpose only. To test this hypothesis, the following regression model is estimated:

$$\text{TRUCK TRIP ENDS} = a \times \text{INDLAND} + b \times I_1 + c \times I_2 \quad \ldots\ldots\ldots (1)$$

in which INDLAND = zonal industrial acres; I_1 = dummy variable having value equal to 1 when employment density = 0.1–20 employees/nonresidential acre, 0 otherwise; I_2 = dummy variable having value equal to 1 when employment

density = 40.1+ employees/nonresidential acre, 0 otherwise; and a, b, c = regression coefficients to be estimated.

After a, b, and c are estimated along with their t statistic (7), the hypothesis that trip rates vary between suburbs and central city is accepted or rejected based upon the values of the t statistic associated with b and c. If b is found to be statistically significant, rates are assumed to be different between the central city and the suburbs. Similarly, by examining the significance of c, a decision can be made whether trip rates vary between the central city and the CBD. Note that for the density range of 20.0–40.0 employees/nonresidential

TABLE 3.—Trips[a] by Destination Land Use and Purpose 1970 Weekday Person Trips

Land use[b] (1)	Home (2)	Work (3)	Business related to work (4)	Shop (5)	School (6)	Social/ recreational (7)	Personal business (8)	Serve passenger (9)	Other (10)
Residential	7,901	95	131	10	2	1,001	180	97	2
Manufacturing	0	959	70	4	0	6	17	47	0
Commercial	0	1,124	243	2,290	4	927	790	126	0
Public buildings	0	314	65	5	666	206	188	174	0
Public open space	0	30	25	1	1	332	11	19	0
Transportation, communication utilities & mining	0	232	32	5	0	30	28	90	13
Total destinations within region	7,901	2,756	567	2,315	673	2,502	1,215	553	16

[a] Trips are in thousands.

[b] Land use categories used by Chicago Area Transportation Study.

Note: Source—a summary of travel characteristics—Chicago Area Transportation Study and Northwestern Indiana Regional Planning Commission, pp. 42, 1977.

acre, I_1 and I_2 assume a value of zero in the equation shown in the foregoing and the value of coefficient a represents the trip rate for this density range.

As observed earlier, it was necessary to determine the strata of pseudo-employment density over which trip attraction rates were different. In order to determine these ranges, zonal observations were allocated to a large number of strata. The lower and upper bound on each stratum was determined by counting the number of at least 50 observations falling within each stratum. Using the dummy variable technique described in the foregoing, each stratum was checked against the adjoining strata for statistical differences in trip attraction

rates. If no statistical differences were found to exist, adjoining strata were collapsed into a single stratum. The process was repeated until all strata were found to be statistically different.

The computer program UREGRE (25) issued by Urban Mass Transportation Administration was used in creating the dummy variables and estimating the regression coefficients. The results obtained for each trip purpose are summarized in the following. The data set used for these runs was the 1963 O-D survey conducted by the Ohio Department of Transportation for the Cleveland Metropolitan Area (3).

Home-Based Work Person Trip Attractions (HBWA)

Using the linear regression analysis technique with dummy variables, the following equation was derived for traffic zones falling outside the Cleveland

TABLE 4.—Values of Calibration Coefficients Used in Eq. 2

Coefficient *a* (1)	Coefficient *b* (2)	Pseudo-employment density range, in employees per nonresidential acre (3)
1.06	0.84	≤1
(5.3)[a]	(2.2)	
2.92	2.17	1–2
(24.9)	(1.9)	
5.13	5.39	2–3
(17.2)	(6.3)	
7.96	9.79	3–5
(21.7)	(44.5)	
11.79	11.26	5–6.5
(21.6)	(9.2)	
17.61	13.17	6.5–10
(34.9)	(22.2)	
24.29	23.05	10–13
(58.9)	(38.2)	
29.75	25.72	13–16
(40.4)	(32.3)	
38.19	33.80	16–20
(49.5)	(52.2)	
45.64	45.98	20–25
(42.9)	(110.1)	
55.45	52.04	25–30
(54.5)	(31.4)	
66.46	70.44	30–40
(58.6)	(60.1)	
93.26	109.88	40–54
(59.7)	(50.7)	
149.22	128.02	54–80
(70.9)	(17.4)	
221.47	175.46	80+
(59.3)	(9.9)	

[a]Numbers within parentheses indicate the values of *t* statistic associated with regression coefficients shown.

CBD. Values of calibration coefficients a and b for different pseudo-employment density ranges are shown in Table 4.

$$\text{HBWA} = a \times \text{COMMLAND} + b \times \text{INDLAND}; \quad R^2 = 0.99,$$

number of observations = 894, F value = 2,903.1,

error of estimate (HBWA) = 166.6 . . . . . (2)

in which HBWA = zonal home-based work person trip attractions; COMMLAND = zonal gross commercial land area, in acres; INDLAND = zonal gross industrial land area, in acres; Pseudo-employment density = (zonal HBWA)/(2. × nonresidential area, in acres); and nonresidential area = zonal gross commercial land area + zonal gross industrial land area.

Home-Based Other Person Trip Attractions (HBOA)

This trip purpose category includes trips made for personal business, eating meals, and medical/dental visits. The equation giving best overall statistical fit is as follows:

$$\text{HBOA} = a \times \text{HH} + b \times \text{COMMLAND} + c \times I_1;$$

$R^2 = 0.91$, number of observations = 902, F value = 725.8,

error of estimate (HBOA) = 270.8 . . . . . (3)

in which HBOA = zonal home-based other person trip attractions; HH = number

TABLE 5.—Values of Calibration Coefficients Used in Eq. 3

Coefficient a (1)	Coefficient b (2)	Coefficient c (3)	Pseudo-employment density range, in employees per nonresidential acre (4)
0.40	0.66	905.2	≤1
(27.9)[a]	(2.1)	(14.9)	
0.40	2.11	905.2	1–3
(27.9)	(11.7)	(14.9)	
0.40	7.12	905.2	3–6.5
(27.9)	(15.2)	(14.9)	
0.40	9.86	905.2	6.5–16
(27.9)	(17.8)	(14.9)	
0.40	18.24	1,052.6	16–30
(27.9)	(16.7)	(17.2)	
0.40	22.64	1,052.6	30–40
(27.9)	(10.5)	(17.2)	
0.40	27.34	1,554.8	40–54
(27.9)	(9.7)	(20.6)	
0.40	41.05	1,554.8	54+
(27.9)	(16.1)	(20.6)	

[a]Numbers within parentheses indicate the values of t statistic associated with regression coefficients shown.

of households in the analysis zone; and I_1 = dummy variable having value equal to 1 if the analysis zone contains a major hospital or a well defined suburban town center, or both, which can satisfy eat meal or personal business trip purpose, 0 otherwise.

Values of calibration coefficients a, b, and c for different pseudo-employment density ranges are shown in Table 5. The coefficients a and b were also estimated without incorporating the dummy variable I_1 in Eq. 3. The statistical fit obtained was much inferior ($R^2 = 0.75$) compared to that obtained when I_1 is included. This indicates that major traffic generators tend to have higher trip attraction rates because of their regional draw and greater awareness on the part of the trip maker. In fact, equations for estimating home-based social recreation trip attractions, shopping trip attractions, school trip attractions, and truck trip ends were all significantly improved when dummy variables indicating the presence of major trip attractor were included in the regression analysis.

Home-Based Social Recreation Person Trip Attractions (HBSRCA)

For this trip purpose, the following equation was developed:

$$\text{HBSRCA} = a \times \text{HH} + b \times \text{COMMLAND} + c \times \text{OPEN SPACE} + d \times I_1;$$

$R^2 = 0.90$, number of observations = 911, F value = 1,031.2,

error of estimate (HBSRCA) = 339.3 . . . . . (4)

in which HBSRCA = zonal home-based social recreation person trip attractions; OPEN SPACE = zonal gross open space area, in acres; and I_1 = dummy variable having value equal to 1 if the analysis zone contains one or more of the following generators: public golf course having large draw area; picnic area, recreational area, beach etc. having regional draw; YMCA, high school

TABLE 6.—Values of Calibration Coefficients Used in Eq. 4

Coefficient a (1)	Coefficient b (2)	Coefficient c (3)	Coefficient d (4)	Pseudo-employment density range, in employees per nonresidential acre (5)
0.84	1.31	0.44	1,047.8	≤2
(25.1)[a]	(6.3)	(3.7)	(28.6)	
0.84	5.14	0.44	1,047.8	2–6.5
(25.1)	(10.5)	(3.7)	(28.6)	
0.84	10.94	0.44	1,047.8	6.5–10
(25.1)	(17.0)	(3.7)	(28.6)	
0.61	10.94	5.51	1,047.8	10+
(34.2)	(17.0)	(10.8)	(28.6)	

[a]Numbers within parentheses indicate the values of t statistic associated with regression coefficients shown.

stadium or baseball diamond having spectator stands, movie theater complex; 0 otherwise. Value of calibration coefficients a, b, c, and d for different pseudo-employment density ranges are shown in Table 6.

Home-Based School Person Trip Attractions (HBSCLA)

Since most school trips are destined to institutional land use (see Table 3), which is only a small subset of the generalized commercial land use category, school person trip attractions cannot be estimated directly as a function of the commercial land-use category. School enrollment totals, however, can be easily compiled at the zonal level using data provided by the state board of education and colleges and universities. Consequently, school person trip attraction rates were developed as a function of zonal school plus college enrollment. Rates were further stratified by residential densities to capture the differences in mode of arrival, since schools located in dense residential areas can be easily

TABLE 7.—Values of Calibration Coefficients Used in Eq. 5

Coefficient a (1)	Coefficient b (2)	Residential density range, in households per residential acre (3)
1.41	NA[b]	≤2
(36.8)[a]		
0.76	NA	2–6
(24.6)		
0.60	317.7	6–15
(21.4)	(2.6)	
0.29	798.1	15+
(7.7)	(6.4)	

[a]Numbers within parentheses indicate the values of t statistic associated with regression coefficients shown.

[b]Not applicable—for residential density less than or equal to 6 households/residential acre, variable associated with coefficient b is not used in Eq. 5.

accessed by walking. The following equation was developed:

$$\text{HBSCLA} = a \times \text{ENROLLMENT} + b \times I_1; \quad R^2 = 0.85,$$

number of observations = 590, F value = 551.8,

error of estimate (HBSCLA) = 474.3 . . . . . (5)

in which HBSCLA = zonal home-based person school trip attractions; ENROLLMENT = zonal school enrollment for grades kindergarten through college; I_1 = dummy variable having value equal to 1 if the analysis zone contains a high school or a college which is commuter oriented, 0 otherwise; and residential density = number of households/gross residential land area, in acres.

Values of calibration coefficients a and b for different residential density ranges are shown in Table 7. It should be noted that for residential density

values less than or equal to six households/acre, the dummy variable I_1 is not used in Eq. 5.

Several attempts were made to improve the R^2 by: (1) Aggregating zonal data to districts to eliminate any bias caused due to poor trip-file coding; (2) disaggregating the enrollment data by different grades; i.e., kindergarten to eighth, eighth to high school, and college; and (3) separating models for school and college enrollment; but none of these efforts proved useful in improving the R^2 further.

Home-Based Shop Person Attractions (HBSHPA)

Home-based shop person trip attraction rates were first calibrated as a function of the generalized commercial land-use category and stratified by employment

TABLE 8.—Values of Calibration Coefficients Used in Eq. 6

Coefficient *a* (1)	Coefficient *b* (2)	Coefficient *c* (3)	Pseudo-employment density range, in employees per nonresidential acre (4)
36.86	2,690.3	11,990.0	≤10
(8.9)[a]	(29.4)	(41.4)	
72.07	2,690.3	11,990.0	10–16
(17.4)	(29.4)	(41.4)	
162.65	2,690.3	11,990.0	16–25
(31.9)	(29.4)	(41.4)	
210.44	2,690.3	11,990.0	25–30
(7.3)	(29.4)	(41.4)	
228.79	2,690.3	11,990.0	30–54
(16.9)	(29.4)	(41.4)	
322.92	2,690.3	11,990.0	54+
(14.7)	(29.4)	(41.4)	

[a]Numbers within parentheses indicate the values of *t* statistic associated with regression coefficients shown.

density, but considerably low R^2 value (0.26) was obtained. An attempt was also made to combine HBOA and HBSHPA into a single trip purpose and estimate models similar to the ones presented earlier for HBOA. This formulation also resulted in a low R^2 (0.40).

It became necessary to base HBSHPA on the retail land-use category rather than on the generalized commercial land use. This puts an additional burden on base year data collection and design year forecasting of land-use changes. Next to work trips, shop trips usually account for the largest portion of overall urban travel demand, so this additional effort seems justified. Using retail land use as the base variable, the following equation was developed:

$$\text{HBSHPA} = a \times \text{RETAIL LAND} + b \times I_1 + c \times I_2;$$

$R^2 = 0.94$, number of observations = 754, F value = 1,466.4,

error of estimate (HBSHPA) = 639.1 . . . . . (6)

in which HBSHPA = zonal home-based shop person trip attractions; RETAIL LAND = zonal gross retail land area, in acres; I_1 = dummy variable having value equal to 1 if the analysis zone contains a subregional shopping center [characterized by discount department store (s)/supermarket and a group of small specialty shops, drug store etc.], 0 otherwise; and I_2 = dummy variable having value equal to 1 if the analysis zone contains a regional shopping mall or center (characterized by two or more nationally known department stores, many small specialty shops, and movie theaters), 0 otherwise. Values of calibration coefficients a, b, and c for different pseudo-employment density ranges are shown in Table 8.

Nonhome-Based Person Trip Ends (NHB)

Since nonhome-based trips originating (O) from a zone are found to be equal to nonhome-based trips destined (D) to that zone, a model was calibrated to estimate total nonhome-based person trip ends (O + D). Estimated trip ends then can be divided by two and set equal to nonhome-based trip origins and trip destinations. Another novel approach used to estimate nonhome-based trip ends was to correlate these trip ends to home-based trip attractions rather than to use number of households and land area measurements by land-use type. The following equation was developed for all zones falling outside the CBD:

$$\underset{t}{\text{NHB}} = \underset{(25.98)}{0.327} \times \text{HBWA} + \underset{(24.29)}{0.959} \times \text{HBOA} + \underset{(17.58)}{0.468} \times \text{HBSRCA} + \underset{(31.54)}{0.250} \times \text{HBSHPA};$$

$R^2 = 0.95$, number of observations = 933, F value = 4750.73, error of estimate (NHB) = 248.53 . . . . . (7)

in which NHB = nonhome-based person trip ends.

Truck Trip Ends

As with nonhome-based trips, truck trips originating from a zone are found to be equal to truck trips destined to that zone. Therefore, models were calibrated to directly estimate total truck trips ends. The following models were estimated:

Truck trip ends = $a \times \text{HH} + b \times \text{COMMLAND} + c \times \text{INDLAND} + d \times I_1$;

$R^2 = 0.92$, number of observations = 887, F value = 673.7,

error of estimate (truck trip ends) = 202.9 . . . . . 8)

in which I_1 = dummy variable having value equal to 1 if the zone contains a truck terminal, industrial park, warehouse, or established suburban town center, 0 otherwise. Values of calibration coefficients a, b, c, and d for different pseudo-employment density ranges are shown in Table 9.

Person Trip Attraction Rates in CBD

It was indicated earlier that for very high density zones such as the CBD,

trip rates cannot be based simply upon the gross land area because of the mixed land-uses found in the same building. Gross floor area was utilized as the base variable. Models calibrated using the Cleveland CBD data are shown in the following. Similar relationships have also been reported by Wright (26).

$$\underset{t}{\text{HBWA}} = \underset{(3.8)}{3.522} \times \text{OFFSPACE} + \underset{(4.9)}{5.876} \times \text{COMMSPACE} + \underset{(0.3)}{0.449} \times \text{INDSPACE};$$

$R^2 = 0.82$, number of observations = 35, F value = 46.7,

error of estimate (HBWA) = 3,313.1 . . . . . (9)

$$\underset{t}{\text{HBOA}} = \underset{(2.5)}{0.789} \times \text{OFFSPACE} + \underset{(4.5)}{1.795} \times \text{COMMSPACE};$$

$R^2 = 0.73$, number of observations = 35, F value = 42.9,

error of estimate (HBOA) = 1,145.7 . . . . . (10)

$$\underset{t}{\text{HBSRCA}} = \underset{(6.9)}{1.058} \times \text{COMMSPACE} + \underset{(1.5)}{1.382} \times \text{RES SPACE};$$

$R^2 = 0.65$, number of observations = 35, F value = 29.7,

error of estimate (HBSRCA) = 599.4 . . . . . (11)

TABLE 9.—Values of Calibration Coefficients Used in Eq. 8

Coefficient *a* (1)	Coefficient *b* (2)	Coefficient *c* (3)	Coefficient *d* (4)	Pseudo-employment density range, in employees per nonresidential acre (5)
0.32	0.67	1.14	827.6	≤3
(28.5)*	(5.5)	(2.7)	(25.1)	
0.32	3.97	1.85	827.6	3–6.5
(28.5)	(9.9)	(3.6)	(25.1)	
0.32	6.00	1.85	827.6	6.5–10
(28.5)	(10.2)	(3.6)	(25.1)	
0.32	9.96	3.35	827.6	10–13
(28.5)	(12.8)	(4.3)	(25.1)	
0.32	12.41	6.27	827.6	13–16
(28.5)	(15.7)	(13.9)	(25.1)	
0.32	14.77	6.27	827.6	16–25
(28.5)	(19.3)	(13.9)	(25.1)	
0.32	14.77	21.65	827.6	25–30
(28.5)	(19.3)	(20.2)	(25.1)	
0.32	23.44	21.65	827.6	30–54
(28.5)	(19.8)	(20.2)	(25.1)	
0.32	23.44	84.26	827.6	54+
(28.5)	(19.8)	(10.9)	(25.1)	

*Numbers within parentheses indicate the values of t statistic associated with regression coefficients shown.

$$\underset{t}{\text{HBSHPA}} = \underset{(18)}{0.017} \times (\text{RETAIL SPACE})^2;$$

$R^2 = 0.91$, number of observations = 35, F value = 324.2,

error of estimate (HBSHPA) = 1,554.3 . . . . . (12)

$$\underset{t}{\text{NHB}} = \underset{(6.6)}{0.462} \times \text{HBWA} + \underset{(1.5)}{0.422} \times \text{HBOA} + \underset{(2.9)}{0.138} \times \text{HBSHPA} + \underset{(2.9)}{0.736}$$

$\times$ HBSRCA $R^2 = 0.99$, number of observations = 35,

F value = 681.9, error of estimate (NHB) = 311.5 . . . . . (13)

$$\underset{t}{\text{Truck Trip Ends}} = \underset{(5.5)}{2.055} \times \text{INDSPACE} + \underset{(4.6)}{0.783} \times \text{COMMSPACE} + \underset{(1.6)}{0.204}$$

$\times$ OFFSPACE; $R^2 = 0.80$, number of observations = 35, F value = 42.6,

error of estimate (truck trip ends) = 470.4 . . . . . (14)

in which OFFSPACE = zonal gross office floorspace area, in thousands of square feet; COMMSPACE = zonal gross commercial floorspace area, in thousands of square feet; RETAIL SPACE = zonal gross retail floorspace area, in thousands of square feet; INDSPACE = zonal gross industrial floorspace area, in thousands of square feet; and RES SPACE = zonal gross residential floorspace area, in thousands of square feet.

It should be noted that home-based school person trip attraction is estimated using student enrollment and trip rates presented earlier. Notice that for the CBD models, office floorspace has been categorized separately rather than being lumped with the general commercial floor use category.

Conclusions

The results reported here indicate that acceptable estimates of person trip attractions can be obtained using readily available data such as the number of households, the school enrollment, the area of industrial, commercial, open space, and retail land. For zones falling within a very high density area such as the CBD, trip attraction should be based upon floorspace measurements rather than upon land area. Categorization of floorspace by office, retail, commercial, and industrial use should be adequate for estimating the person-trip attractions by trip purpose.

Stratification of zones by a locational variable is also shown to be essential because trip rates based upon gross land area vary significantly from low-employment to high-employment density areas. Use of pseudo-employment density was found to be adequate in stratifying the zones. Introduction of a dummy variable to reflect the presence of a major trip attractor relevant to the trip purpose under consideration significantly improves the statistical correlation between trips attracted and the gross land area present within a zone.

For the model calibration year, pseudo-employment densities can be easily calculated from the O-D survey and land-use inventory data. The year model validation has to be undertaken as part of the continuing planning process, pseudo-employment densities for zones falling within the mature portion of an urban area can be assumed to have the same values as in the base year (model calibration year).

For traffic zones belonging to that portion of the urban area which underwent new development/redevelopment, adjustment to pseudo-employment density values can be made in two ways. One approach is based upon the assumption that if a zone was partially developed (about 60–70%), the new development would follow the density that prevailed in the base year. If a zone was underdeveloped, employment density can be estimated by averaging the prevailing densities of neighboring zones.

The second approach is suitable if the precise nature of new development is known. The analyst could either refer to the comprehensive tabulation prepared by Ide (8) which gives employment densities for establishments classified by two-digit SIC codes, or consult Ref. 23. Densities shown in Ref. 23 are based upon the pseudo-employment densities observed in northeast Ohio. These sources can also aid in the selection of proper equations for assessing traffic impact associated with specific land development proposals.

For long-range planning purposes, it is suggested that pseudo-employment densities be used in a recursive manner, that is, base year densities be used for estimating trip attractions for the first time increment (usually 5 yr). Calculated work attractions then should be used to calculate the revised pseudo-employment densities, which in turn should be used for calculating trip attractions for the next time increment and so on.

Trip-estimating equations presented in this paper can be aggregated to produce total person trip attraction. If modal split and auto-occupancy of these trips can be estimated, vehicular trip generation estimates similar to those reported by the Institute of Transportation Engineers (21) and the Maricopa Association of Government (22) can be obtained. It should be emphasized that certain traffic generators such as airports, military bases, post offices, stadiums, large universities, hospitals, museums, and libraries may require special adjustments or independent trip-generation estimates. It should also be noted that trips calculated using the equations presented in this paper account for travel occurring entirely within the cordon line.

Acknowledgments

The preparation of this paper was financed through a grant for technical studies from the Urban Mass Transportation Administration and the Federal Highway Administration of the United States Department of Transportation with joint sharing in cost by the counties and municipalities within Cuyahoga, Geauga, Lake, Lorain, and Medina.

Appendix I.—References

1. "A Summary of Travel Characteristics," Chicago Area Transportation Study and Northwestern Indiana Regional Planning Commission, 1977, pp. 42.
2. "An Introduction to Urban Development Models and Their Use in Urban Transportation Planning," Urban Development Branch, Federal Highway Administration, Washington, D.C., 1976.
3. "Accuracy Checks & Adjustments on the 1963 Origin-Destination Survey," Seven County Transportation and Land Use Study, Cleveland, Ohio, Nov., 1967.
4. Black, A., "Comparison of Three Parameters of Non-residential Trip Generation," *Highway Research Record No. 114*, 1966, pp. 1–7.

5. "Census Use Study: The DIME Geocoding System," United States Bureau of Census, United States Government Printing Office, Washington, D.C., 1970.
6. Godfrey, K. A., "What Future for Remote Sensing From Space?," *Civil Engineering*, ASCE, Vol. 42, No. 7, July, 1979, pp. 61–65.
7. "Guidelines for Trip Generation Analysis," United States Department of Transportation/Federal Highway Administration, Washington, D.C., 1967.
8. Ide, E. A., *Estimating Land and Floor Area Implicit in Employment Projections—How Land and Floor Area Useage Rates Vary by Industry and Site Factors*, Vol. I & II, reports prepared for Bureau of Public Roads, United States Dept. of Transportation, July, 1970 (available from National Technical Information Service, PB 200 069, PB 200 070, Springfield, Va.)
9. Kolifarth, M., and Shuldiner, P. W., "Covariance Analysis of Manufacturing Trip Generation," *Highway Research Record No. 165*, 1967, pp. 117–128.
10. Lathrop, G. T., and Hamburg, J. R., "An Opportunity Accessibility Model for Allocating Regional Growth," *Journal of the American Institute of Planners*, Vol. XXXI, No. 2, 1965, pp. 90–94.
11. Nakkash, T. Z., and Grecco, W. L., "Activity Accessibility Models of Trip Generation," *Highway Research Record No. 392*, 1972, pp. 98–110.
12. "1975 Population Households, and Average Household Income Estimates by Census Tracts within Standard Metropolitan Statistical Area," National Planning Data Corporation, Ithaca, N.Y., 1975.
13. *NOACA Land Use Element: First-Year Working Edition*, Northeast Ohio Areawide Coordinating Agency, Cleveland, Ohio, May 3, 1978.
14. Ondecko, J. D., "Procedures and Software of the Ohio Capability Analysis Program," *Misc. Report No. 18*, Ohio Department of Natural Resources, Columbus, Ohio.
15. "Revised Implementation Manual for the Interim Design Concept: Land Use Suitability Analysis," Parsons, Brinckerhoff, Quade and Douglas, prepared for Northeast Ohio Areawide Coordinating Agency, Cleveland, Ohio, Jan. 16, 1977.
16. Shuldiner, P. W., "Land Use, Activity and Non-Residential Trip Generation," *Highway Research Record No. 141*, 1966, pp. 73–88.
17. "Standard Industrial Classification Manual," Executive Office of the President, Office of Management and Budget, United States Government Printing Office, Washington, D.C., 1972.
18. Suits, D. B., "Use of Dummy Variables in Regression Equations," *American Statistical Association Journal*, Dec., 1957, pp. 548–551.
19. "The Direct Trip Allocation Model in SCOTS Modeling Process," Cleveland-Seven County Transportation Land Use Study, Cleveland, Ohio, 1968.
20. "Trip Generation Analysis," United States Department of Transportation, Federal Highway Administration, Washington, D.C., 1975.
21. "Trip Generation," Institute of Transportation Engineers, Arlington, Va., 1976.
22. "Trip Generation Intensity Factors," Transportation Planning Division, Arizona Department of Transportation, Phoenix, Ariz., 1976.
23. "Trip Generation Analysis-Vol. 2; Home Based Person Trip Attraction Models, Non-Home Based Trip Ends, and Truck Trip Ends Estimation Models," prepared by Northeast Ohio Areawide Coordinating Agency, Cleveland, Ohio, May, 1980.
24. "U.S. Census Bureau—Urban Transportation Planning Package," Federal Highway Administration Notice, Washington, D.C., Apr. 18, 1972.
25. "Urban Transportation Planning System (UTPS) Software, Program UREGRE," United States Department of Transportation/Urban Mass Transportation Administration/Federal Highway Administration, Washington, D.C., Sept., 1977.
26. Wright, P. H., "Relationships of Traffic and Floor Space Use in Central Business District," *Highway Research Record No. 114*, Washington, D.C., 1966.

Appendix II.—Notation

The following symbols are used in this paper:

COMMLAND = zonal gross commercial land area, in acres;

COMMSPACE = zonal gross commercial floorspace area, in thousands of square feet;
ENROLLMENT = zonal school enrollment for grades kindergarten through college;
HBOA = zonal home-based other person trip attractions;
HBSCLA = zonal home-based school person trip attractions;
HBSHPA = zonal home-based shop person trip attractions;
HBSRCA = zonal home-based social recreation person trip attractions;
HBWA = zonal home-based work person trip attractions;
HH = number of households in zone;
I_1 = dummy variable used in regression analysis;
I_2 = dummy variable used in regression analysis;
INDLAND = zonal gross industrial land area, in acres;
INDSPACE = zonal gross industrial floorspace area, in thousands of square feet;
NHB = zonal nonhome-based person trip ends;
OFFSPACE = zonal gross office floorspace area, in thousands of square feet;
OPEN SPACE = zonal gross open space area, in acres;
RES SPACE = zonal gross residential floorspace area, in thousands of square feet;
RETAIL LAND = zonal gross retail land area, in acres;
RETAIL SPACE = zonal gross retail floorspace area, in thousands of square feet;
a = calibration coefficient;
b = calibration coefficient;
c = calibration coefficient; and
d = calibration coefficient.

TRANSPORTATION
ENGINEERING JOURNAL

DISCUSSION

Note.—This paper is part of the Transportation Engineering Journal of ASCE, Proceedings of the American Society of Civil Engineers, © ASCE, Vol. 107, No. TE1, January, 1981. ISSN 0569-7891/81/0001-0101/$01.00.

Discussions

Discussions may be submitted on any Proceedings paper or technical note published in any *Journal* or on any paper presented at any Specialty Conference or other meeting, the *Proceedings* of which have been published by ASCE. Discussion of a paper/technical note is open to anyone who has significant comments or questions regarding the content of the paper/technical note. Discussions are accepted for a period of 4 months following the date of publication of a paper/technical note and they should be sent to the Manager of Technical and Professional Publications, ASCE, 345 East 47th Street, New York, N.Y. 10017. The discussion period may be extended by a written request from a discusser.

The original and three copies of the Discussion should be submitted on 8-1/2-in. (220-mm) by 11-in. (280-mm) white bond paper, typed double-spaced with wide margins. The length of a Discussion is restricted to two *Journal* pages (about four typewritten double-spaced pages of manuscript including figures and tables); the editors will delete matter extraneous to the subject under discussion. If a Discussion is over two pages long it will be returned for shortening. All Discussions will be reviewed by the editors and the Division's or Council's Publications Committees. In some cases, Discussions will be returned to discussers for rewriting, or they may be encouraged to submit a paper or technical note rather than a Discussion.

Standards for Discussions are the same as those for Proceedings Papers. A Discussion is subject to rejection if it contains matter readily found elsewhere, advocates special interests, is carelessly prepared, controverts established fact, is purely speculative, introduces personalities, or is foreign to the purposes of the Society. All Discussions should be written in the third person, and the discusser should use the term "the writer" when referring to himself. The author of the original paper/technical note is referred to as "the author."

Discussions have a specific format. The title of the original paper/technical note appears at the top of the first page with a superscript that corresponds to a footnote indicating the month, year, author(s), and number of the original paper/technical note. The discusser's full name should be indicated below the title (see Discussions herein as an example) together with his ASCE membership grade (if applicable).

The discusser's title, company affiliation, and business address should appear on the first page of the manuscript, along with the *Proceedings* paper number of the original paper/technical note, the date and name of the *Journal* in which it appeared, and the original author's name.

Note that the discusser's identification footnote should follow consecutively from the original paper/technical note. If the paper/technical note under discussion contained footnote numbers 1 and 2, the first Discussion would begin with footnote 3, and subsequent Discussions would continue in sequence.

Figures supplied by the discusser should be designated by letters, starting with A. This also applies separately to tables and references. In referring to a figure, table, or reference that appeared in the original paper/technical note use the same number used in the original.

It is suggested that potential discussers request a copy of the *ASCE Authors' Guide to the Publications of ASCE* for more detailed information on preparation and submission of manuscripts.

Basic Pipe Stress Evaluation Summary[a]

Closure by Gerald F. Mouser,[3] A. M. ASCE

The writer would like to thank the discusser for his interest in the paper and for offering comments regarding hoop stress analysis.

Load Response of Transportation Support Systems[b]

Errata

The following correction should be made to the original paper:

Page 124, Eq. 7: Should read $\sigma_T = -2c \tan\left(45 - \frac{\phi}{2}\right)$ instead of $\sigma_T = -2c \tan^2\left(45 - \frac{\phi}{2}\right)$

Cracking in Concrete Pavements[c]

Discussion by Clyde N. Laughter,[5] M. ASCE

As performance of concrete pavements with cracking is a major concern and a field with broad experimental and observational background, expansive and complex theoretical development and often a gulf exists between the two.

[a]July, 1979, by Gerald F. Mouser (Proc. Paper 14691).
[3]Operations Engr., Mountain Fuel Supply Co., 625 Connecticut Ave., P.O. Box 1129, Rock Springs, Wyo. 82901.
[b]January, 1980, by Lufti Raad and Jose L. Figueroa (Proc. Paper 15146).
[c]March, 1980, by Robert C. Deen, James H. Havens, Assaf S. Rahal, and W. Vernon Azevedo (Proc. Paper 15273).
[5]Chf. Soil Engr., Wisconsin Dept. of Transportation, Div. of Highways, 3502 Kinsman Blvd., Madison, Wisc. 53704.

The authors are to be complimented for another effort to bridge this gulf.

The writer has several comments that are essentially questions. Buckling and blowups are attributed to expansion and it is implied these can be prevented with expansion joints. At this time there is a prevalent theory that expansion, growth, joint impaction or other phenomena coupled with gravational forces cause creep of pavement slabs down hill with forces sufficient to move bridge abutments. To attentuate this many agencies cut or form an expansion space back of bridge ends. If these forces exist and the expansion forces set forth by the authors combine, should not almost all blowups occur at sag points having no bridges such as those that fill over culverts in rolling terrain? Is this the authors' observation?

The comments on D-cracking are interesting as most researchers have previously attributed it to aggregate or other mix properties with no explanation of lack of edge deterioration at midlengths of the slab. This of course lends credence to the hypothesis of fatigue loading of the concrete by temperature expansion-contraction as presented in the paper. But if this hypothesis is valid, D-cracking would occur at all or at least most of the joints for similar slab lengths built with similar joints. Is this true in the pavements observed by the authors? Naturally, one variation that could affect this is different expansive properties of the different pavements. If this is the reason that some pavements have D-cracking while others do not, then the aggregate quality again probably becomes the major factor. If some pavements D-cracked and others did not, were the thermal expansion or wet-dry expansion properties of the mix components, or of the cured concrete in the various pavements determined?

Diesel Fuel Forecasts in Virginia[a]

Errata

The following corrections should be made to the original paper:

Page 176, Table 4, heading for Col. 2: Should read "DIESEL FUEL USED" instead of "GALLONS TAXED (MILLIONS)"

Page 181, paragraph 4, line 6: Should read "for 5% and 10% diesel automobiles respectively." instead of "5% and 10% diesel automobiles, respectively."

[a]July, 1980, by Antoine G. Hobeika and Frank Tamberrino, *Transportation and Development Around the Pacific*, pp. 172–183.